BEARING CAPACITY OF A THIN LAYERED JOINTED ROCK SYSTEM

A THESIS

Presented to

The Faculty of the Graduate Division

by

Allen Campbell Johnson

In Partial Fulfillment

of the Requirements for the Degree

Master of Science in Civil Engineering

Georgia Institute of Technology

April, 1966

BEARING CAPACITY OF A THIN LAYERED

JOINTED ROCK SYSTEM

Approved:

Date approved by Chairman: 7/25/66

ACKNOWLEDGMENTS

The writer wishes to express his gratitude to Professor George F. Sowers, Thesis Advisor, and to Professor B. B. Mazanti and Dr. Charles E. Weaver, members of the reading committee, for advice and direction during this investigation. The writer also wishes to thank Mr. C. E. Pavey, machinist, for his assistance in constructing some of the items of equipment used in the research, and the Sherwood Cut Stone Company for supplying the Indiana Limestone used in this project.

TABLE OF CONTENTS

LIST OF TABLES

LIST OF ILLUSTRATIONS

LIST OF SYMBOLS AND ABBREVIATIONS

Symbol	
α	Semi-wedge angle
c	Cohesion
φ	Angle of Internal Friction
q	Pressure
q_o	Unit Load (Bearing capacity)
q_u	Unconfined Compression Strength
p_t	Tensile Strength
p_h	Horizontal splitting pressure
Q	Total Failure Load
γ	Effective Unit Weight of Limestone
b	Footing Width
t	Individual block thickness
W	Individual block width
H	Height of system
eq.	Equation
vs.	Versus
N_γ, N_c, N_q	General Bearing Capacity Factors
D_f	Depth of surcharge
psi	Pounds per square inch

SUMMARY

The purpose of this research project was to investigate certain behaviors of a thin layered, jointed rock system when loaded in various positions with various sizes of square model footings. The aspects of behavior of the system that were investigated included bearing capacity, load-settlement relationships, and lateral load development. The thin layered, jointed system was composed of small blocks (four inches square by 0.25 inch thick) of Indiana Limestone stacked as closely as possible by hand to form a mass 12 inches square and four inches high. The system was placed in a rigid aluminum retaining box, two adjacent sides of which were fitted with SR 4 strain gauges for measuring the lateral loads which developed during testing. Model footings were made of steel and ranged from 1.25 inches square to six inches square. The rate of deformation was 0.01 inches per minute.

The purposes of the investigation were satisfied in that a general trend for bearing capacity as a hyperbolic function of the ratio of footing width, b, to block width, W, was developed for the range of testing. The amount of settlement occurring in the loaded blocks was found to be dependent upon the magnitude of separations occurring in a horizontal plane between the stacked blocks. Lateral loads appeared to reach critical magnitudes with regard to foundation failure only after the loaded blocks had failed in bearing.

The conclusions reached from this investigation follow:

1. The bearing capacity failure occurring in the loaded blocks is always the splitting type described by Meyerhof.

2. The bearing capacity of the loaded blocks can be represented by a power function of the form

$$q_o = a(\frac{b}{w})^n$$

in which the coefficient a is in psi units and n is a fractional negative exponent.

3. The magnitudes of the coefficient a and exponent n vary according to the position of the footing on the loaded blocks.

4. The total amount of settlement occurring in such a system prior to failure can be attributed to the following: an initial component due to the reduction of void spaces occurring in a horizontal plane between stacked blocks, and a subsequent quasi-elastic component resulting from deformation of the individual blocks under load.

5. In order to predict the amount of settlement which would result in the loaded blocks, it would be necessary to determine the amount of void spaces present in the system prior to loading, and to determine the behavior of the quasi-elastic deformation of the system.

6. The lateral load developing in such a system under a footing load is probably dependent upon the Poisson's ratio of the rock, the irregularities in individual blocks and stacking, and the magnitude of void spaces occurring in a vertical plane within the system prior to loading.

7. The lateral load developing in such a system prior to failure is not of sufficient magnitude to be a factor in foundation failure.

8. Lateral load developing after failure of the loaded blocks is due to the forcing aside of adjacent blocks by the wedge of material formed underneath the footing as it is forced downward.

CHAPTER I

INTRODUCTION

Excavations for projects such as mines, tunnels, highway or railroad cuts, or foundations for buildings, dams, or bridges frequently encounter rock deposits. In order that the engineer involved may effectively design and construct his particular structure, he must have an accurate understanding of the manner in which the underlying rock (and soil) will react to the future imposed load.

In foundation design, the engineer is interested in two aspects of behavior displayed by the underlying rock under load. These aspects are the bearing capacity and the relationship between load and settlement. Bearing capacity is important as it is the maximum load per unit area that the rock can support without rupture. The relationship between load and settlement is important since the foundation must not deflect sufficiently either to cause failure of the structure or to impair its use (1).

If there are foundations of other structures nearby, the engineer will be interested in the effect of the load on the underlying rock upon the adjacent foundations. Should the installation of the new foundation cause damage to adjacent foundations, the engineer could have a damage suit for negligence brought against him in a court of law. Therefore, the engineer is often interested in the relationship between footing load and lateral load produced by the new foundation.

Although rock has been used as a building material since before the dawn of history, very little research was conducted to determine its shear strength under *in situ* conditions prior to the beginning of the 20^{th} century. This lack of research probably was due to the following factor: stresses imposed by foundations were almost always much lower than the bearing capacity of the supporting rock deposits. (It is emphasized at this point that shear strength and bearing capacity are not synonamous. Rather, shear strength is a physical property of a substance, while bearing capacity is a behavior of a substance that is dependent upon a number of physical properties of the material and the geometric boundaries of the mass of material. Other physical properties besides shear strength contributing to bearing capacity are the unit weight of a material, the depth of overburden, the width of the footing, and the nature of joints within the mass of material.)

Prior to 1900, the shear strength of small rock samples was determined by an unconfined compression test. Since the results of this test did not reflect the effects of lateral confining pressure on shear strength, investigators began to search for a new method of testing that would do so. The triaxial test as used in soil and rock testing today is the result of these efforts. This test employs lateral confining pressures and pore fluid pressures in order to simulate *in situ* conditions on rock samples during testing. The results furnish a reasonably representative value of *in situ* shear strength. (Since the actual *in situ* stresses acting upon a soil or rock mass are unknown, the true *in situ* shear strength cannot be obtained in a laboratory test.)

While there has been great progress in determining _in situ_ shear strength of rock samples, there still remain many unanswered questions concerning the bearing capacity of rock masses under _in situ_ conditions. In comparison with the number of triaxial tests conducted upon rock samples to determine the shear strength, there have been relatively few model or prototype footing tests on rock to investigate its bearing capacity.

The great majority of triaxial tests on rock are conducted upon small, solid cylindrical samples. According to Klaus W. John (2), a great difference exists between these laboratory samples and rock masses in the field. He states the following:

> _In situ_ rock, however, contrary to the widespread assumption in foundation engineering, is rarely homogeneous; rarely without mechanical discontinuities. Therefore, rock mechanics is, in most cases, to be a study of a discontinuum. This marks a distinct difference between soil and rock mechanics.

John (2) then states the fundamentals of rock mechanics which are as follow:

> 1. For most engineering problems, the technological properties of a rock mass depend far more on the system of geological separation within the mass than on the strength of the rock material itself. Therefore, rock mechanics is to be a mechanics of a discontinuum, that is, a jointed system.
>
> 2. The strength of a rock mass is considered to be a residual strength that, together with its anisotropy, is governed by the interlocking bond of the unit rock blocks representing the rock mass.
>
> 3. The deformability of a rock mass and its anisotropy result primarily from the internal displacements of the unit blocks within the structure of the rock mass.

In view of the lack of research on the bearing capacity of rock and John's hypothesis that rock masses in the field are rarely homogeneous and rarely without mechanical discontinuities, it was proposed to investigate several previously mentioned behaviors of a thin layered (i.e., the thickness of the individual rock layers is less than the width of the footings), jointed rock system. The system could be considered as a model of a jointed sedimentary rock such as limestone or sandstone, or a fissile rock such as shale or slate that might occur in the field. The behaviors of the system which were investigated included the following:

1. Bearing Capacity
2. Footing load vs. Settlement
3. Footing load vs. Lateral load

The system itself was composed of blocks of Indiana Limestone four inches square and 0.25 inches thick. The individual blocks were stacked closely by hand as shown in Figure 1 in a aluminum retaining box. Various different sizes of model footings were used to load the system with ratios of footing width, b, to block width, W, ranging from 0.313 to 1.5. Tests were conducted with footings at the positions on the system indicated in Figure 2.

One purpose of conducting a model study is to obtain information which may be used to predict accurately the performance of a prototype system in the desired respect (3). One purpose of conducting the model footing tests on the thin layered, jointed rock system was to obtain information about the bearing capacity of the loaded blocks which could be used to predict the bearing capacity of prototype footings on similar jointed rock systems occurring in the field.

In applying the data obtained from a model footing test on the thin layered jointed rock system to predict the bearing capacity of a

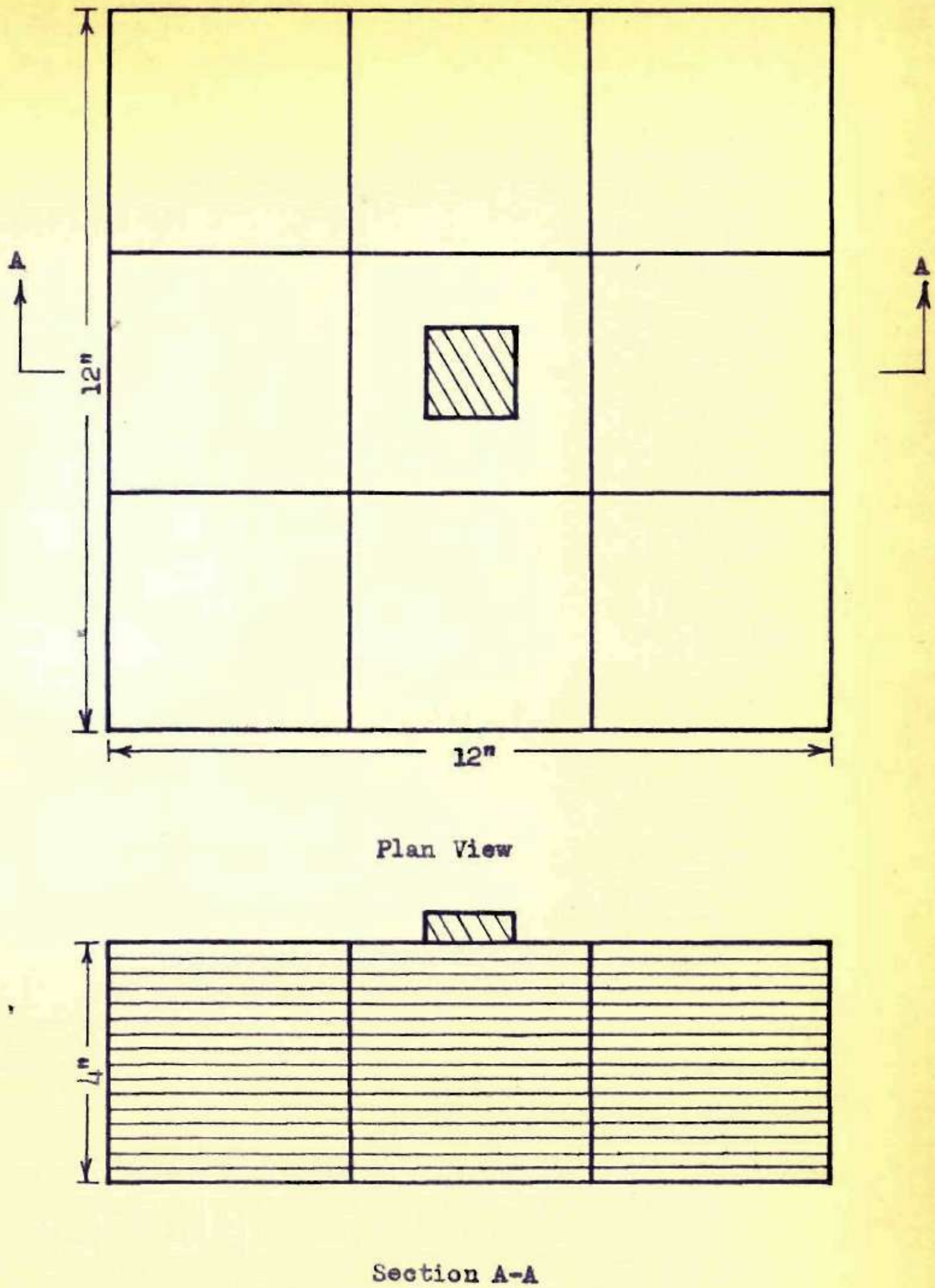

Figure 1. Entire Thin Layered Jointed System Showing Footing at the Center of a Block

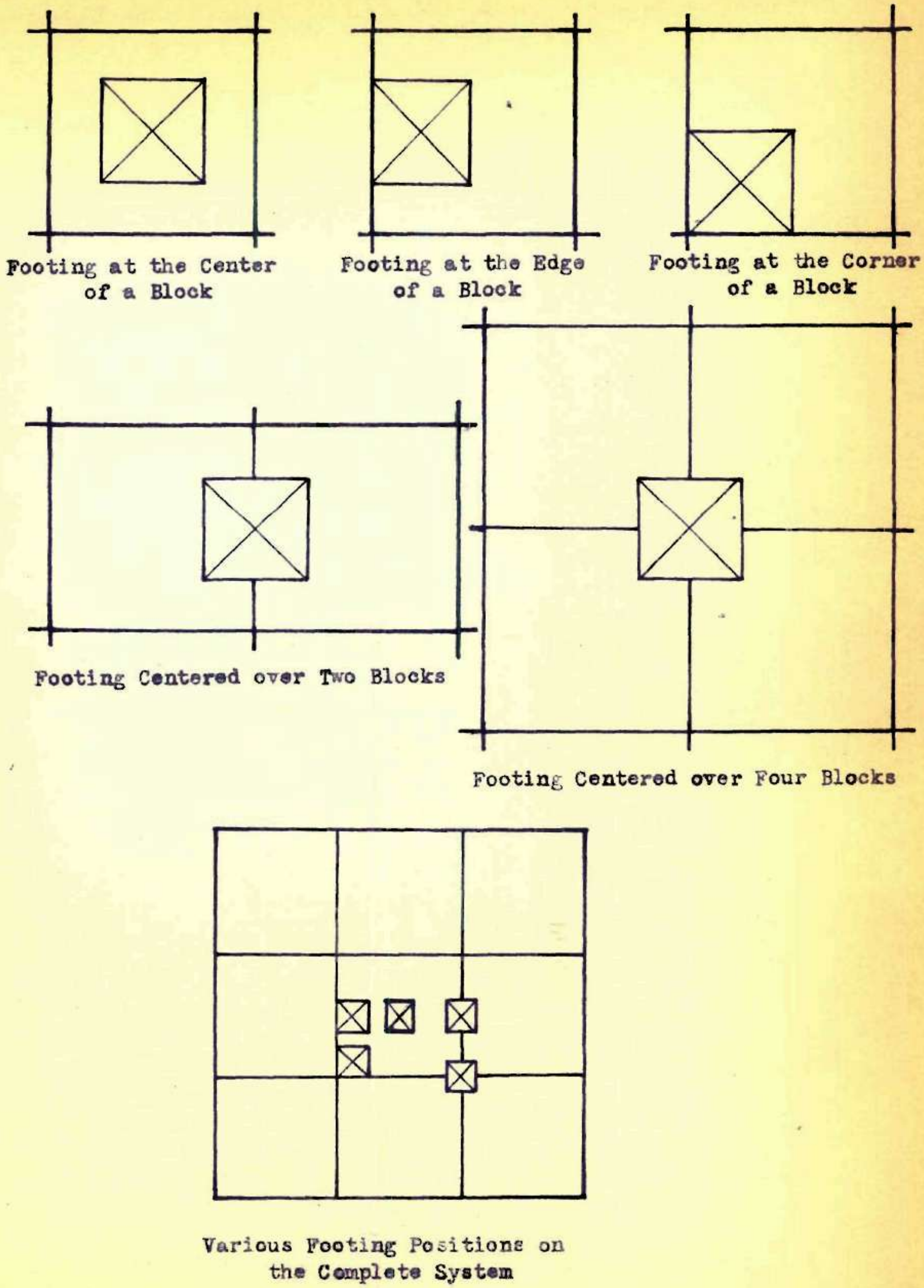

Figure 2 . Positions of Footings in the Various Tests

prototype footing, the scale effects of the footing width, b, must be considered if the predicted value of the bearing capacity of the prototype footing is to be an accurate one. Likewise, if a surcharge is involved, scale effects due to the depth of surcharge, D_f, must be considered in predicting the bearing capacity of the prototype footing. The following procedure is proposed as a means of accounting for the scale effects due to these two dimensions in a material in which the bearing capacity may be expressed by the general bearing capacity equation

$$q_o = \frac{\gamma b}{2} N_\gamma + c N_c + \gamma D_f N_q \quad . \; . \; . \; . \; . \; . \qquad (1)$$

where γ = effective unit weight of material

b = width of footing

c = soil cohesion

D_f = depth of overburden

N_γ, N_c, and N_q = general bearing capacity factors depending upon φ and the assumed shape of the failure surface.

(It is not implied that the bearing capacity of the thin layered jointed rock system tested in this project either can or can not be expressed by means of the general bearing capacity equation (1). It was chosen for use in this illustration for reasons of its relatively wide application and convenience of form.)

If model tests are conducted upon representative samples of the material occurring in the field, then the values of c, φ, and γ would be approximately equal in both the cases of the model system and the prototype. Similarly, values of N_γ, N_c, and N_q, would be identical in both cases if the shapes of the two failure surfaces were similar. Thus, the variables between the two cases would be the footing widths, b, and the depths of surcharge, D_f, according to the general bearing capacity equation (1). As this equation states, q_o varies directly with both b and D_f. Therefore, the increases in b and D_f from the model to the prototype would produce proportionate increases in the bearing capacity of the prototype over that of the model. Consider a model footing of width b_m and having a depth of surcharge D_{fm}. The bearing capacity of the model footing, q_{om}, could be expressed by the general bearing capacity equation as follows:

$$q_{cm} = \frac{\gamma b_m}{2} N_\gamma + c\, N_c + \gamma\, D_{fm} \cdot N_q \; . \; . \; . \; . \; . \qquad (1)$$

The bearing capacity, q_{op}, of a prototype footing of width b_p and depth of surcharge D_{fp} on a deposit of the same material as used in the model test could be expressed by the general bearing capacity equation as follows:

$$q_o = \frac{\gamma b_p}{2} N_\gamma + c\, N_c + \gamma\, D_{fm} N_q \; . \; . \; . \; . \; . \qquad (1)$$

If the ratio of $\frac{b_p}{b_m}$ were K_b, and the ratio of $\frac{Df_p}{Df_m}$ were K_D, then q_{op} might be expressed as

$$q_{op} = q_{om} \text{ modified} = \frac{\gamma b_m}{2} N_\gamma \cdot K_b + c\, N_c + \gamma D_{fm} N_q K_D \qquad (2)$$

a relationship which would account for the differences in bearing capacities of the prototype and model footings due to scale effects arising from footing width, b, and depth of surcharge, D_f.

CHAPTER II

REVIEW OF THE LITERATURE

A number of German investigators were among the first to study the bearing capacity of small concrete and rock blocks when loaded with strip and circular model footings. The investigators and dates of their investigations are as follow: Bauschinger, 1876; Bach and Baumann, 1924; and Graf, 1921 and 1934. The original articles were published in German, and no information as to footing and block dimensions, rate of loading, or nature of the block material was found. G. G. Meyerhof (4) gives the following synopsis of their results:

> Previous loading tests (5, 6, 7, 8) on strip and circular model footings resting on cubes of concrete and rock indicate that the material fails by a combination of shearing and splitting. Immediately beneath the footing a wedge or cone of the material, corresponding to an angle of internal friction of 40° to 50° is formed by shearing along a rupture surface and is forced into the material below. By exceeding the tensile strength of the surrounding material, it is split progressively downwards and displaced sideways. The following simple theory may therefore be suggested for the two dimensional case. (Refer to Figure 3a.)
>
> At the bearing capacity q of a strip footing of width B resting on a block of thickness H and width L ($\geq H$), the horizontal splitting pressure can (in accordance with Coulomb-Mohr's theory for linear portions of the Mohr Envelope) be shown to be
>
> $$p_h = q \tan^2 \alpha - 2c(\tan \alpha) \tag{3}$$
>
> whose resultant acts at a depth $\frac{B}{4} \cot \alpha$, where the semiwedge angle $\alpha = 45° - \varphi/2$. The maximum bending tensile stress at the point of the wedge of material below the footing is

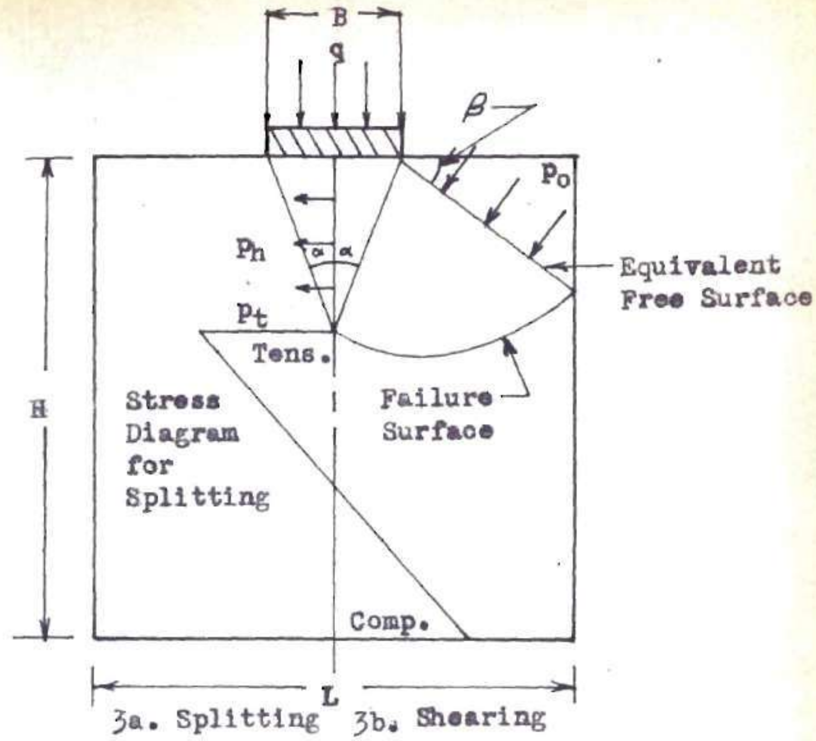

Figure 3. Failure of a Small Block, after Meyerhof

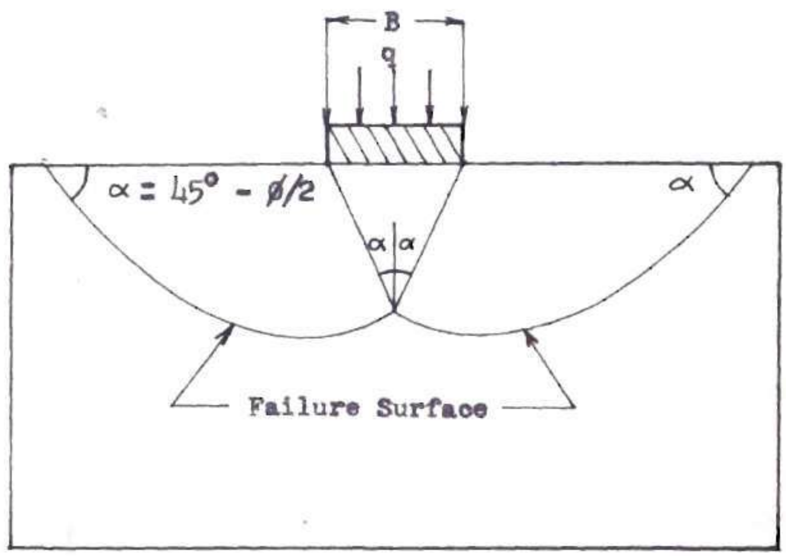

Figure 4. Shearing Failure of a Large Block, after Meyerhof

$$p_t = \left(1 + \frac{6H}{2H - B\cot\alpha}\right)\left(\frac{B\cot\alpha}{2H - B\cot\alpha}\right) p_h \tag{4}$$

Substituting for p_h from (3) into (4) and simplifying

$$q = \frac{\left(\frac{2H}{B} - \cot\alpha\right)^2 (\cot\alpha) p_t}{\frac{8H}{B} - \cot\alpha} + 2c(\cot\alpha) \tag{5}$$

For large values of H/B and substituting the unconfined prism strength $p_u = 2c(\cot\alpha)$

$$\frac{q}{p_u} = 1 + \frac{H \cdot p_t}{4B \cdot c} \tag{6}$$

This relationship indicates that the bearing capacity of surface footings is directly proportional to the ratio of block thickness to footing width (H/B) for a given ratio P_t/c depending on the properties of the material....

Where splitting of the material is prevented by reinforcement or the use of blocks that are large in relation to the size of a footing, the bearing capacity is mainly governed by the shearing strength of the material. At failure, a wedge or cone is formed below the footing as before, but the material at the side is forced outwards and upwards by shearing along a curved rupture surface. (Refer to Figure 3b.) The bearing capacity of a strip footing on the surface as before can then in accordance with Terzaghi (9) approximately be represented by

$$q = c \cdot N_c \tag{7}$$

where N_c is the general bearing capacity factor. This factor depends mainly on the angle of internal friction φ and the ratio L/B (or the inclination B of the equivalent free surface as indicated in Figure and can be determined from plastic theory.... For a very large value of L/B the bearing capacity becomes equal to that of a strip footing on the surface of a semi-infinite solid. (Figure 4)

Results of bearing capacity tests performed by Meyerhof (4) with 1.5 inch diameter model footings on small concrete and rock blocks ranging in size from six inches square by 1.25 inches thick to 18 inches square by six inches thick are in close agreement with predicted values obtained by application of equation (5).

Von Kolnitz (10) investigated the bearing capacity, footing load vs. settlement relationship of a thin layered, jointed rock system as shown in Figure 5. The rate of deformation was 0.15 inches per minute. Lateral loads were measured by means of two flat plate load cells placed between the blocks and the inside of the plywood box employed to confine the system. The results of Von Kolnitz's investigation (10) are as follow:

1. There was no significant transfer of stress across the discontinuities. The only blocks affected were those directly beneath the footing.

2. Based on the above statement and results, no attempt should be made to analyze the bearing capacity of a jointed rock system with the general bearing capacity equation (1).

3. The bearing capacity of the jointed system can be conveniently predicted by a simple modification to the Meyerhof equation (5) for the bearing capacity of rock. Meyerhof's equation and the modification may be expressed as

$$q = \left[\frac{(\frac{2H}{B} - \cot\alpha)^2 (\cot\alpha) p_t}{\frac{8H}{B} - \cot\alpha} + 2c(\cot\alpha) \right] (\frac{t}{B}) \qquad (8)$$

4a. Small footings: When the footing is small compared to the block size, there is a slight increase in bearing capacity when the footing is moved from the center to the edge of a block. Further, there is a significant drop in bearing capacity when the footing is moved to the corner of a block and over a discontinuity.

4b. Large footings: When the footing size approaches the block size, position of the footing affects the bearing capacity very little until a discontinuity is covered. This results in a significant drop in bearing capacity.

5. Failure occurs in a splitting manner followed by a punching

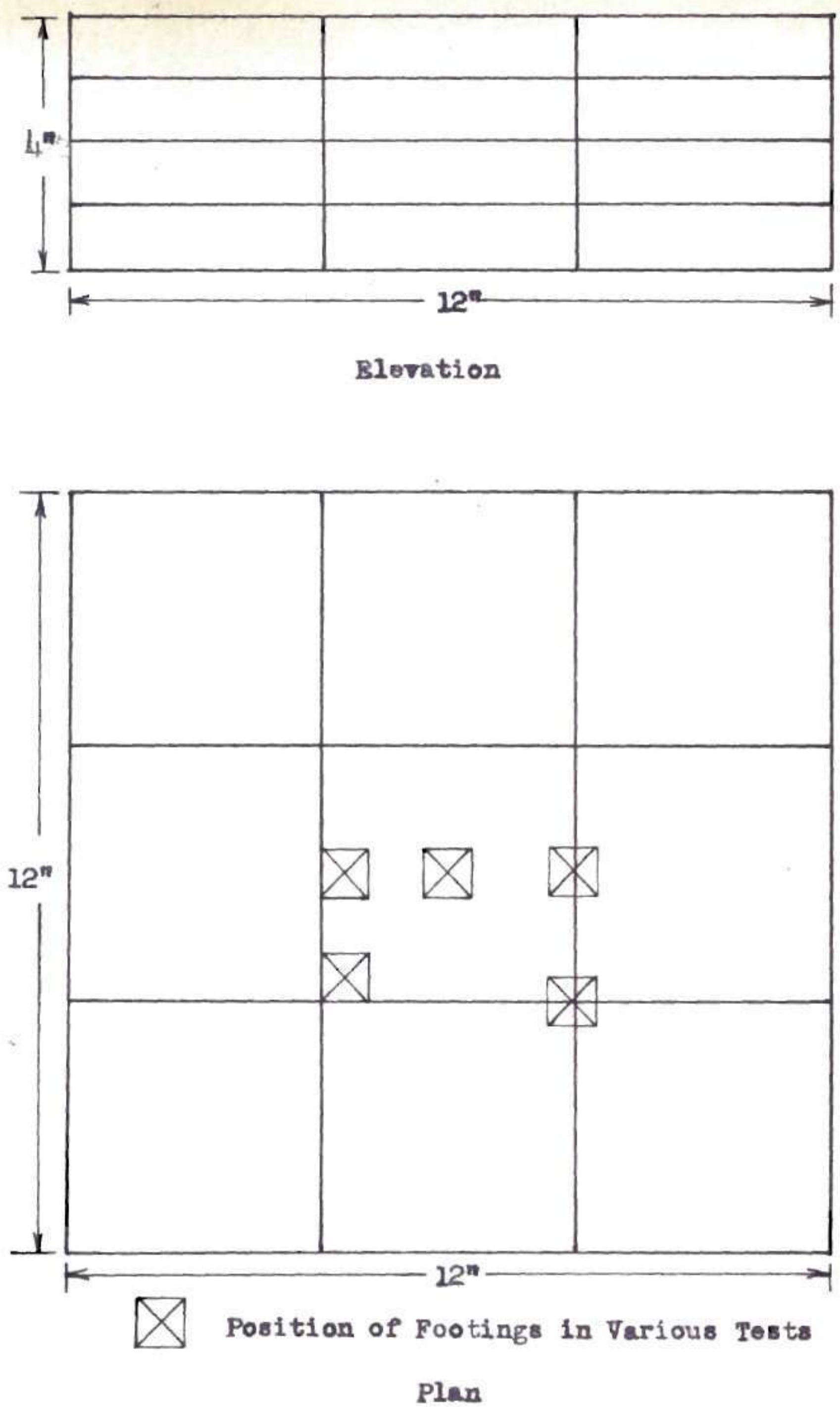

Figure 5. Thin Layered Jointed System used by Von Kolnitz

out of lower blocks.

6. Settlement depends greatly upon the tightness of the packing of individual blocks and would be most difficult to predict.

CHAPTER III

ROCK DESCRIPTION AND EQUIPMENT

Rock Description

General

The rock chosen for testing in this project was Indiana Limestone from the quarries of the Indiana Limestone Company of Bedford, Indiana. Local purchases were made from the Sherwood Cut Stone Company of Atlanta, Georgia. The limestone is accurately described by the following quotation from the specifications pamphlet of the Indiana Limestone Company (11):

> Indiana Limestone is the type of rock termed by geologists as Oolitic Limestone. It is a calcite cemented calcareous stone formed of shells and shell fragments, practically non-crystalline in character. It is characteristically a free stone without cleavage plane, possessing a remarkable uniformity of composition, texture and structure, and equality of strength in all directions regardless of the plane of its original bedding.
>
> The average analysis (in per cent) as developed by carefully prepared composite samples is given below.

Calcium Carbonate	($CaCO_3$)	97.39
Magnesium Carbonate	($MgCO_3$)	1.20
Silica	(SiO_2)	.69
Alumina	(Al_2O_3)	.44
Iron Oxide	(Fe_2O_3)	.10
Water and Loss		.10
Total		100 per cent

The average weight of dry (seasoned) Indiana Limestone is 144 pounds per cubic foot.

The term "free stone" is defined in Webster's New Intercollegiate Dictionary (12) as "any stone, but especially a sand stone or limestone, that may be cut freely without splitting."

Physical Properties

In order to determine the magnitudes of internal friction (φ), cohesion (c), tensile strength (p_t), and unconfined compression strength (q_u) of the Indiana Limestone used in this project, the following tests were conducted: quick triaxial tests, unconfined compression tests, and direct tension tests. All test samples were 2.5 inches in length and 0.875 inches in diameter; each sample was oven dried at 110°C for 24 hours to insure a uniform moisture content in all samples of zero per cent. All tests were conducted at a rate of deformation of 0.01 inches per minute, the same rate of deformation employed in testing the thin layered jointed system. The results of these tests are presented in Figures 6 through 11.

Table 1 presents the average values of c, φ, p_t, and q_u obtained from all test results. The maximum variation between the mean value and a single test result for each parameter is also recorded.

Table 1. Average Values of Strength Test Results on Indiana Limestone

Parameter	Test	Mean Value	Max. Variation From Mean For a Single Test Result
Cohesion (c)	Quick Triaxial	910 psi	63 per cent
Internal friction (φ)	Quick Triaxial	37°	15 per cent
Unconfined Compression Strength (q_u)	Unconfined Compression	3980 psi	62 per cent
Tensile Strength (p_t)	Direct Tension	410 psi	14 per cent

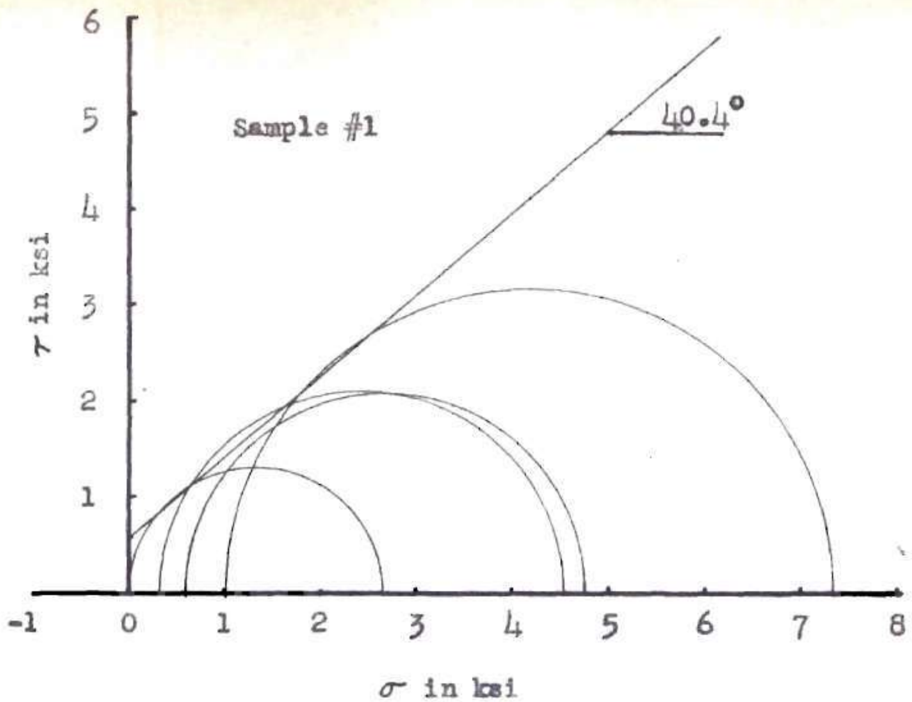

Figure 6. Mohr's Circles for Indiana Limestone

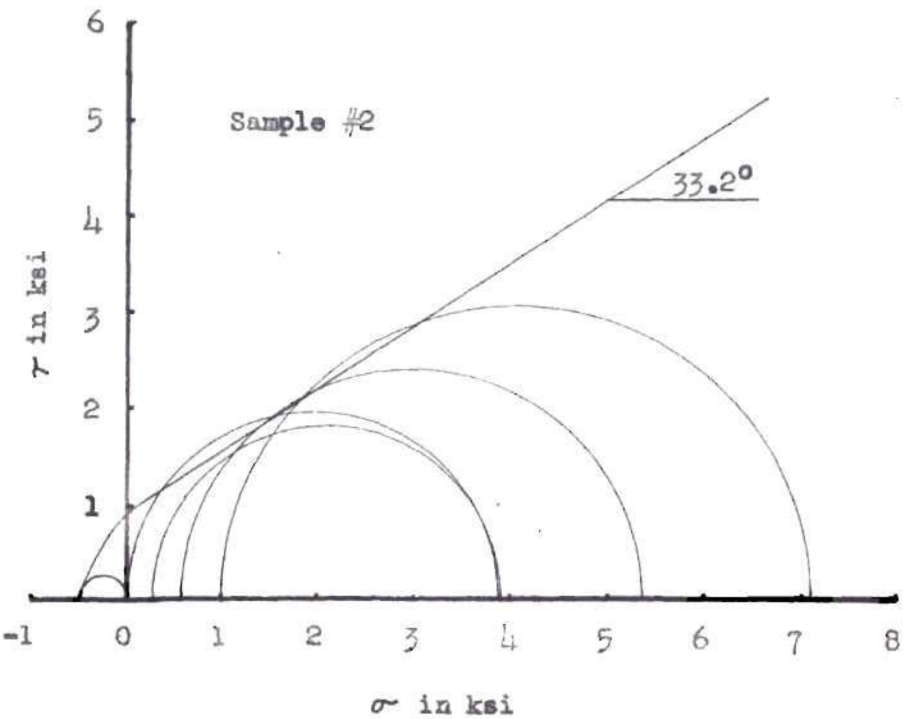

Figure 7. Mohr's Circles for Indiana Limestone

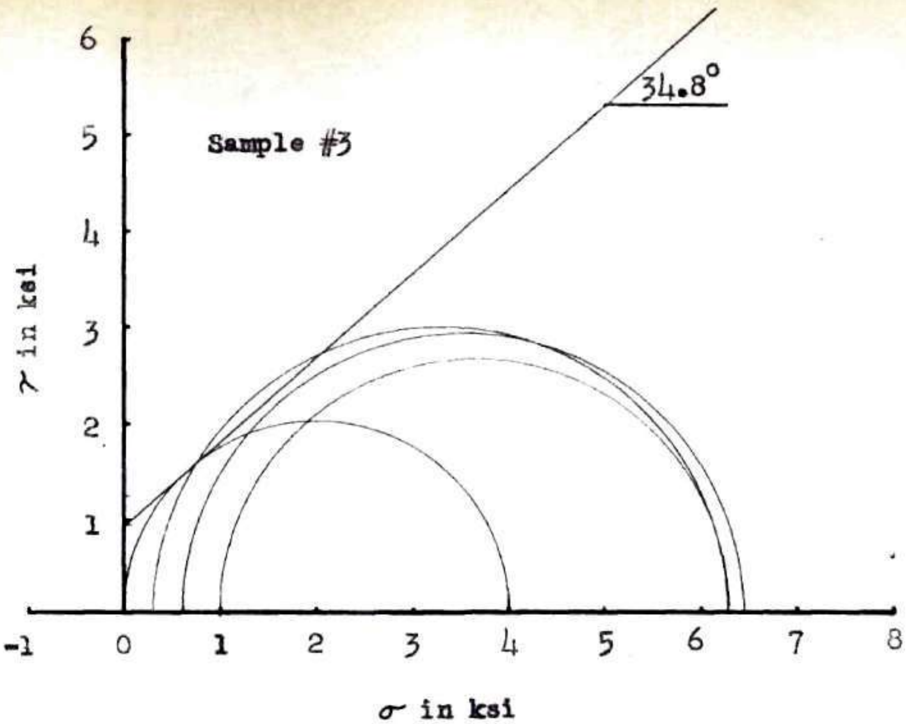

Figure 8 . Mohr's Circles for Indiana Limestone

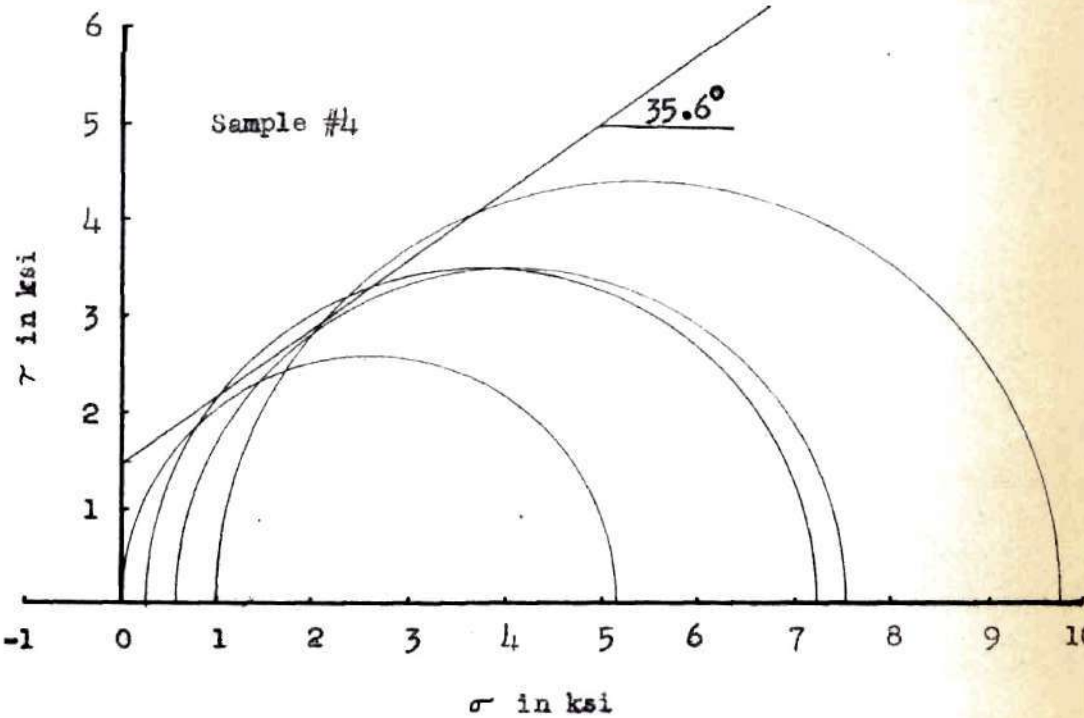

Figure 9 . Mohr's Circles for Indiana Limestone

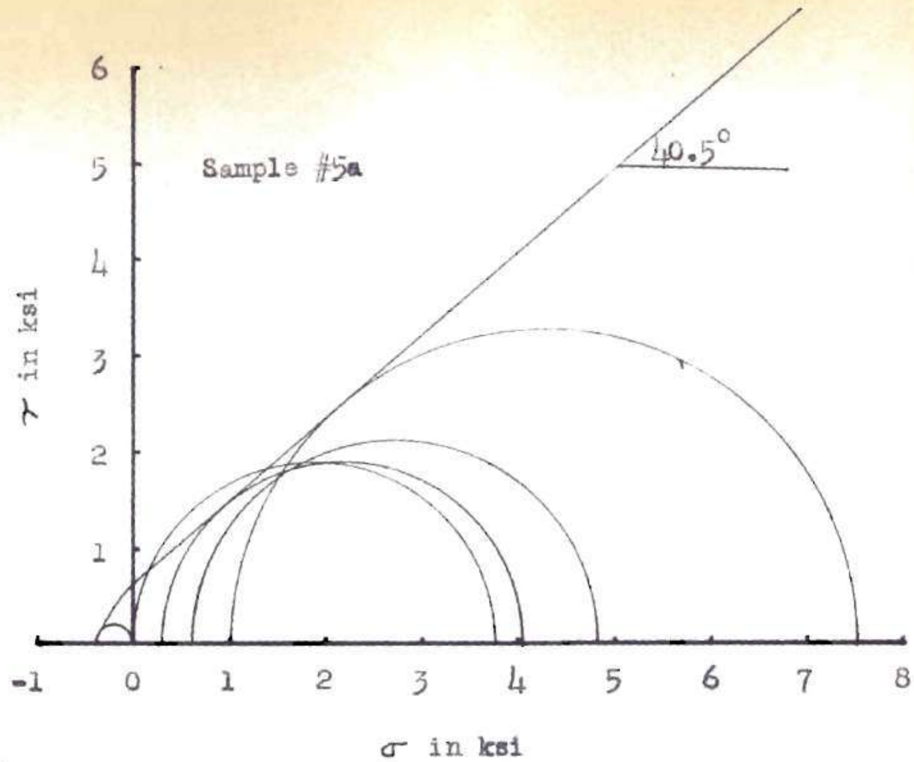

Figure 10 . Mohr's Circles for Indiana Limestone

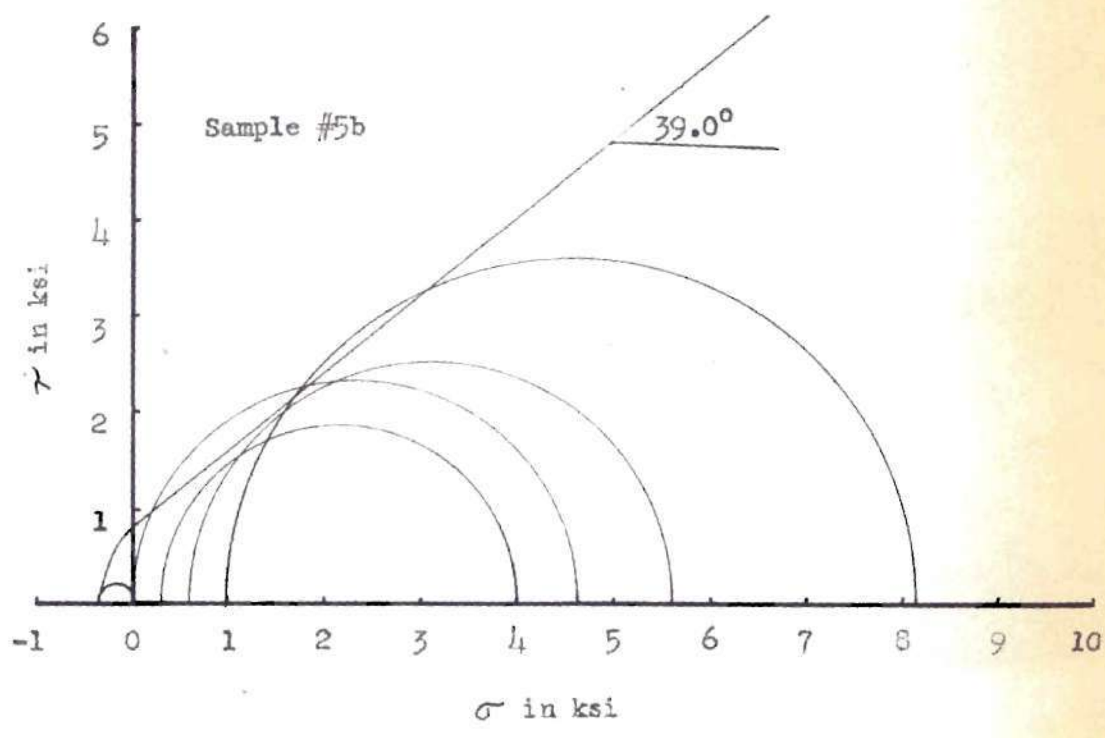

Figure 11 . Mohr's Circles for Indiana Limestone

It is of interest to note that for a set of samples taken from a single block of stone four inches square and 12 inches long, the maximum variations in q_u and p_t between mean values for the set and a single test result are 22 per cent and 3.7 per cent respectively. Considering two sets of samples taken from a block, one set taken with the longitudinal axes perpendicular to the longitudinal axes of the other set, the mean values of q_u for the two sets varied by 9.3 per cent from the average of the two means. Tensile strength variation for this condition was only 1.3 per cent. These variations are cited in order to emphasize that variations in bearing capacity test results can be expected to vary considerably.

Schwartz (13) found values of c and φ for Indiana Limestone of 1,100 psi and 46° respectively, and Robertson (14) found values of these parameters as 1,800 psi and 28° respectively. Anderegg (15) states that the unconfined compression strength of Indiana Limestone may range from 6000 psi to 7000 psi. Schwartz (13) found a tensile strength of 400 psi for Indiana Limestone.

The variations in these parameters between rock used in this project and rock tested by Schwartz, Robertson and Auderegg is due to the fact that the rock used in this project was much weaker than that tested by the other investigators.

Equipment

Sample Preparation Equipment

The individual limestone blocks were cut from pieces of Indiana Limestone four inches square and 12 inches long with a water cooled masonry saw. The saw blade had small diamond chips embedded in the teeth to facilitate cutting the stone. The samples used in the various strength tests were cored from the same size pieces of limestone as were the individual blocks. A diamond bit, water cooled core drill having an inside diameter of 0.875 inch was used to cut these samples. The core drill was powered by a drill press. A belt sander was utilized to grind the faces of the individual blocks and the ends of the cylindrical samples in order to eliminate irregularities.

<u>Strength Test Equipment</u>

Quick triaxial tests were conducted with a Tinius Olsen hydraulically driven, multiple range testing machine having a maximum capacity of 120,000 pounds. A special high pressure triaxial cell constructed at the Georgia Institute of Technology was employed to conduct these tests. The cell was capable of withstanding confining pressures of 10,000 psi, a maximum axial load of 50,000 pounds, or a maximum deviator stress of 73,000 psi. The loading piston and base were constructed with spherically concave upper and lower ends respectively. Loading caps having one spherically convex end and one flat end were placed between the sample and both the piston and the base with the flat ends in contact with the sample. This arrangement allowed for correcting any misalignment due to non-uniformities in the samples. Vinyl membranes were secured to the base and both the top and bottom loading caps with rubber "O" rings. The piston, loading caps, sample and base were all 0.875 inches in diameter (13).

Confining pressures were applied in the quick triaxial tests with a portable hydraulic pressure accumulator, also constructed at the Georgia

Institute of Technology. The accumulator was capable of producing a maximum pressure of 10,000 psi. Pressure was applied with a hand operated hydraulic pump and regulated during testing with a screw operated piston which operated in a pressure cylinder connected to the hydraulic pump pressure line. Pressures were measured with a gauge capable of withstanding a gauge pressure of 10,000 psi (13).

Unconfined compression tests were conducted with a Tinius-Olsen mechanically driven, constant strain, multiple range testing machine having a maximum capacity of 20,000 pounds. Deformations were recorded on a dial gauge calibrated in 0.001 inch units.

Direct tension tests developed by Schwartz (13) were conducted with the Tinius Olsen testing machine used in conducting the quick triaxial tests. Each end of the cylindrical sample was fastened with an epoxy resin cement into the cylindrically recessed end of an aluminum chuck. The other end of the aluminum chuck was threaded and was screwed into the tensile testing attachment of the machine loading head.

Model Footing Test Equipment

Two multiple range, mechanically driven, constant strain testing machines were employed in conducting the model footing tests on the thin layered, jointed rock system. One was the Tinius-Olsen machine used in conducting the unconfined compression tests on the cylindrical samples. The other was a Riehle machine with a maximum capacity of 450,000 pounds. Deformations of the loaded blocks were measured with a micrometer dial gauge calibrated in 0.0001 inch units.

A specially constructed, rigid aluminum retaining box enclosed on four sides and the bottom was used to retain the system. The sides of the box were made from six inches x 0.25 inch aluminum flat stock, and were fitted with two pieces of one inch x 0.25 inch aluminum angle which acted as stiffeners. The bottom of the box was 13.625 inches square and 0.25 inch thick. It was attached to two adjacent sides of the box with one 0.125 inch brass screw per side. Each of the other two sides of the retaining box had one SR4 strain gauge mounted on it, and had previously been loaded as a simple beam. The response to load of the SR4 strain gauge attached to the side was then calibrated. Metal shims were placed between the rock system and the sides bearing strain gauges to insure transmission of any lateral load that developed during testing to the sides of the box. A simple switch box and a Baldwin-Lima-Hamilton Type N Strain Recorder were also employed in monitoring the footing load vs. lateral load relationship during testing. Figure 12 illustrates the arrangement of the system, retaining box, switch box, and recording device during testing.

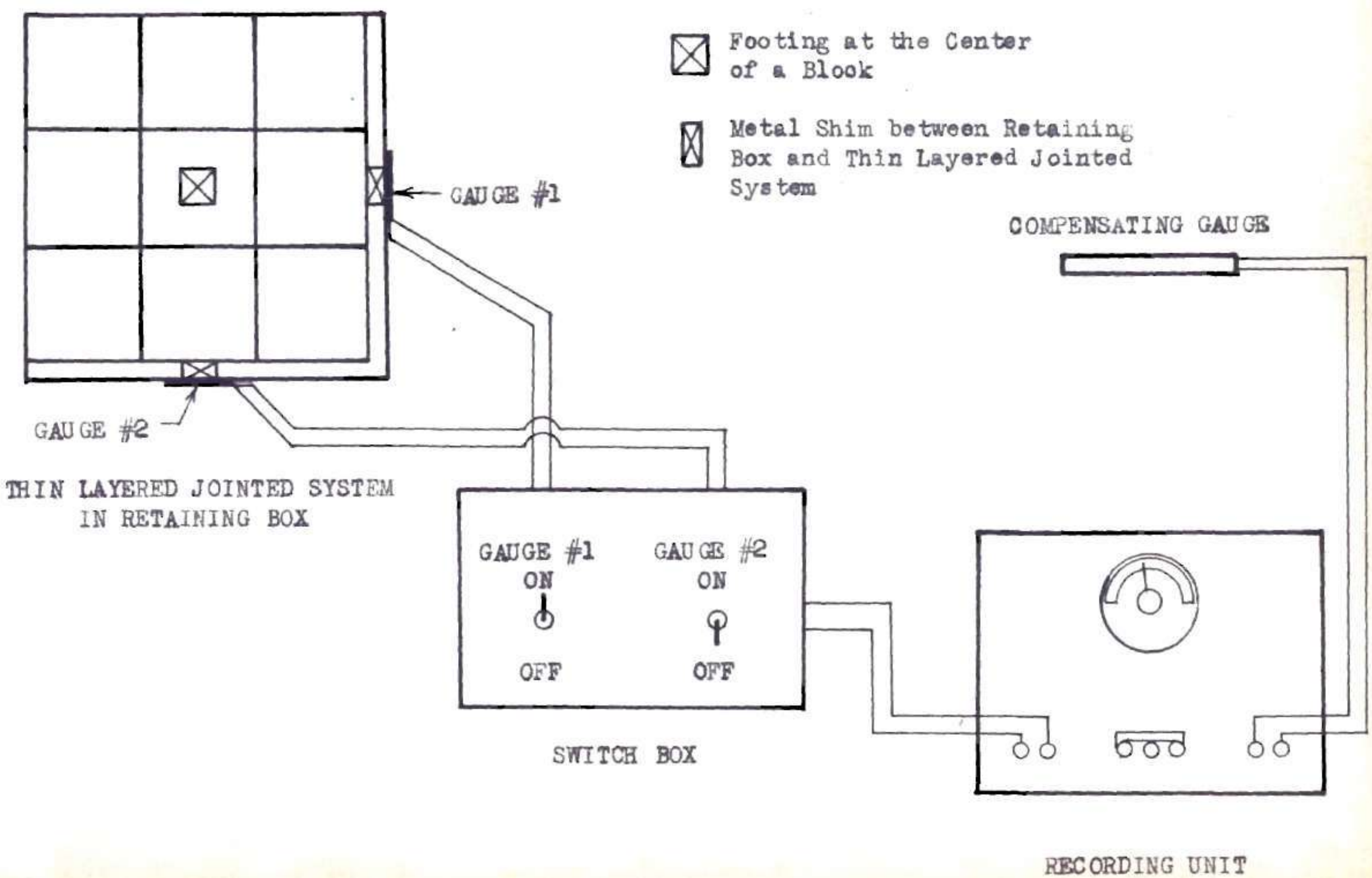

Figure 12. Schematic Diagram of System Used to Monitor Lateral Load Development

CHAPTER IV

PROCEDURE

Sample Preparation

The rock samples used in the model footing tests, quick triaxial tests, extension tests and unconfined compression tests were obtained from individual pieces of Indiana Limestone four inches square and 12 inches long.

The samples used in the model footing tests were sawn with the masonry saw previously described. These blocks were 0.25 inches ±0.02 inches in thickness. After sawing, the blocks were oven dried for 24 hours at +110°C to insure a uniform moisture content of zero per cent in all samples. In order to provide as smooth a bearing surface as possible and minimize flexural deformation of the blocks both faces of the samples were ground on a belt sander. The final tolerances in the block thickness were +0.015 inches and -0.025 inches.

The cylindrical samples tested in quick triaxial, unconfined compression, and direct tension tests were cored with the core drill previously described. They were then cut into lengths of 2.5 inches and oven dried for 24 hours at 110°C to insure a uniform moisture content in all samples of zero per cent. The ends of the samples were then ground on a belt sander to provide a smooth bearing surface for the loading caps.

Testing Procedure

Quick Triaxial Tests, Unconfined Compression Tests, and Direct Tension Tests

The procedures for this series of tests have been previously outlined in the section of Chapter III entitled "Physical Properties," and will not be reiterated.

Model Footing Tests

The aluminum retaining box was assembled on the bed of the testing machine as previously described, and the SR4 strain gauge system was inspected to insure that it was functioning properly. The individual blocks were then stacked as closely as possible by hand in the retaining box as illustrated in Figure 1. Metal shims were placed between the system and the two adjacent sides of the box bearing the SR 4 strain gauges to insure transmission of any lateral load which developed during testing from the system to the sides of the retaining box. The model footing was then placed in the appropriate position for the particular test, and a three inch square aluminum section eight inches in length was centered over the footing to prevent bending of the footing and to serve as a spacer between the loading head and footing. The loading head was then brought into contact with the aluminum block, and a seating load of approximately 10 pounds was placed on the footing. At this point, the micrometer dial gauge employed to measure deformation in the loaded blocks was placed in position and adjusted to read 0.0000 inches. The reading on each strain gauge was also recorded. The footing load was applied at a rate of loading head travel (rate of deformation) of

0.01 inch per minute. Due to the rapid rotation of the micrometer dial gauge needle and the time required to record the SR 4 strain gauge readings, it was necessary to stop loading when a set of readings were being taken. The system was loaded until the footing load reached a maximum value and then declined to a magnitude of 75 per cent at most of the maximum value.

CHAPTER V

DISCUSSION OF RESULTS

Sequence of Events Occurring During Testing

During the course of each model footing test conducted on the thin layered, jointed rock system, a sequence of events occurred which was the same in nearly every test. The conditions under which the model footing tests were conducted were as follows: the thin layered, jointed rock system composed of four inch square by 0.25 inch thick Indiana Limestone blocks was stacked in a rigid aluminum retaining box and loaded with various sized model footings at various positions as illustrated in Figure 2. The rate of travel of the loading head was 0.01 inches per minute. The footing load vs. lateral load and footing load vs. settlement relationships were monitored during the model footing tests. Henceforth, these conditions will be referred to as "test conditions."

Under test conditions, the model footing load accumulated very slowly immediately following the beginning of a test, while settlement occurred at a very rapid rate. The lateral load developed during this phase of testing was usually less than 0.5 per cent of the model footing load on the blocks at the time.

As load was applied to the model footing at a constant rate of loading head travel of 0.01 inches per minute, when the magnitude of load on the footing reached approximately one per cent of the total failure load, the model footing load began to build up at a rate more rapid than in the beginning phase of testing. The pressure vs. settlement curves assumed a flatter, constant slope at this point. Figures 26 through 42 illustrate this phenomenon. This change in slope of the pressure vs. settlement curves usually occurred at a settlement ranging from 0.03 inch to 0.07 inch, with the former occurring most frequently. This represented a deformation of 0.75 per cent of the height of the system.

Under test conditions, the lateral load began to develop at different stages in each of the various model footing tests. The relationships between footing load and lateral load for a number of tests are shown in Figures 43 through 51. As these figures indicate, the relationship between the model footing load and lateral load was not constant, and there was rarely any similarity between the magnitudes of the lateral loads on the two adjacent sides of the retaining box in any one test.

As failure was approached under test conditions, the model footing load would reach a maximum value and remain there for a short period of time while settlement continued. The rate of settlement increased considerably at this point, as did the rate of accumulation of the lateral load. Then, the model footing load would usually decline to a value of approximately 75 per cent or less of the maximum load. In a few tests, it remained at the maximum value and did not decline. The occurrence of either of these two behaviors in model footing load development under test conditions and the accompanying increase in the rate of settlement were considered to signify failure of the loaded blocks, and testing was halted at that point. After failure, the blocks surrounding the loaded blocks were pushed upward in a bulging manner.

Interpretation of Events Occurring During Testing

Three phenomena occurred immediately following the beginning of loading. These include the following: the very slow, irregular buildup of the model footing load with a constant deformation rate; the steep slope of the pressure vs. settlement curves (3×10^{-4} inches per psi) as opposed to the slower rate of settlement (8.25×10^{-6} inches per psi) observed in model footing tests conducted on solid four inch cubes of linestone (the slopes of cited were observed in tests conducted with a four inch square footing at the center of the blocks.); and the absence or very small magnitude (i.e., < 0.5 per cent of the model footing load at that point) of lateral load. These are attributed to the presence of separations in horizontal planes between stacked blocks. Figures 2b through 42 showing relationships between pressure and settlement, and Figures 43 through 51 showing relationships between footing load and lateral load illustrate these phenomena.

The increase in the rate of model footing load accumulation and the decrease in the rate of settlement which occurred at a model footing load of approximately one per cent of the total failure load in the model footing tests are considered as indications that the majority of the separations occurring in a horizontal plane between the stacked blocks had been closed. The relationship between pressure and settlement in the subsequent phase of testing was usually constant, which indicated that the settlement occurring in the loaded portion of the system was analogous to the deformation of an elastic body under load. From Figure 24, the slope of the pressure vs. settlement curve for a four inch footing at the center of a solid block of limestone is 8.25×10^{-6} inches per psi. The slope of the middle straight portions of the pressure vs. settlement curves for a four inch footing at the center of a thin layered jointed system presented in Figure 24 is 2.5×10^{-5} inches per psi. The magnitude of the two slopes are quite different, but as they appear to remain constant for a certain phase of testing, the comparison is a valid one. It is possible that any remaining separations in a horizontal plane between the stacked blocks are the cause of the greater rate of settlement in the thin layered jointed system during this phase of loading.

The tendency of the lateral load to begin to develop prior to failure of the loaded blocks during the model footing tests is attributed to the Poisson effect. During this phase of testing, both the magnitude of lateral load developed and the relationship between footing load and lateral load varied among the tests. These variations are attributed to the effects of irregularities in individual blocks and stacking. As the system adjusts under model footing load to accommodate these irregularities, the lateral load fluctuates in the manner previously described.

It is probable that any separations occurring in a vertical plane prior to loading of the system would affect the magnitude of lateral load which could develop in the system. These separations would have to be closed before appreciable lateral load could be transferred to adjacent blocks. The greater the width of such separations, the less the amount of lateral load which could develop, and vice versa.

The tendency of the model footing load to remain constant after reaching a maximum value while settlement increases indicates the existence of a condition within the system analogous to the plastic yielding of a loaded body. This in turn indicates the occurrence of a shearing failure in the loaded blocks. The decrease in model footing load that followed in some tests indicated that the loaded blocks could no longer support the load which caused failure. The tendency of the model footing load to remain at the maximum value in other tests was possibly due to the confining effects of the rigid retaining box. The restraint upon the system provided by the box partially prevented the wedge of material formed under the model footing at failure from being forced downward under the imposed load, thereby causing the model footing load to remain constant.

The rapid accumulation of lateral load after failure is attributed to the forcing aside by the wedge of material formed under the model footing at failure as it is forced downward by the model footing load.

The formation of the wedge of material beneath the model footing, the rapid rate of settlement occurring after failure of the loaded blocks, and the upward bulging of the blocks adjacent to the loaded blocks are all characteristic of the general shearing failure of a soil mass as described by Sowers (1).

Bearing Capacity

General

In order to investigate the general behavior of the thin layered, jointed rock systems with respect to bearing capacity, the results of each test conducted with each footing in each of the five different test positions were plotted versus the ratio of $\frac{b}{w}$. The arithmetic mean of the bearing capacity results at each value of the $\frac{b}{w}$ ratio was computed, and by applying the mathematical principle of least squares to the arithmetic means, a hyperbolic function of the form

$$q_o = a\left(\frac{b}{w}\right)^n \tag{9}$$

where a = a coefficient in psi units

n = a negative fractional exponent

was developed as a method of representing the bearing capacity of the thin layered jointed system when loaded with model footings.

Figure 13 illustrates the results of this investigation. The hyperbolic function

$$q_o = 3500 \left(\frac{b}{w}\right)^{-0.134} \tag{10}$$

was developed as a method of representing the bearing capacity of the thin layered jointed system under model footing loads.

Figure 14 illustrates the results of Von Kolnitz's investigation (10) conducted on the thin layered jointed rock system illustrated in Figure 5. The hyperbolic function

$$q_o = 1950 \left(\frac{b}{w}\right)^{-0.68} \tag{11}$$

was developed to represent the bearing capacity of that thin layered, jointed rock system under model footing load.

While the results of both investigations indicate that bearing capacity decreases with an increase in the $\frac{b}{w}$ ratio, the two hyperbolic

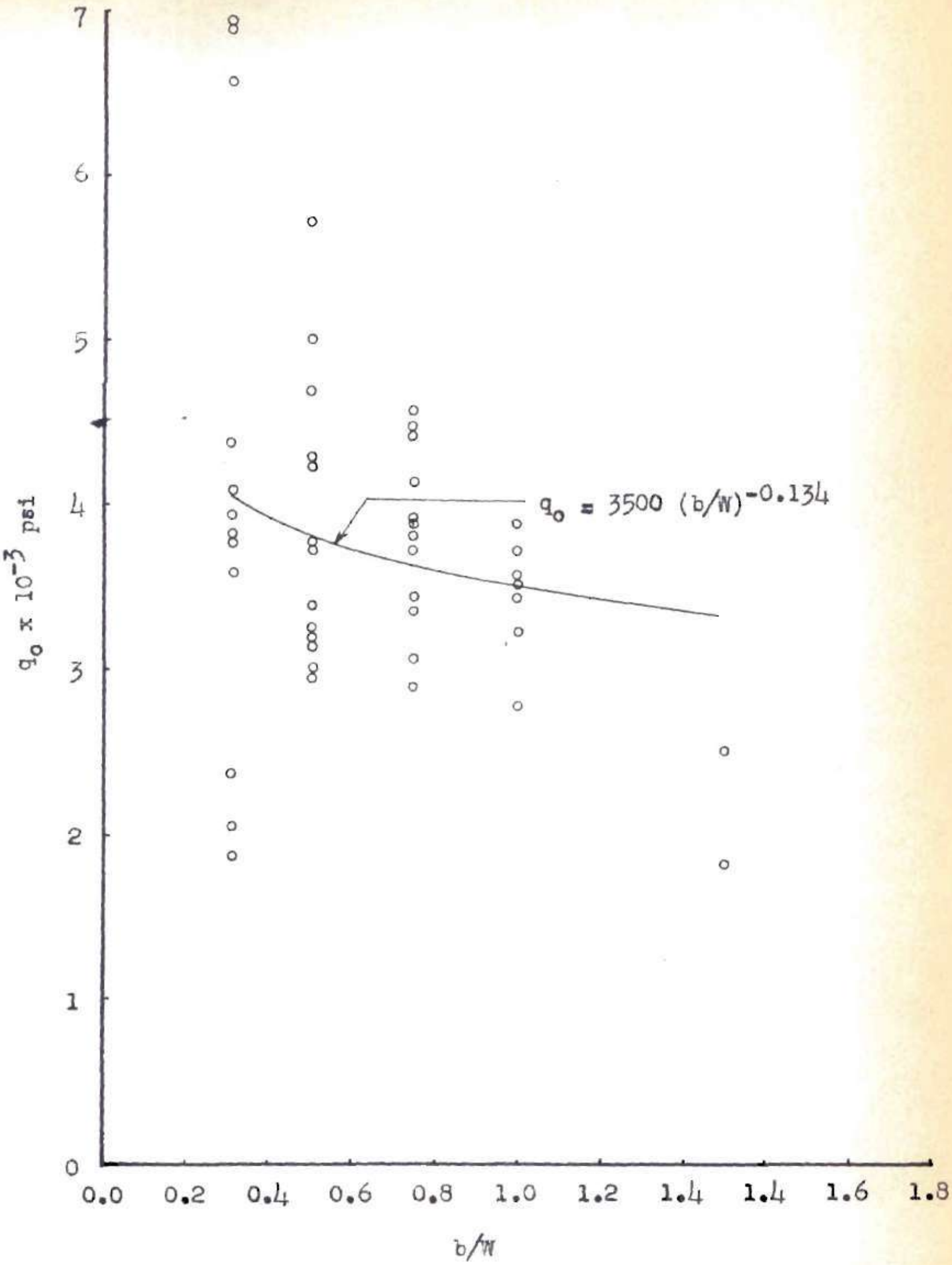

Figure 13. Unit Load (q_o) vs. b/W, Combined Results of This Investigation

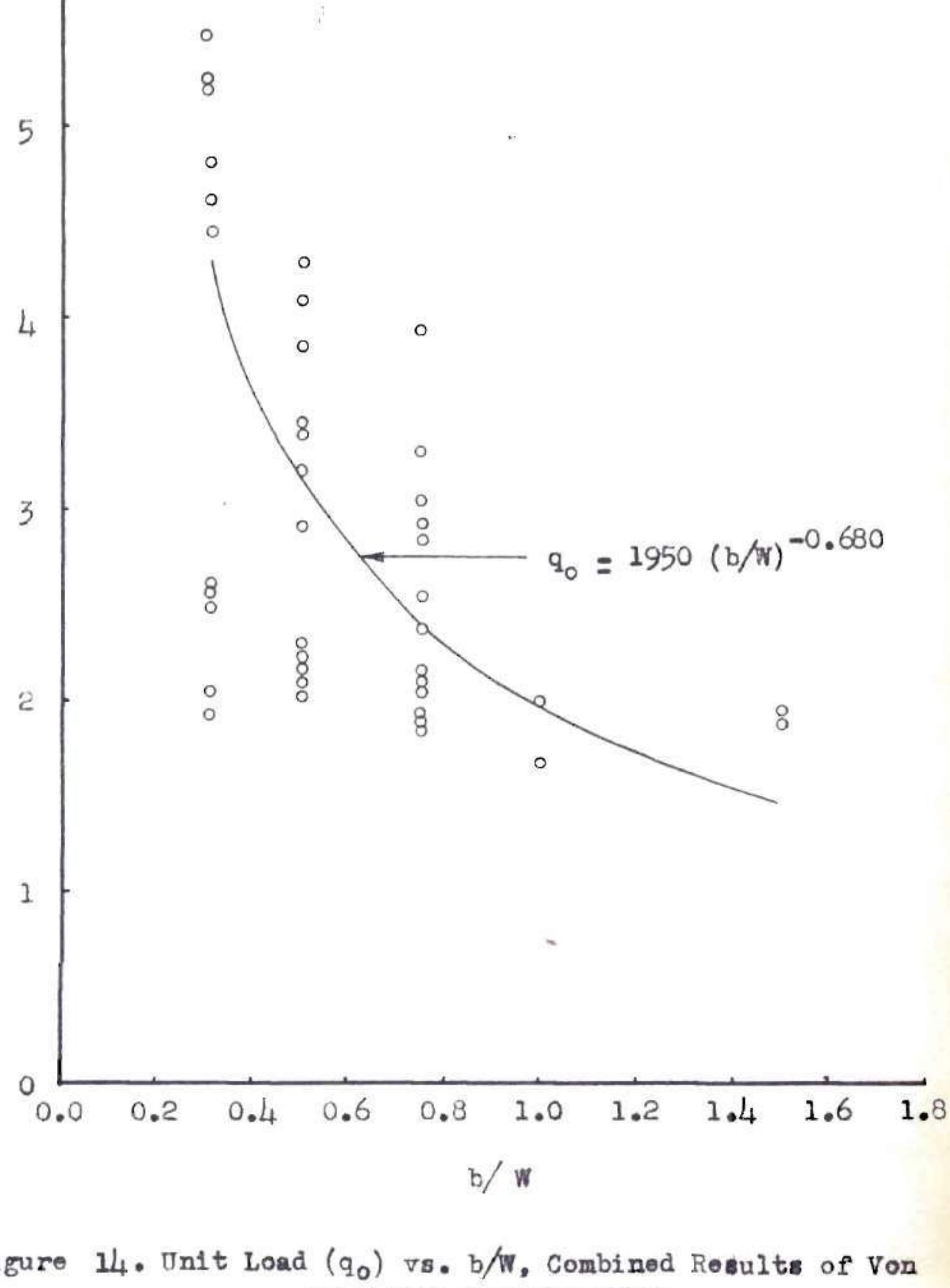

Figure 14. Unit Load (q_o) vs. b/W, Combined Results of Von Kolnitz's Investigation

functions (10) and (11) differ in the magnitudes of the coefficients a and the exponents n. No explanation of these variations was determined from the results of either investigation. However, it is believed that any or all of the following items could possibly affect these variations: cohesion, internal friction, and tensile strength of the rock samples; dimensions of the individual blocks; widths of footings; and rate of load application. It is suggested that further research be conducted to investigate the effects of these items upon the variations in the coefficient a and exponent n in the hyperbolic function (9).

The results of both Von Kolnitz's investigation (10) and this investigation were combined and are presented in Figure 15. The hyperbolic function

$$q_o = 2750 \left(\frac{b}{w}\right)^{-0.38} \tag{12}$$

was developed as a method of representing the bearing capacity for the combined results. As the two systems were dissimilar in block thickness (one inch in Von Kolnitz's system, 0.25 inches in the system tested in this project), and the rates of loading head travel (0.15 inch per minute in Von Kolnitz's investigation, 0.01 inches per minute in this investigation) were different, the power function (12) should be considered as only a qualitative representation of the bearing capacity of a thin layered, jointed rock system under model footing load. As in the cases of the individual investigations, the bearing capacity decreased hyperbolically with an increase in the ratio of $\frac{b}{w}$.

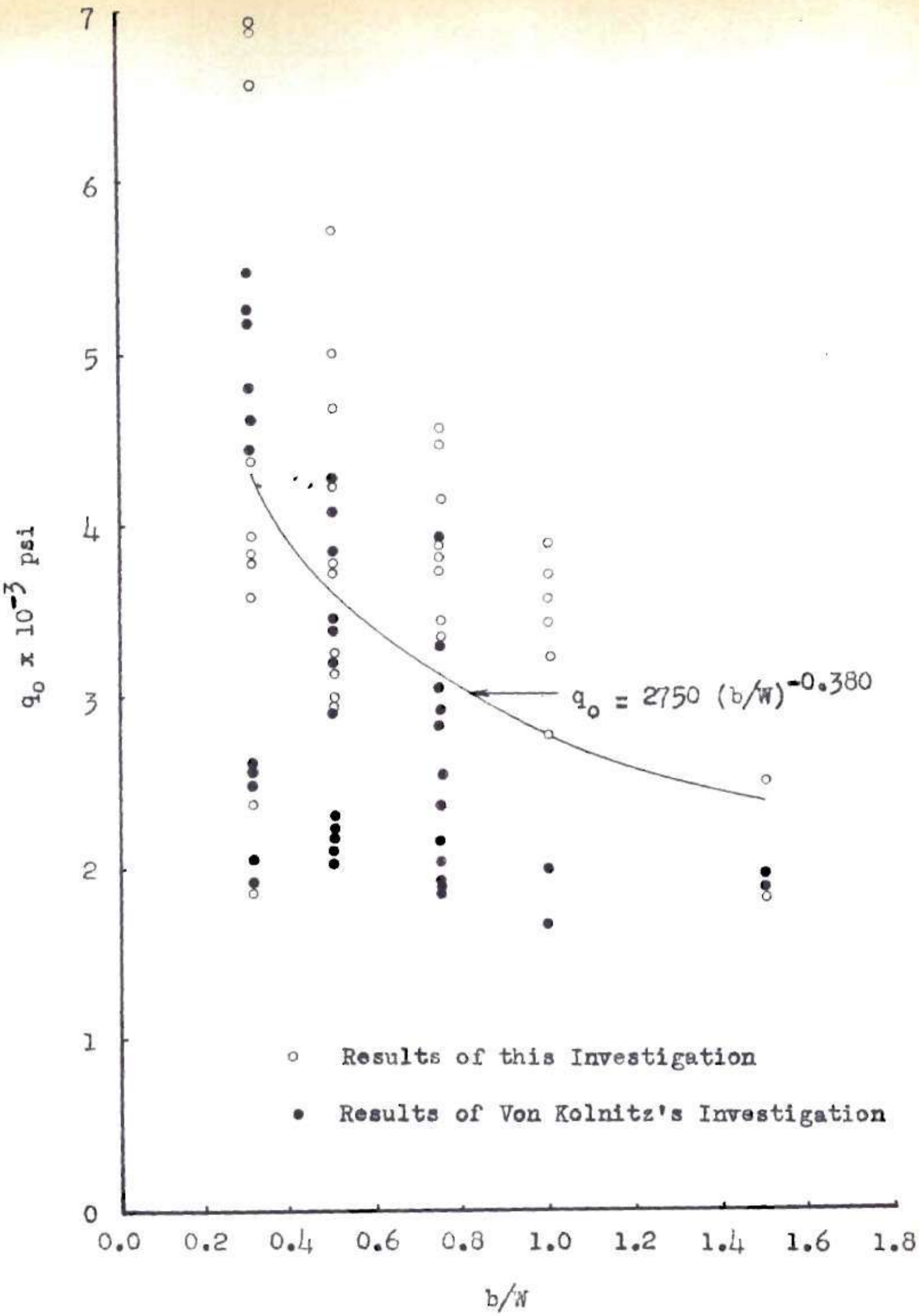

Figure 15. Unit Load (q_o) vs. b/W, Combined Results of This and Von Kolnitz's Investigations

Bearing Capacity at the Individual Test Positions

The bearing capacity of the various footings in each different test position are presented in Figures 16 through 20. The results of Von Kolnitz's investigation (10) are also presented in these figures for the purpose of comparison.

Power functions of the form

$$q_o = a(\frac{b}{w})^n$$

were developed as a means of expressing the bearing capacity of the loaded blocks with the model footings in each test position. The magnitudes of the coefficients a and exponents n varied among the different power functions, and some power functions were hyperbolic and others parabolic. In some instances, the power function for the results of this investigation was hyperbolic while that for Von Kolnitz's results (10) was parabolic, and vice versa. It is suggested that these discrepancies could be the results of extreme variations in rock strength, or that there may be insufficient data available to properly define the curves in some cases. Nevertheless, no explanation for these discrepancies were determined as a result of either investigation, and it is recommended that further research be conducted to investigate the cause or causes of these discrepancies.

Footings at the Center of a Block

The results of this series of tests are presented in Figures 16, and Table 5. As Figure 16 indicates, unit load (bearing capacity), q_o,

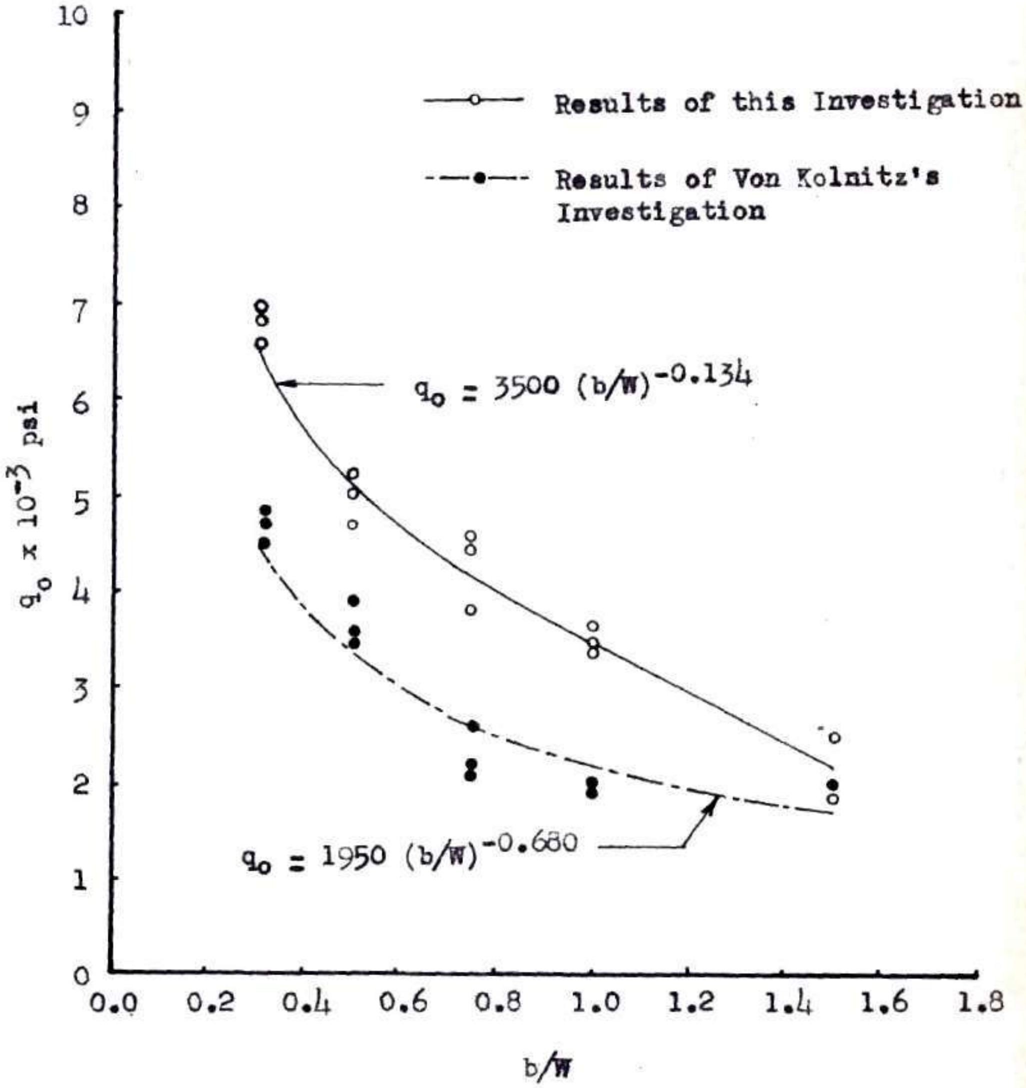

Figure 16. Unit Load (q_o) vs. b/W, Footings at the Center of a Block

decreases as the ratio of $\frac{b}{w}$ increases. The following well defined relationship was developed for representing the bearing capacity of the loaded blocks under this loading:

$$q_o = 3500 \left(\frac{b}{w}\right)^{-0.536} \tag{13}$$

The bearing capacities of most of the footings in this position were greater than with the footings in any other position on the system. For the 1.25 inch footing, it was 57 per cent greater than the next highest value; for the two inch footing, 20 per cent greater; and for the three inch footing, two per cent greater. The bearing capacity of the four inch footing was 92 per cent of the maximum value observed with that footing centered over four blocks.

Footings at the Edge of a Block

The results of this series of tests are presented in Figure 17 and Table 6. Tests were conducted with the 1.25 inch, two inch and three inch footings in this position. Results of the four inch footing at the center of a block are shown for the purpose of comparison.

Figure 17 indicates that the bearing capacity increases with an increase in the $\frac{b}{w}$ ratio. A power function

$$q_o = 4400 \left(\frac{b}{w}\right)^{0.10} \tag{14}$$

was developed to represent the bearing capacity of the loaded blocks under this loading condition. The results of the four inch footing at the center of a block do not fit the locus of points of the function (14).

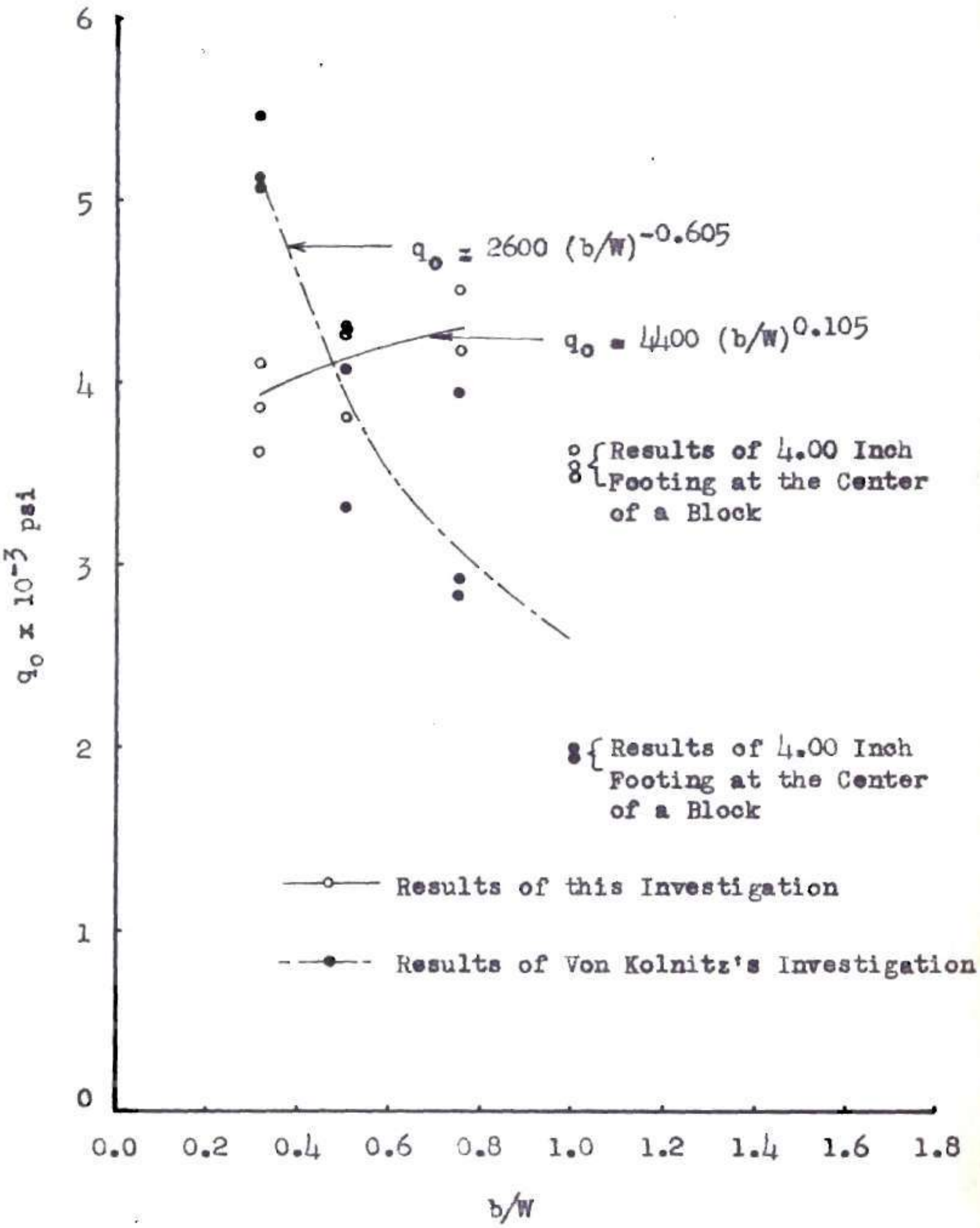

Figure 17. Unit Load (q_o) vs. b/W, Footings at the Edge of a Block

The power function (14) is parabolic instead of hyperbolic as in previous instances. It is possible that either extreme variations in rock strength or a lack of sufficient data to properly define a relationship may be the reasons for the relationship (14) being of parabolic form.

The bearing capacities of the two inch and three inch footings were greater in this position than in any other position except that of a footing at the center of a block. The bearing capacities of the two inch and three inch footings as a percentage of the maximum bearing capacity observed for each footing were 83 per cent and 98 per cent respectively. The bearing capacities of these two footings varied by less than one per cent. The bearing capacity of 1.25 inch footing was 56 per cent of the maximum value observed with that footing at the center of a block.

Footings at the Corner of a Block

Results of this series of tests are presented in Figure 18 and Table 7. The 1.25 inch, two inch, and three inch footings were used in this series of tests, and the results of the four inch footing at the center of a block are shown for the purpose of comparison.

As Figure 18 indicates, the bearing capacity increases with increasing $\frac{b}{w}$ ratios. The power function

$$q_o = 3550 \left(\frac{b}{w}\right)^{0.358} \tag{15}$$

was developed for expressing the bearing capacity of the system under this loading condition. The results of tests conducted with the four

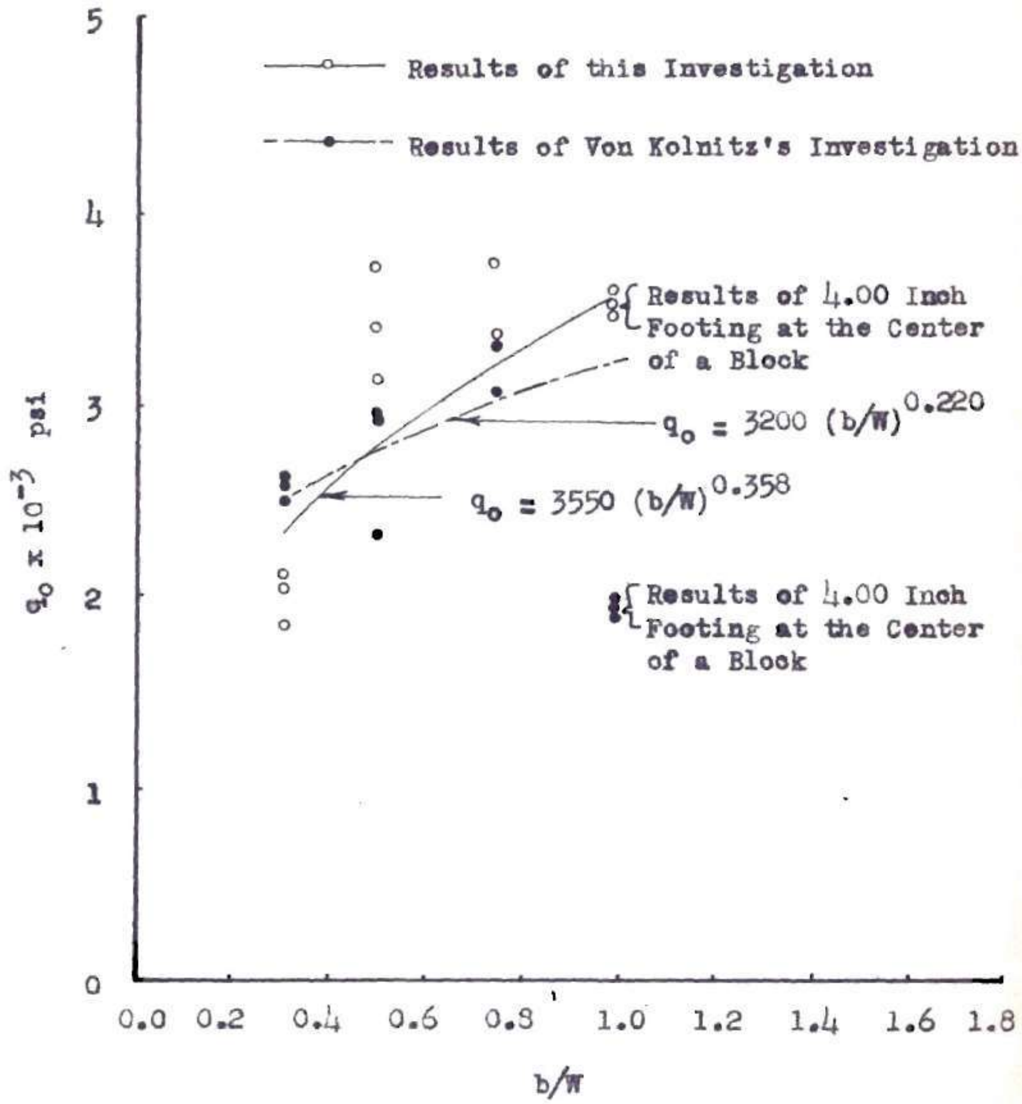

Figure 18 . Unit Load (q_o) vs. b/W, Footings at the Corner of a Block

inch footing at the center of a block fit the locus of points of the function (15) very well.

As in the tests conducted with the footings at the edge of a block, the bearing capacities of the two inch and three inch footings varied by less than one per cent. The bearing capacity of these two footings were within one per cent of the bearing capacity of a four inch footing at the center of a block. The bearing capacity of the 1.25 inch footing in any other test position, and was 31 per cent of the maximum value observed with that footing at the center of a block. The bearing capacities of the two inch and three inch footings were 69 per cent and 81 per cent respectively of the maximum values of bearing capacity observed for each footing at the center of a block.

Footings Centered over Two Blocks

The results of this series of tests are presented in Figure 19 and Table 8. As Figure 19 indicates, bearing capacity decreases with increasing ratios of $\frac{b}{w}$. The power function

$$q_o = 3050 \left(\frac{b}{w}\right)^{-0.250} \qquad (16)$$

was developed to express the bearing capacity of the blocks when loaded in this position.

The bearing capacity of the 1.25 inch footing in this case is nearly double that of the same footing when placed at the corner of a block. The bearing capacity of this footing in this position is 59 per cent of the maximum value observed with that footing at the center of a block.

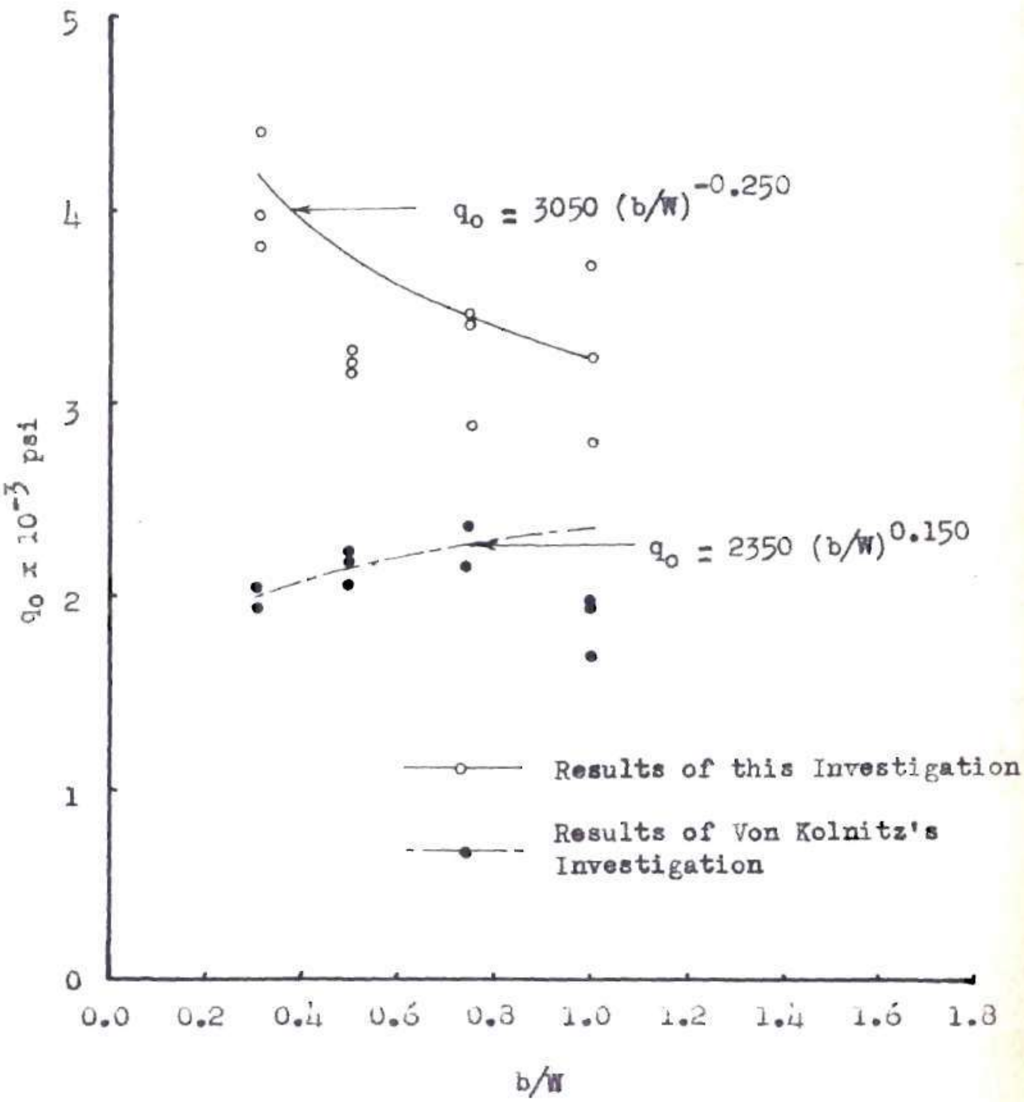

Figure 19. Unit Load (q_o) vs. b/W, Footings Centered over Two Blocks

The bearing capacities of the two inch, three inch, and four inch footings vary by only 1.25 per cent. The bearing capacity of the four inch footing varies by only eight per cent from the bearing capacity of that footing when tested at the center of a block. The bearing capacity of the four inch footing in this position is 85 per cent of maximum value observed with that footing centered over four blocks. The bearing capacities of the two inch and three inch footings are 65 per cent and 76 per cent of the respective maximum values observed for these footings when placed at the center of a block.

Footings Centered over Four Blocks

Results of this series of tests are presented in Figure 20 and Table 9. As Figure 20 indicates, the bearing capacity increases with increasing ratios of $\frac{b}{w}$. The power function

$$q_o = 3790 \left(\frac{b}{w}\right)^{0.325} \qquad (17)$$

was developed to represent the bearing capacity of the loaded blocks under this loading conditions. The bearing capacities of the two inch and three inch footings are 43 per cent and 80 per cent of the respective maximum values observed with each footing at the center of a block. The bearing capacity of the four inch footing was a maximum in this position, and it varied by only 7.5 per cent from the bearing capacity of that footing when placed at the center of a block.

Footing Tests on Solid Blocks

Four tests were conducted on solid four inch cubes of limestone

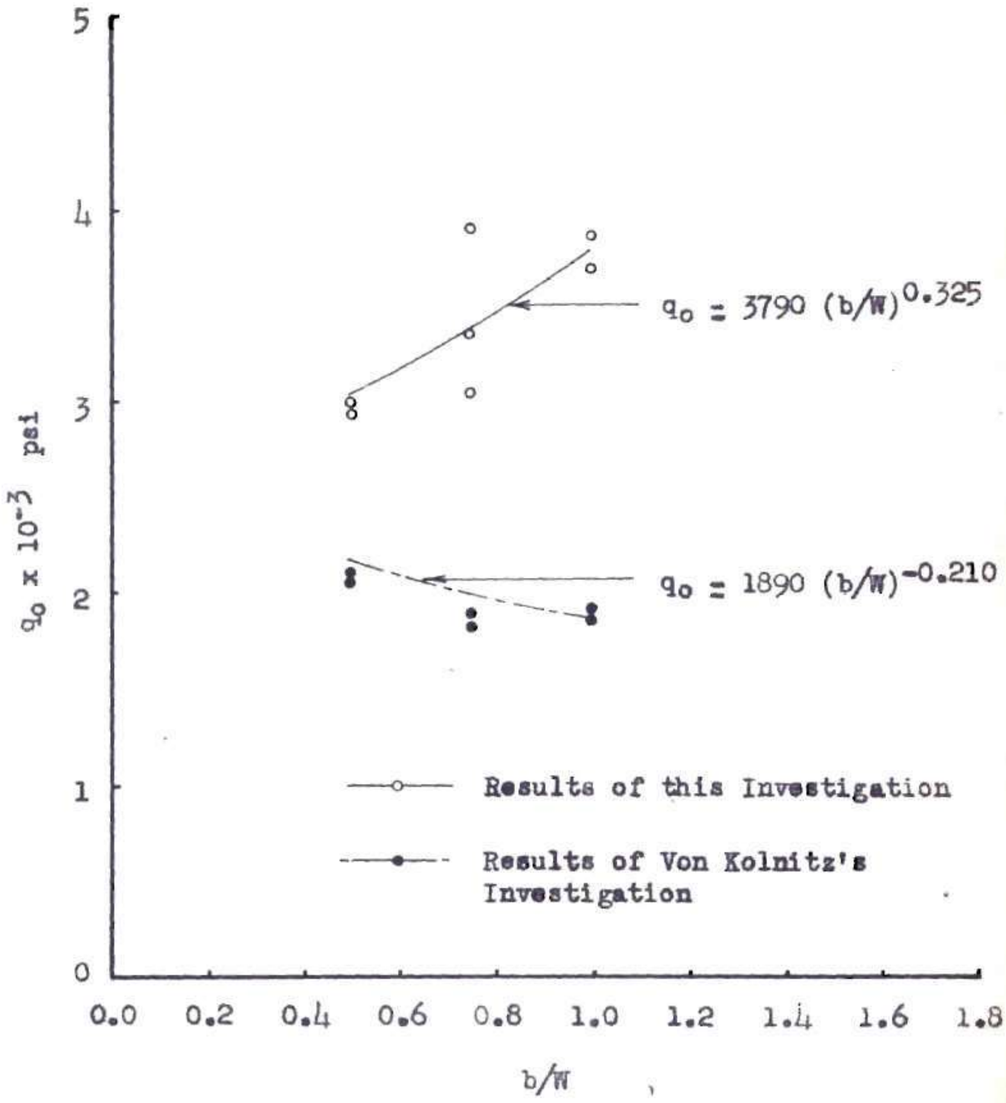

Figure 20 . Unit Load (q_o) vs. b/W, Footings Centered over Four Blocks

in order to obtain values of bearing capacity and total settlement and to obtain pressure vs. settlement relationships for comparison with these behaviors in the thin layered, jointed system. In these tests, 1.25 inch, two inch, three inch, and four inch footings were placed at the center of a block and loaded at a rate of deformation of 0.01 inches per minute until the blocks failed in a splitting manner. Figure 25 illustrates pressure vs. settlement curves for the various footings used in this set of tests. Table 2 presents values of bearing capacity and total settlement for the various footings used in these tests.

Table 2. Bearing Capacity and Total Settlement in Model Footing Tests on Solid Blocks

Footing Size (inches)	Bearing Capacity (psi)	Settlement at Failure (inches)
1.25	6400	0.0095
2.00	6625	0.0126
3.00	5940	0.0220
4.00	3750	0.0291

The type of failure which occurred in these tests was the splitting type which occurred in the thin layered jointed system. The semi-wedge angle, α, in each test was approximately 23°, which agreed well with the values of 17° to 26° observed in tests on the thin layered jointed system.

The relationships between pressure and settlement for this series of tests were constant at all times, but varied with footing size. This was not the case in tests conducted on the thin layered, jointed rock system.

Discussion of Bearing Capacity

The combined results of all model footing tests conduct in this project and by Von Kolnitz (10) suggest that the bearing capacity of a thin layered, jointed rock system under model footing load can be expressed by a power function of the form

$$q_o = a\left(\frac{b}{w}\right)^n \tag{9}$$

where a = a coefficient in psi units

n = a negative fractional exponent

The relationship established for representing the bearing capacity of the system tested in this project can be expressed as

$$q_o = 3500 \left(\frac{b}{w}\right)^{-0.134} \tag{10}$$

The bearing capacity of the system tested by Von Kolnitz (10) can be represented by the power function

$$q_o = 1950 \left(\frac{b}{w}\right)^{-0.680} \tag{11}$$

No explanation for the differences in the magnitudes of the coefficient a and exponent n between the power functions (10) and (11) were determined from the results of either investigation. However, it is believed that the two terms are affected by changes in the sample strength parameters such as cohesion, internal friction, and tensile strength; block dimensions; and rate of loading. It is suggested that further investigations be conducted to examine the effects of the above items upon the variation of the coefficients a and exponents n in the relationship (9).

From the combined results of the two investigations, the power function

$$q_o = 2750 \left(\frac{b}{w}\right)^{-0.380} \tag{12}$$

was developed to represent the bearing capacity. However, due to the differences in individual block thickness (one inch in Von Kolnitz system, 0.25 inch in the system tested in this investigation) and differences in the rate of deformation (0.15 inches per minute in Von Kolnitz's investigation, 0.01 inches per minute in this investigation) between the two investigations, it is necessary to consider the power function (12) only as a qualitative representation of the bearing capacity trend of a thin layered jointed rock system under model footing loads.

The results of the model footing tests conducted in this project at each test position were analyzed and relationships of the form

$$q_o = a\left(\frac{b}{w}\right)^n \tag{9}$$

where a = a coefficient in psi units

n = a fractional exponent

were established to represent the bearing capacity of the loaded blocks with the footings in the respective positions. The results of Von

Kolnitz's (10) investigation were treated similarly, and Figure 16 through 20 illustrate the results of both investigations and the various relations developed to represent the bearing capacity of the respective systems for the various footing positions.

In tests conducted in this investigation with the footings at the center of a block and centered over two blocks, the relationships developed were hyperbolic. In tests conducted in this investigation with the footings at the edge of a block, at the corner of a block, and centered over four blocks, the relationship was parabolic. No explanations for these discrepancies were determined from the results of this investigation. It is possible that extreme variations in the rock strength could cause these discrepancies, or, it is possible that there was insufficient data available to define properly a relationship to represent the bearing capacity as a function of the b/w ratio. It is suggested that further investigation be conducted in order to determine what factors influence these behaviors. In addition to the variations in form between the relationships established to represent the bearing capacity of the thin layered jointed system among the various model footing test positions, there were also variations among the magnitudes of the coefficients a and exponents n. It is again suggested that further investigations be conducted in order to determine what properties of the rock and/or variables in load application affect the magnitudes of the coefficients a and exponents n as no explanation for such variations were determined as a result of this investigation.

The failure pattern which occurred in the thin layered, jointed system under footing load was the splitting type described by Meyerhof (4). The same type failure occurred in model footing tests on solid four inch cubes of limestone. In this type of failure, a wedge of material forms below the footing at failure, and as the wedge is forced downward, it splits the underlying portions of the block. Figures 21, 22, and 23 illustrate the wedge formation and failure patterns in certain tests. Values of the semi-wedge angle, α, in the tests on solid blocks were approximately 23°. In tests conducted on the thin layered jointed system, values of α ranged from 17° to 26°. The similarities in the mode of failure occurring in both systems indicate that the separations occurring in a horizontal plane within the thin layered, jointed system do not affect the mode of failure.

Before any discussion of variations in the actual magnitudes of bearing capacity observed in the various model footing tests is presented, the variations in the values of unconfined compression strength, cohesion, internal friction, and tensile strength determined for limestone used in this project are re-emphasized. This information is presented in Table 1 and Figures 6 through 11. The variations in these strength parameters among the different pieces of limestone from which samples were obtained undoubtedly will cause variations in the bearing capacity of the loaded blocks. The variations in the sample strength parameters can be attributed to the following factors (among others): The variations in depth below the surface from which the limestone pieces were obtained; variations in mineralogical composition among samples obtained from various locations in a quarry; and variations in the parameters according to the plane

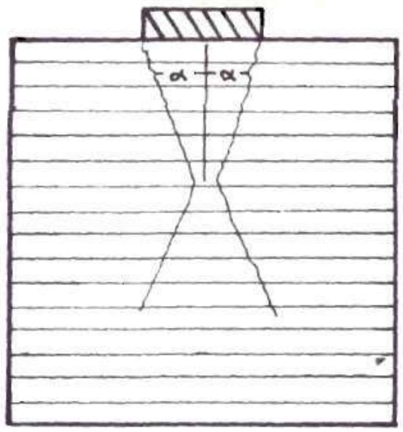

1.25 Inch Footing
$\alpha \sim 25^{\circ}$

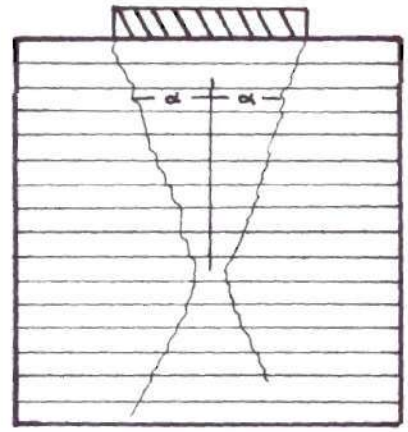

2.00 Inch Footing
$\alpha \sim 26^{\circ}$

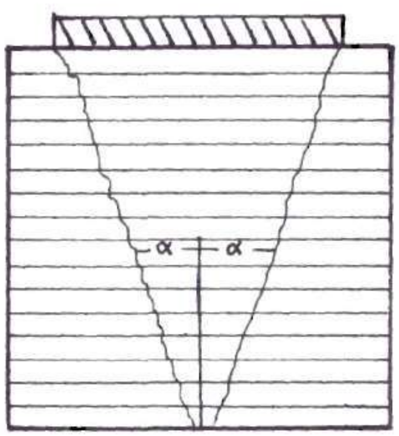

3.00 Inch Footing
$\alpha \sim 18^{\circ}$

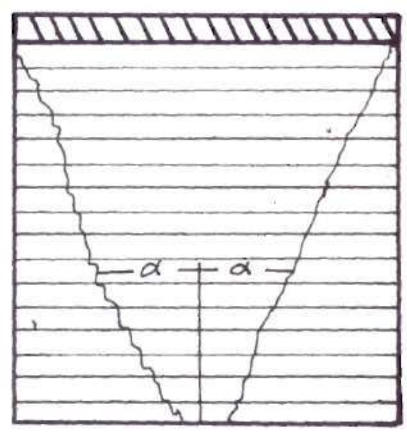

4.00 Inch Footing
$\alpha \sim 17^{\circ}$

Figure 21 . Observed Failure Patterns, Profile View Showing Wedge Angle $\sim 2\alpha$

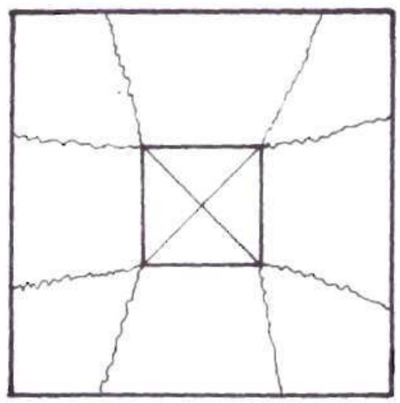

Footing at the Center of a Block

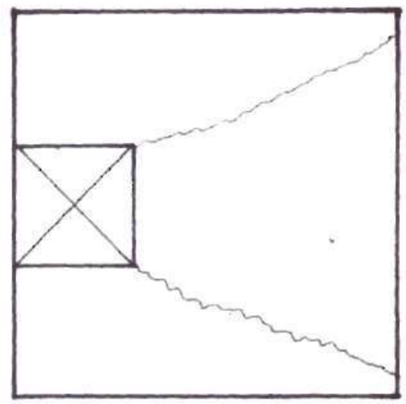

Footing at the Edge of a Block

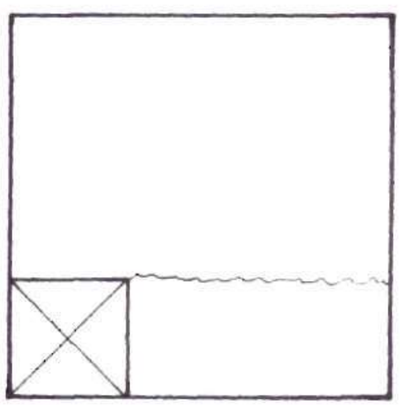

Footing at the Corner of a Block

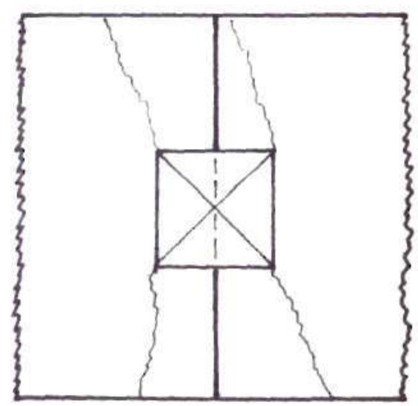

Footing Centered over Two Blocks

Figure 22 . General Failure Pattern, 1.25 Inch Footing
Plan View

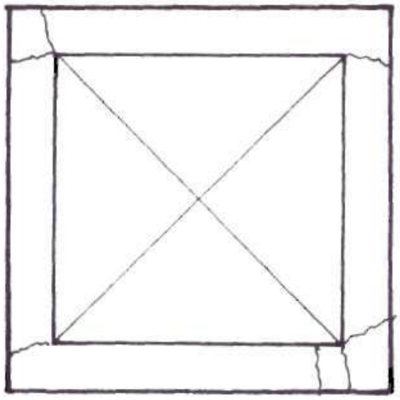

Footing at the Center of
a Block

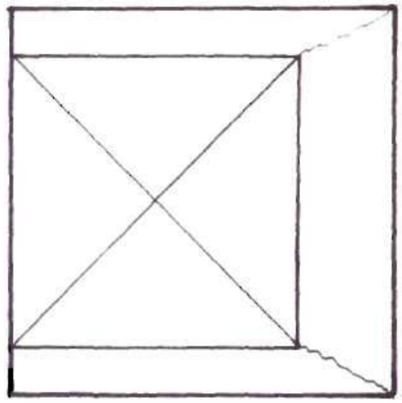

Footing at the Edge of a
Block

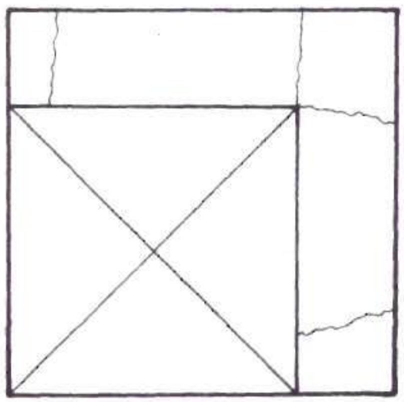

Footing at the Corner of
a Block

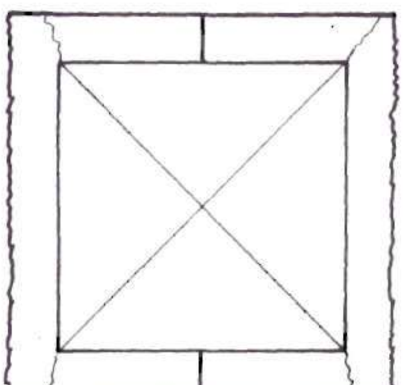

Footing Centered over Two
Blocks

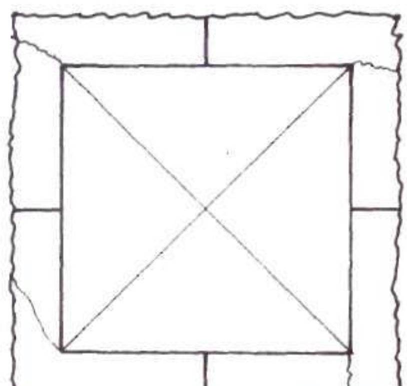

Footing Centered over Four
Blocks

Figure 23 . General Failure Pattern, 3.00 Inch Footing, Plan View

of load application. It was assumed but not proven that the plane of load application in this project was perpendicular to the original direction of deposition, the direction in which strength parameters should reach a maximum value. Thus, the strength of the samples which was mobilized was probably not a maximum value, but exceptions to this assumption could have occurred and gone undetected.

Table 3 presents values of bearing capacity obtained for each footing at the different positions on the system. The bearing capacity appears to approach a constant value of approximately 3500 psi as the $\frac{b}{w}$ ratio approaches unity. In tests conducted with the four inch footing at the center of a solid block, the bearing capacity of the four inch block is 3750 psi or 94 per cent of the unconfined compression strength of the limestone. In tests conducted with the four inch footing at the center of a block in the thin layered, jointed system, the bearing capacity of the four inch footing is 3500 psi or 88 per cent of the unconfined compression strength of the limestone. These similarities in bearing capacity suggest that as the ratio of $\frac{b}{w}$ approaches unity, the bearing capacity approaches the unconfined compression strength of the material.

Bearing capacities for footings smaller than four inches placed at the center of a block and at the edge of a block were greater than the bearing capacity of the four inch footing at the same positions. The effects of lateral confining pressure on the failure zone could be the reason for this occurrence. However, it seems that the use of weaker rock in tests conducted with footings at the center of a block would be a possible reason for the bearing capacities of the two inch and three

Table 3. Comparison of Bearing Capacity at Various Footing Positions

Footing Size (inches)	Position	Sketch	Q_{ave} (lbs.)	q_{ave} (psi)
1.25	At the Center of a Block		10,610	6810
1.25	At the Edge of a Block		5980	3830
1.25	At the Corner of a Block		3260	2090
1.25	Centered over Two Blocks	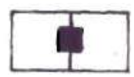	6300	4040
2.00	At the Center of a Block		19,800	4950
2.00	At the Edge of a Block		16,420	4100
2.00	At the Corner of a Block		13,630	3410
2.00	Centered over Two Blocks		12,810	3200
2.00	Centered over Four Blocks	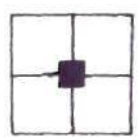	11,900	2980
3.00	At the Center of a Block		38,400	4270
3.00	At the Edge of a Block		37,500	4170
3.00	At the Corner of a Block		31,200	3470
3.00	Centered over Two Blocks		29,200	3240
3.00	Centered over Four Blocks		30,800	3420

Table 3. (continued)

Footing Size (inches)	Position	Sketch	Q_{ave} (lbs.)	q_{ave} (psi)
4.00	At the Center of a Block		56,000	3500
4.00	Centered over Two Blocks		51,700	3220
4.00	Centered over Four Blocks		60,600	3790

inch footings at the edge of a block being greater than that of the four inch footing at the center of a block.

The progressive decrease in bearing capacities of the 1.25 inch, two inch, and three inch footings as they are moved from the center of a block to the edge of a block and then to the corner of a block is attributed to the reduction in the effects of lateral confining pressure on the failure zone.

An inspection of the results of bearing capacity tests conducted with the footings centered over the blocks and centered over four blocks indicates that in general, the bearing capacity tends to approach a value of 75 per cent to 95 per cent of the unconfined compression strength of the material as the $\frac{b}{w}$ ratio approaches unity. It is believed that the results of further investigations are required to explain this trend. However, it seems highly possible that the presence of macroscopic separations occurring in a vertical plane within the center of the failure zone affects the bearing capacity of the loaded blocks under these conditions to a great degree.

The total footing load at failure Q, increased linearly with an increasing rate of $\frac{b}{w}$ for all sets of tests. This is analogous to the usual occurrence in plate load tests on soils in which total load increases with increased bearing area.

Comparison of Results with Those of Previous Investigations

As previously discussed, Meyerhof (4) has proposed the following relationship as a means of representing the bearing capacity of a strip or circular model footing of width $b(D)$ on the surface of a concrete or rock block of height H and width L (Refer to Figure 3):

$$q = \frac{(\frac{2H}{B} - \cot \alpha)^2 (\cot \alpha) p_t}{\frac{8H}{B} - \cot \alpha} + 2c(\cot \alpha) \qquad (5)$$

Von Kolnitz (10) proposed that the bearing capacity of square model footings having ratios of $\frac{b}{w} < 1.5$ on a thin layered, jointed system could be expressed by applying a modification factor, $\frac{t}{b}$, to Meyerhof's relation (5). Meyerhof's relation and Von Kolnitz's modification may be expressed in the following manner:

$$q_o = \left[\frac{(\frac{2H}{B} - \cot \alpha)^2 (\cot \alpha) p_t}{\frac{8H}{B} - \cot \alpha} + 2c(\cot \alpha) \right] (t/b) \qquad (8)$$

Using the values of c, α, and p_t listed in Table 1, the bearing capacity of the system tested in this project was predicted for the various sized footings at the center of a block using relations (5) and (8). These predicted values did not agree with the observed values of bearing capacity for the footings in this position. Since the predicted values did not match the observed values, it was concluded that the bearing capacity of the thin layered, jointed system tested in this project could not be predicted by the application of either relationship (5) or (8). The power functions of the form

$$q_o = a(\frac{b}{w})^n$$

previously discussed for predicting the bearing capacity of the thin layered, jointed system under the various loading conditions were then developed by curve fitting by the method of least squares. Table 4 presents observed values of bearing capacity for the various sized footings at the center of a block and predicted values obtained by applying the relationships (5), (8), and (13).

Table 4. Comparison of Predicted and Observed Values of Bearing Capacity for Footings at the Center of a Block

Footing Size (inches)	Meyerhof's Relation (5) (psi)	Von Kolnitz's Relation (8) (psi)	Power Function (13) (psi)	Observed Value (psi)
1.25	11,390	2,280	6,500	6,810
2.00	10,060	1,260	5,000	4,950
3.00	9,630	800	4,100	4,270
4.00	9,550	600	3,500	3,500
6.00	9,340	300	2,800	2,160

Settlement

Pressure vs. settlement curves for a number of tests conducted upon the thin layered, jointed rock system are presented in Figures 26 through 42. In the majority of tests, the initial portion of the curve was approximately straight and had a very steep slope. At a settlement which ranged from 0.03 inches to 0.07 inches (0.75 per cent to 1.75 per cent of the height of the system), the slope of the curve usually decreased, but it remained constant until failure was approached. At failure, the curve usually assumed a very steep slope. In contrast to this behavior, the pressure vs. settlement curves for model footing tests conducted on solid four inch cubes of limestone with various size footing at the center of the block maintained a constant slope from the beginning to failure, an indication of elastic deformation of the limestone. These curves are presented in Figure 25.

The initial straight portions of steep slope which occur in pressure vs. settlement curves for tests conducted on the thin layered jointed system suggest that the void spaces occurring in a horizontal plane between stacked blocks are being reduced during this phase of loading. The reduction of these void spaces is attributed to flexural deformation of the individual blocks rather than crushing of any irregularities for the following reason: grinding of the faces of the individual blocks removed all small sharp irregularities but left dome-like irregularities of areas large enough to be safe against crushing failure. In addition, all loose grains of material were brushed from the block faces before blocks were stacked.

The changes in slope of the pressure vs. settlement curves for tests conducted on the thin layered jointed system occurring at settlements ranging from 0.03 inches to 0.07 inches (0.75 per cent to 1.75 per cent of the height of the system) indicate that the void spaces occurring in a horizontal plane between stacked blocks have been reduced to a great extent. The subsequent constant slope of the curve indicates the occurrence of a type of settlement in the loaded blocks analogous to the deformation of an elastic body under load. In tests conducted with a four inch footing at the center of a block in the thin layered

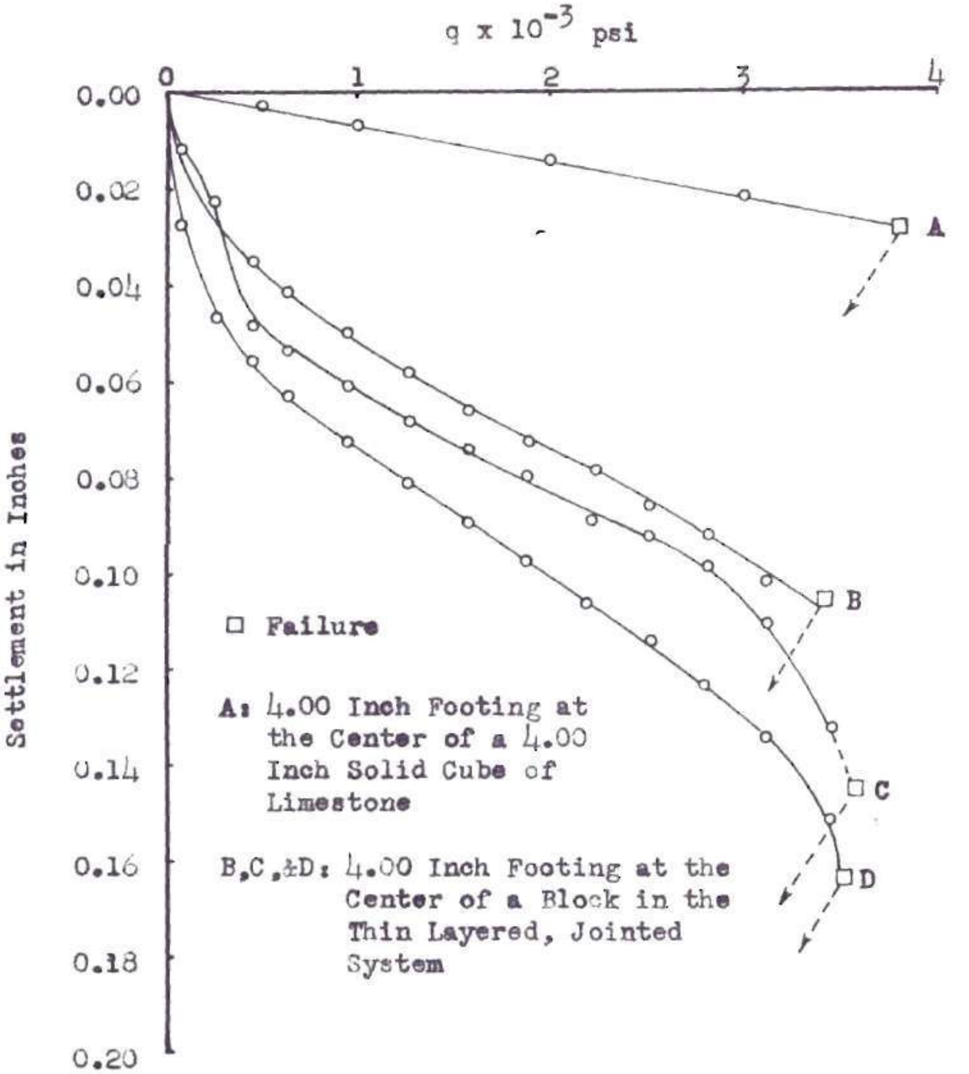

Figure 24 . Pressure (q) vs. Settlement Curves for 4.00 Inch Footings at the Center of a Block on Solid Cubes of Limestone and in the Thin Layered, Jointed System

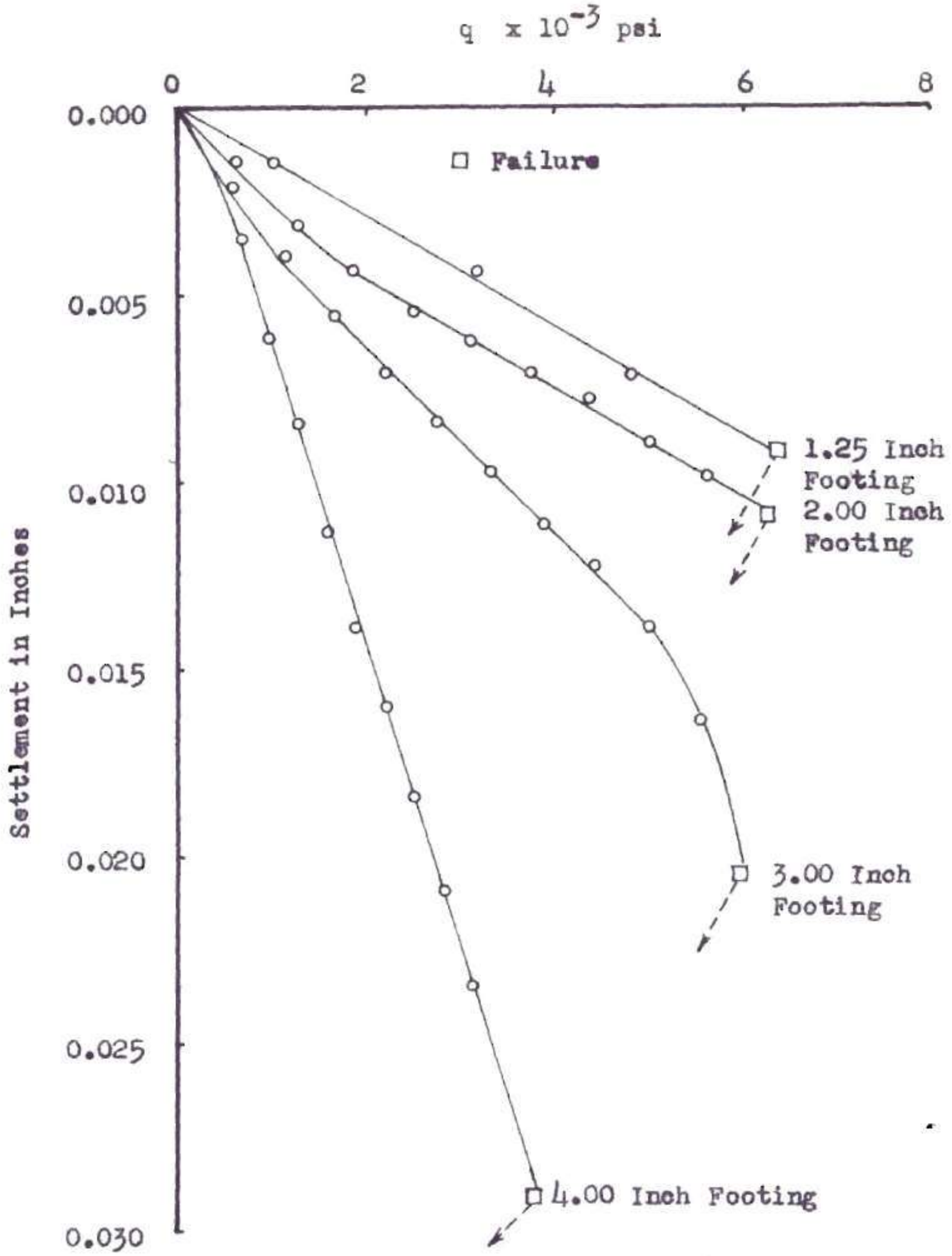

Figure 25. Pressure (q) vs. Settlement Curves for Model Footing Tests Conducted on Solid 4.00 Inch Limestone Cubes

jointed system, the slope of this portion of the pressure vs. settlement curve was approximately 2.5×10^{-5} inches per psi. The slope of the pressure vs. settlement curve for a four inch footing at the center of a solid cube of limestone was 8.25×10^{-6} inches per psi. Figure 24 illustrates these differences between pressure vs. settlement relationships in the two types of systems.

The tendency for the rate of settlement to increase rapidly at a certain maximum value of footing load indicates that the loaded blocks can no longer support the imposed load, and that failure has occurred.

In general, the total amount of settlement occurring in the thin layered, jointed system at failure increased with increasing model footing size. This suggests that the total load rather than unit load governs the amount of settlement which will occur in the system under load. Pressure vs. settlement curves for model footing tests on solid blocks support this suggestion.

It seems that the governing factor in the total amount of settlement which can occur in a thin layered, jointed system is the magnitude of the void spaces occurring in a horizontal plane between the stacked blocks prior to loading as John (2) hypothesized. In order to predict the magnitude of settlement occurring in such a system under load, it will be necessary to determine the magnitude of these void spaces. No measurements of the magnitudes of these void spaces were made in this investigation. In order to estimate the amount of settlement occurring in the system during the quasi-elastic phase of deformation, it is suggested that model tests be conducted, and the pressure vs. settlement relationship during this phase be analyzed to obtain data which can be used to estimate the magnitude of settlement occurring during this phase of deformation. The reason for this suggestion is that the pressure vs. settlement relationships are not the same in the case of model footing tests on the solid cubes of limestone and on the thin layered, jointed system during the quasi-elastic phase of deformation. Therefore, the use of data obtained from model footing tests on solid cubes of limestone in estimating settlement occurring during the quasi-elastic phase of deformation in the thin layered jointed system would produce erroneous results.

Due to the limited time available for testing in this project, the settlements occurring in the thin layered, jointed system resulting from the effects of creep and rock consolidation were not considered. However, under actual field conditions, these two phenomena would possibly have a considerable effect upon the amount of settlement occurring in a prototype system under footing load. It is suggested that further research be conducted to study the effects of creep and consolidation upon the settlement occurring in a loaded thin layered jointed system.

For identical size footings at the center of a block, the total settlement in the thin layered jointed system was usually four to five times the magnitude of the settlement which occurred in the solid cube tests.

Lateral Load Development

Figures 43 through 51 illustrate Footing load vs. Lateral load relationships for a number of tests.

The system employed in monitoring the lateral loads developed during testing is described in the section of Chapter III entitled "Model Footing Test Equipment" and is illustrated in Figure 12. The lateral loads on two adjacent sides of the aluminum retaining box were monitored during testing. An inspection of Figures 43 through 51 will verify that there was not always a similarity between these two loads, either in magnitudes or the manner in which they increased with increasing model footing load. In some cases, one SR 4 strain gauge would show no appreciable amount of lateral load at failure, while the other gauge might register as much as 375 pounds or three per cent of the footing load at that time.

The development of lateral load in the system prior to failure is attributed to Poisson's effect and the adjustment of the system under load to accommodate irregularities in individual blocks and the resulting irregularities in stacking. The fluctuations in magnitude and rate of development of lateral load in this phase of testing are attributed to the effects of irregularities and local failure occurring in individual blocks. The consequential adjustments of the system to accommodate these irregularities and local failures cause fluctuations in the magnitude and rate of buildup of lateral loads.

It seems that the magnitude of void spaces occurring in a vertical plane between adjacent blocks will affect the magnitude of lateral load that can develop in a jointed system. If displacements occurring within such a system can be accommodated by reduction of the separations, then relatively little or no lateral load will develop. However, if the magnitudes of these separations are small and the system is confined, then any lateral displacements occurring in the system will first eliminate the separations and then begin to cause lateral load to accumulate.

The lateral load developed in the system due to Poisson's effect in such a system would be difficult to evaluate due to the separations occurring in vertical planes within the system. As limestone is not an isotropic material, values of Poisson's ratio would vary with the orientation of the sample with respect to the original bedding plane, thereby introducing further variation into the lateral load developing in the system due to this effect. It is suggested that further investigations be undertaken to determine the Poisson's effect upon the development of lateral load in a jointed system.

The increase in the rate of lateral load development after failure of the loaded blocks is attributed to the forcing aside of adjacent blocks by the wedge of material formed under the footing as it is forced downward by the footing load.

The significance of lateral load development in such a model or prototype system under a footing load is that should one footing in a foundation fail under its imposed loading, the lateral loads produced at that footing could cause failure of a nearby adjacent footing. A chain reaction failure of the entire foundation system could then occur, and failure of the superstructure would follow. The most effective method of preventing such an occurrence is to insure that the factor of safety of the foundation with respect to bearing capacity is substantial.

CHAPTER VI

CONCLUSIONS

The purposes of this project were to investigate the following behaviors of thin layered, jointed rock system when loaded with square model footings: bearing capacity, footing load vs. settlement and footing load vs. lateral load.

As a result of the tests conducted in the laboratory, the following conclusions have been reached:

1. The bearing capacity failure occurring in the loaded blocks is always the splitting type described by Meyerhof (4).

2. The bearing capacity of the loaded blocks can be represented by a power function of the form

$$q_o = a\left(\frac{b}{w}\right)^n$$

in which the coefficient a is in psi units and n is a negative fractional exponent.

3. The magnitudes of the coefficient a and the exponent n vary according to the position of the footing on the loaded blocks.

4. The total amount of settlement occurring in such a system prior to failure can be attributed to the following: an initial component due to the reduction of void spaces occurring in a horizontal plane between loaded blocks, and a subsequent quasi-elastic component resulting from deformation of the individual blocks under load.

5. In order to predict the amount of settlement which could result in such a system under a load, it will be necessary to determine the amount of void spaces present in the system prior to loading, and to determine the behavior of the quasi-elastic deformation of the system.

6. The lateral load developing in such a system under a footing load is probably dependent upon the Poisson's ratio of the rock, the irregularities in individual blocks and stacking, and the magnitude of void spaces occurring in a vertical plane within the system prior to loading.

7. The lateral load developing in such a system prior to failure is not of sufficient magnitude to be a factor in foundation failure.

8. Lateral load developing after failure of the loaded blocks is due to the forcing aside of adjacent blocks by the wedge of material formed underneath the footing as it is forced downward.

CHAPTER VII

RECOMMENDATIONS FOR FURTHER STUDY

After the testing conducted in this project was completed and the results analyzed, a number of questions regarding the bearing capacity, load vs. settlement relationships, and lateral load vs. footing load relationships, and lateral load vs. footing load relationship of a thin layered, jointed rock system still existed. It is suggested that the investigation of the following items might provide information useful in answering those questions:

1. Investigate the effects of using rock samples having various amounts of cohesion, internal friction, and tensile strength upon the coefficient a and exponent n in the power function

$$q_o = a\left(\frac{b}{w}\right)^n \tag{9}$$

2. Investigate the effects of variations in individual block thickness, width and breadth upon the coefficient a and exponent n in the power function (9).

3. Study the effects of using rock samples having varying values of Poisson's ratio on the amount of lateral load developed prior to failure.

4. Study the settlement occurring in such a system under footing loads, and endeavor to develop a method of estimating the magnitude of void spaces occurring in the horizontal plane between stacked blocks so

as to facilitate estimating the amount of settlement under a footing load due to such void spaces.

5. Investigate the settlement occurring in the quasi-elastic phase of deformation to determine if any relationship can be established between it and the deformation of a solid block under a footing load.

6. Investigate the bearing capacity, settlement, and lateral load development in a thin layered, jointed system in which successive layers of blocks are overlapped to determine if these behaviors are similar to those occurring in a system in which the blocks are not overlapped.

APPENDIX

Table 5. Results of Tests Conducted with Footings at the Center of a Block

Footing Size (inches)	b/W	Q_1 (lbs)	Q_2 (lbs)	Q_3 (lbs)	q_1 (psi)	q_2 (psi)	q_3 (psi)	Q_{ave} (lbs)	q_{ave} (psi)	Failure Settlement (inches) 1	2	3
1.25	.313	10,740	10,820	10,280	6880	6940	6560	10,610	6810			
2.00	.500	18,700	20,000	20,700	4670	5000	5710	19,800	4950			
3.00	.750	34,200	40,000	41,000	3800	4450	4560	38,400	4270		.0846	.0820
4.00	1.000	56,000	57,100	54,800	3500	3560	3420	56,000	3500	.1650	.1338	.1065
6.00	1.500	89,500	65,000		2500	1810		77,250	2160	.1773	.2340	

Table 6. Results of Tests Conducted with Footings at the Edge of a Block

Footing Size (inches)	b/W	Q_1 (lbs)	Q_2 (lbs)	Q_3 (lbs)	q_1 (psi)	q_2 (psi)	q_3 (psi)	Q_{ave} (lbs)	q_{ave} (psi)	Failure Settlement (inches)		
										1	2	3
1.25	.313	6360	5600	5960	4080	3590	3820	5980	3830	.0724		.0760
2.00	.500	16,900	15,090	17,180	4240	3770	4290	16,420	4105	.0953	.0820	.0945
3.00	.750	35,000	40,200	37,300	3890	4460	4140	37,500	4170	.0848	.0298	.0438

Table 7. Results of Tests Conducted with Footings at the Corner of a Block

Footing Size (inches)	b/W	Q_1 (lbs)	Q_2 (lbs)	Q_3 (lbs)	q_1 (psi)	q_2 (psi)	q_3 (psi)	Q_{ave} (lbs)	q_{ave} (psi)	Failure Settlement (inches) 1	2	3
1.25	.313	2900	3700	3200	1860	2370	2050	3260	2090	.0330	.0560	.0430
2.00	.500	13,500	12,500	14,900	3380	3130	3730	13,630	3410	.0623	.0420	.1181
3.00	.750	30,000	30,000	33,600	3340	3340	3730	31,200	3470	.0795	.0520	.0542

Table 8. Results of Tests Conducted with Footings Centered over Two Blocks

Footing Size (inches)	b/W	Q_1 (lbs)	Q_2 (lbs)	Q_3 (lbs)	q_1 (psi)	q_2 (psi)	q_3 (psi)	Q_{ave} (lbs)	q_{ave} (psi)	Failure Settlement (inches) 1	2	3
1.25	.313	6850	5900	6150	4390	3780	3940	6300	4040	.0950	.0933	
2.00	.500	13,000	12,800	12,700	3250	3200	3180	12,810	3200	.0291	.0864	.0956
3.00	.750	25,800	31,000	30,700	2870	3440	3410	29,200	3240	.0958		.0732
4.00	1.000	59,200	44,400	51,400	3700	2770	3210	51,700	3220	.1230	.0880	.1200

Table 9. Results of Tests Conducted with Footings Centered over Four Blocks

Footing Size (inches)	b/W	Q_1 (lbs)	Q_2 (lbs)	Q_3 (lbs)	q_1 (psi)	q_2 (psi)	q_3 (psi)	Q_{ave} (lbs)	q_{ave} (psi)	Failure Settlement (inches) 1	2	3
2.00	.500	11,800	12,000		2950	3000		11,900	2980	.0632	.1090	
3.00	.750	30,000	35,000	27,400	3340	3900	3050	30,800	3420	.1200	.1650	.1212
4.00	1.000	59,200	62,000		3700	3880		60,600	3790	.0935	.1130	

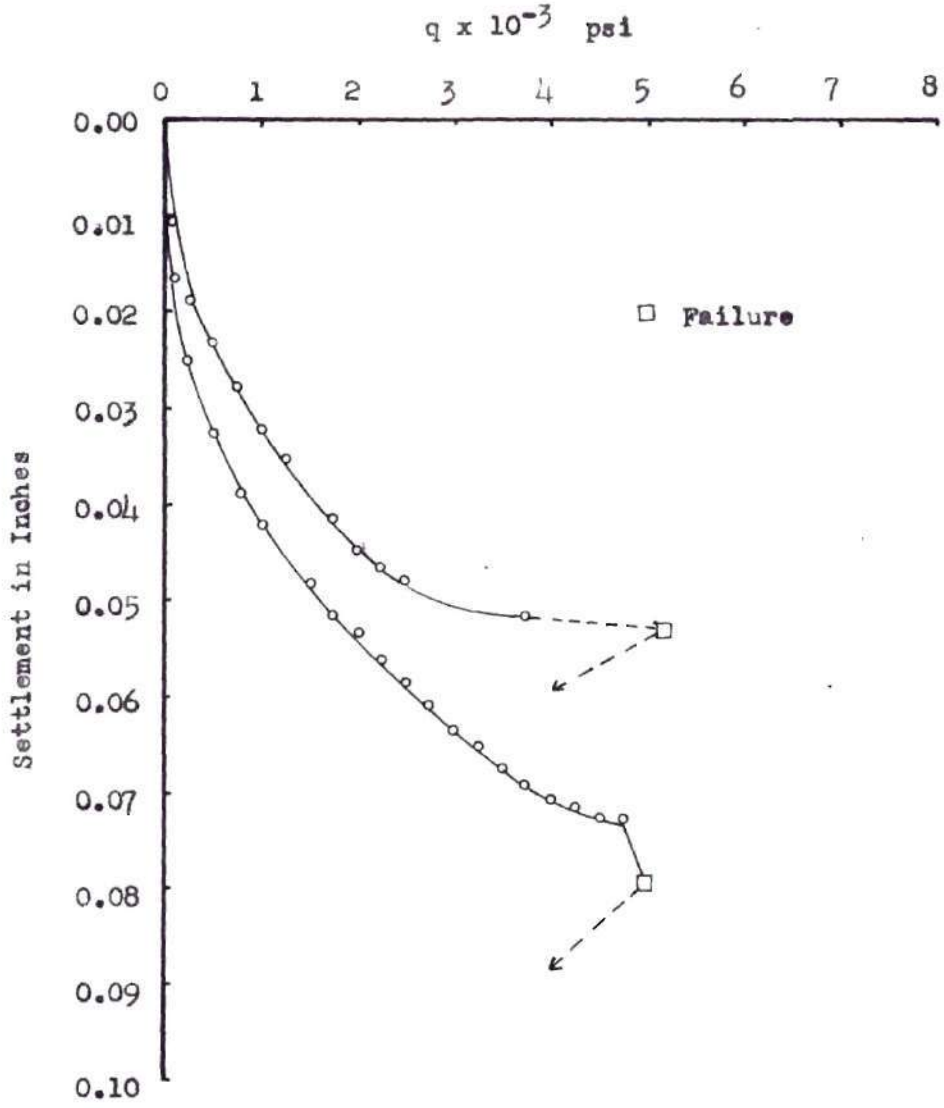

Figure 26. Pressure (q) vs. Settlement, 2.00 Inch Footing at the Center of a Block

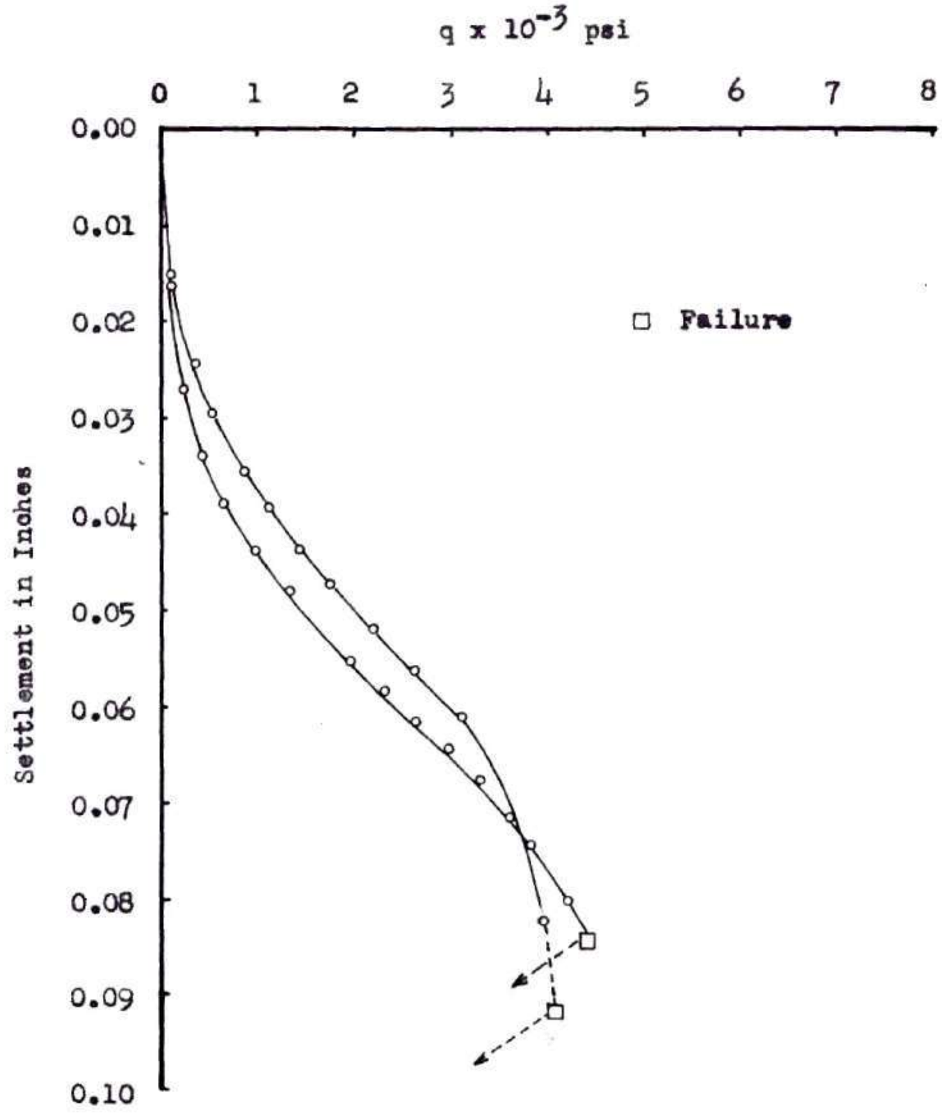

Figure 27. Pressure (q) vs. Settlement, 3.00 Inch Footing at the Center of a Block

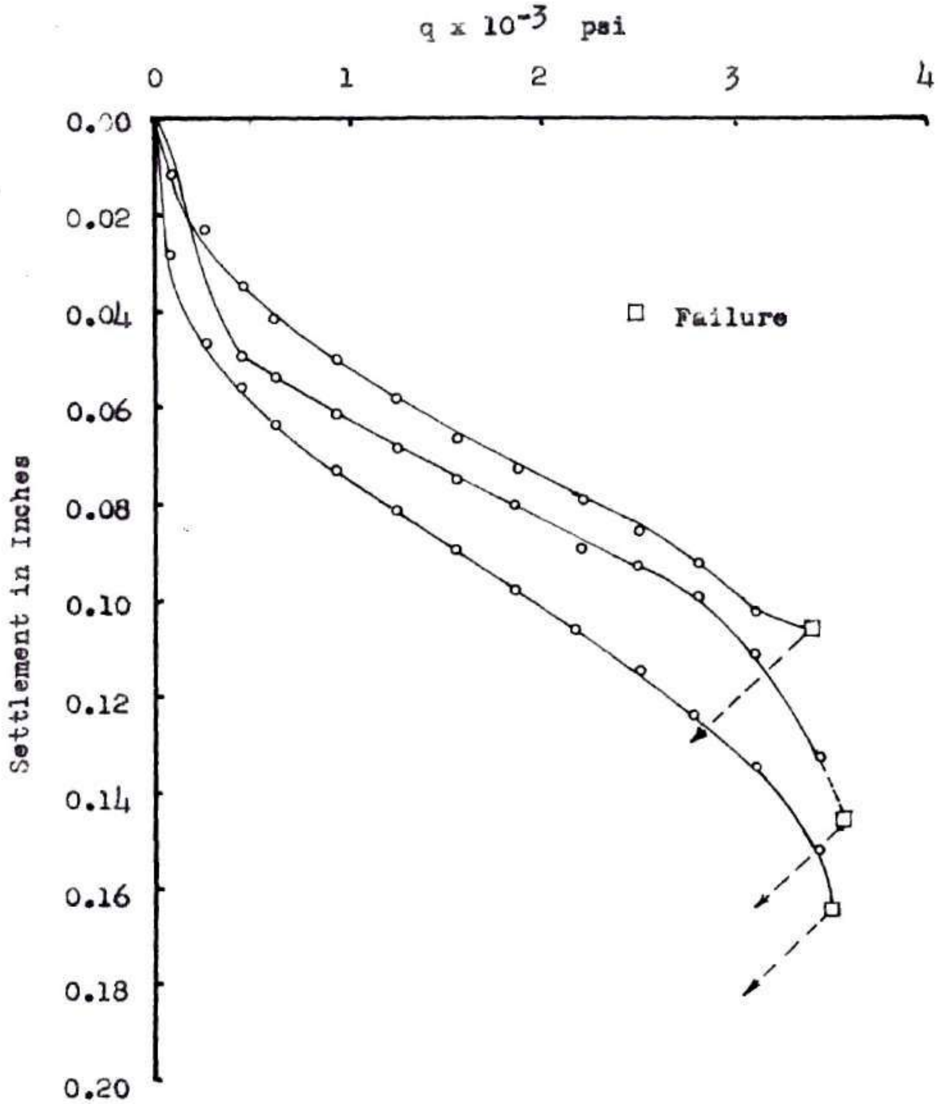

Figure 28. Pressure (q) vs. Settlement, 4.00 Inch Footing at the Center of a Block

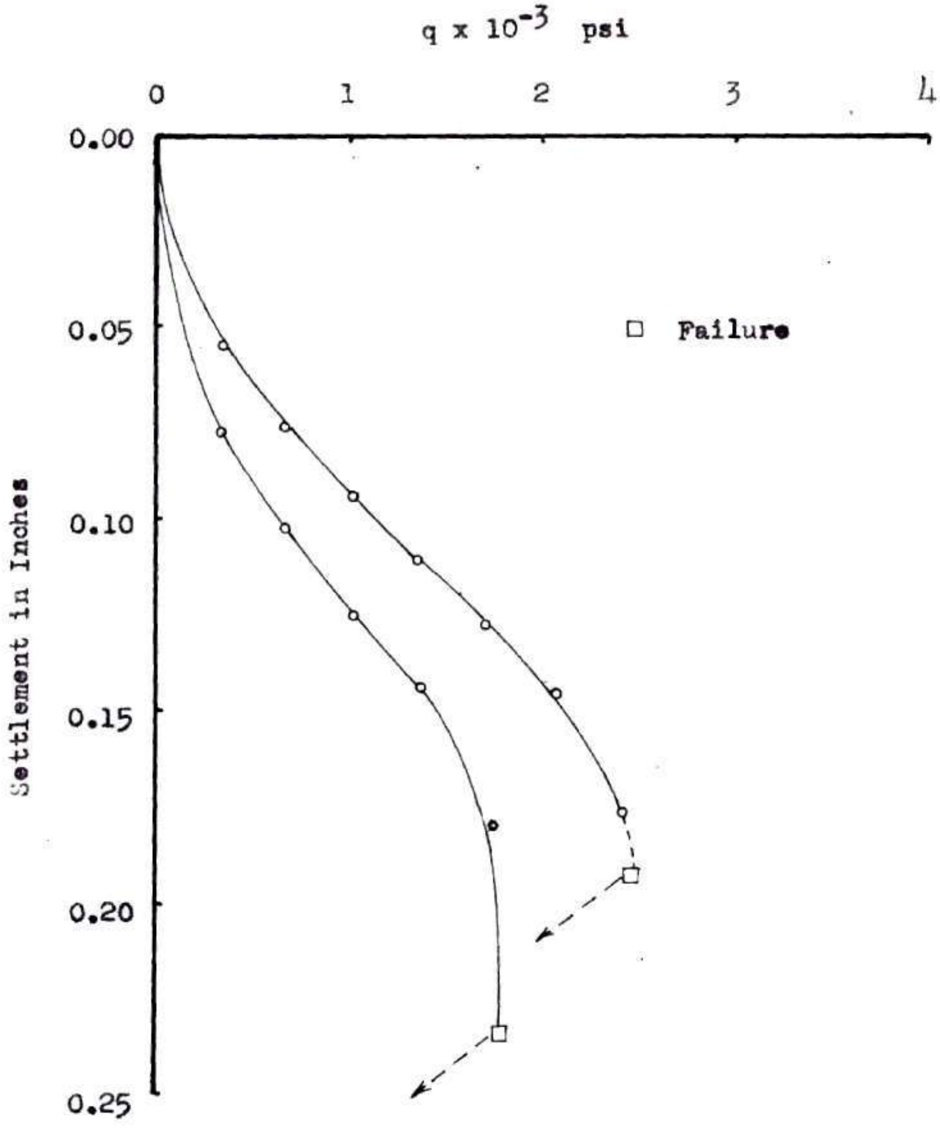

Figure 29. Pressure (q) vs. Settlement, 6.00 Inch Footing at the Center of a Block

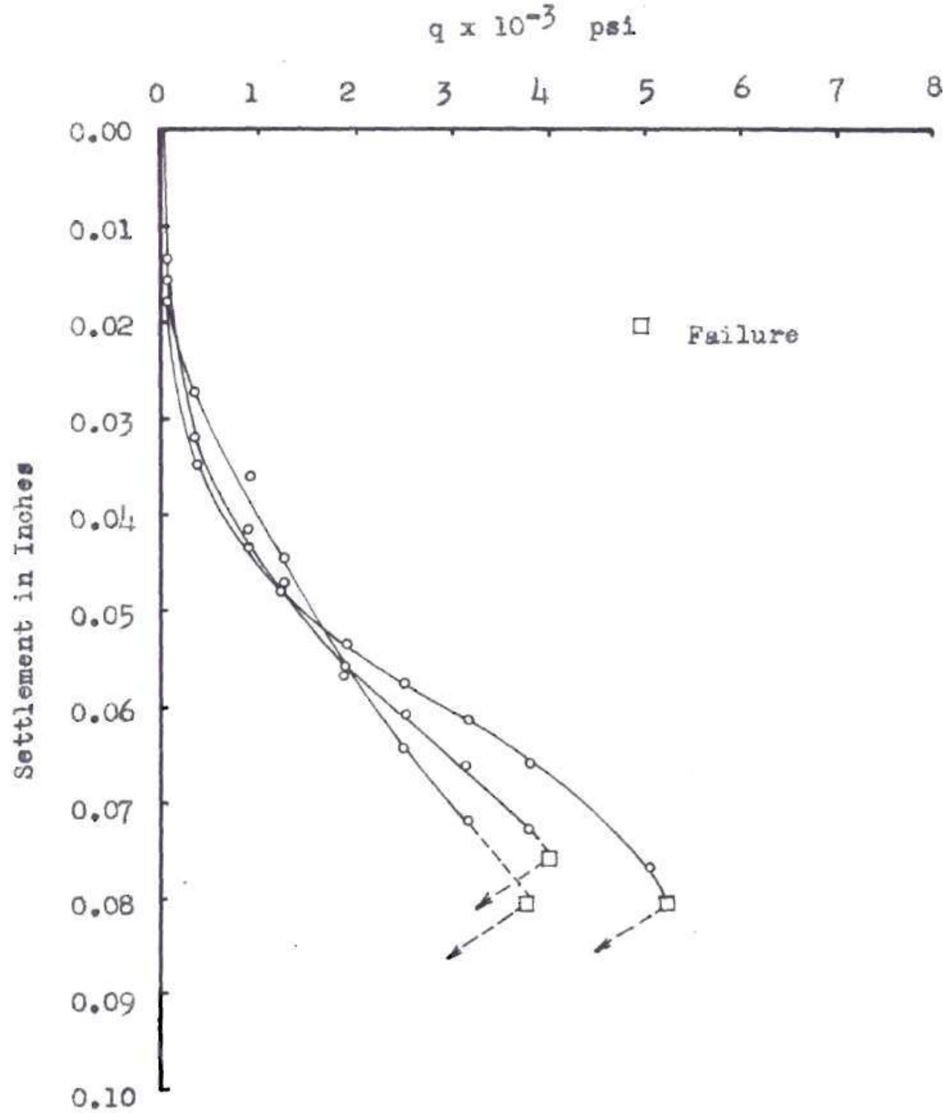

Figure 30. Pressure (q) vs. Settlement, 1.25 Inch Footing at the Edge of a Block

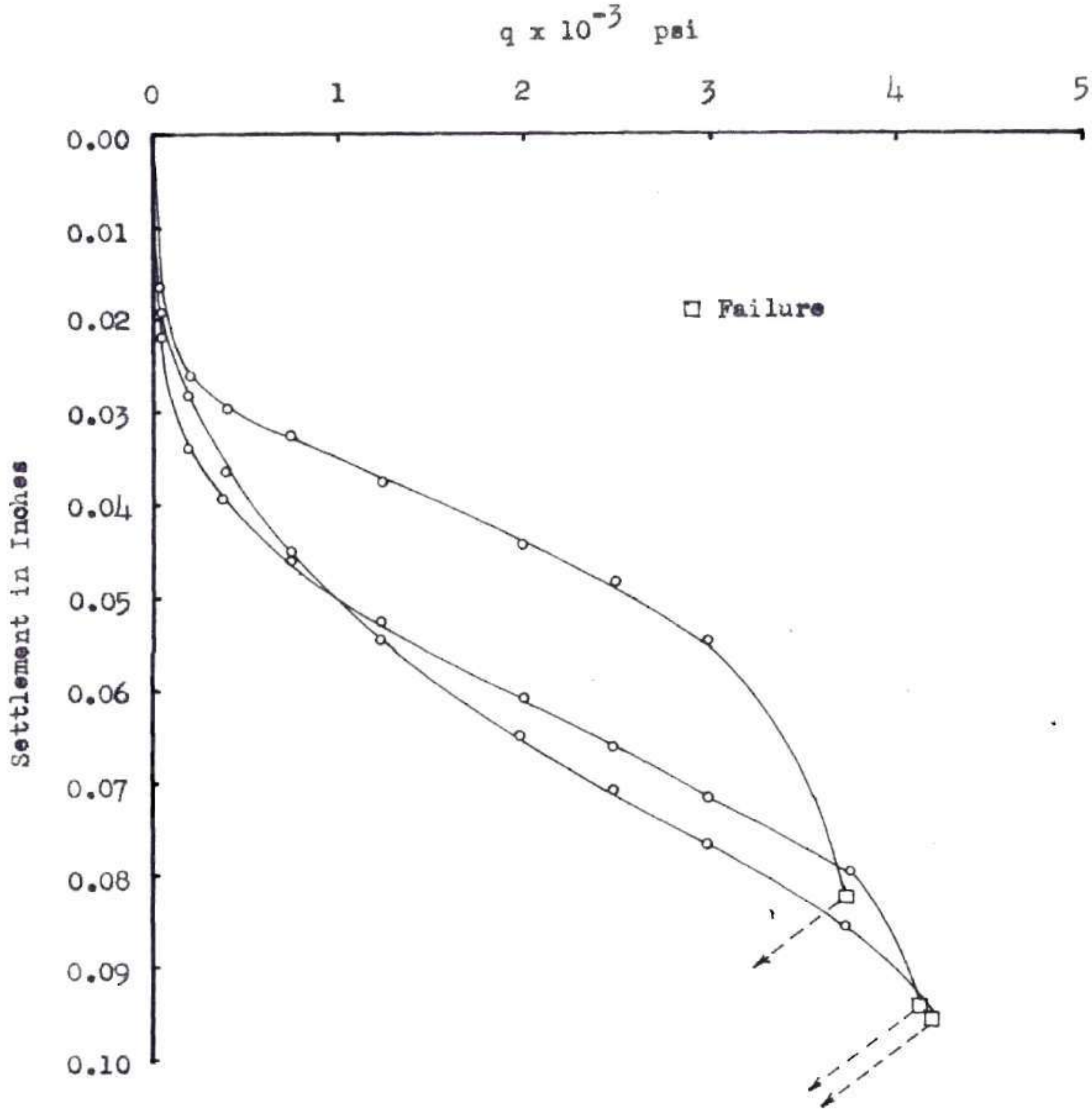

Figure 31. Pressure (q) vs. Settlement, 2.00 Inch Footing at the Edge of a Block

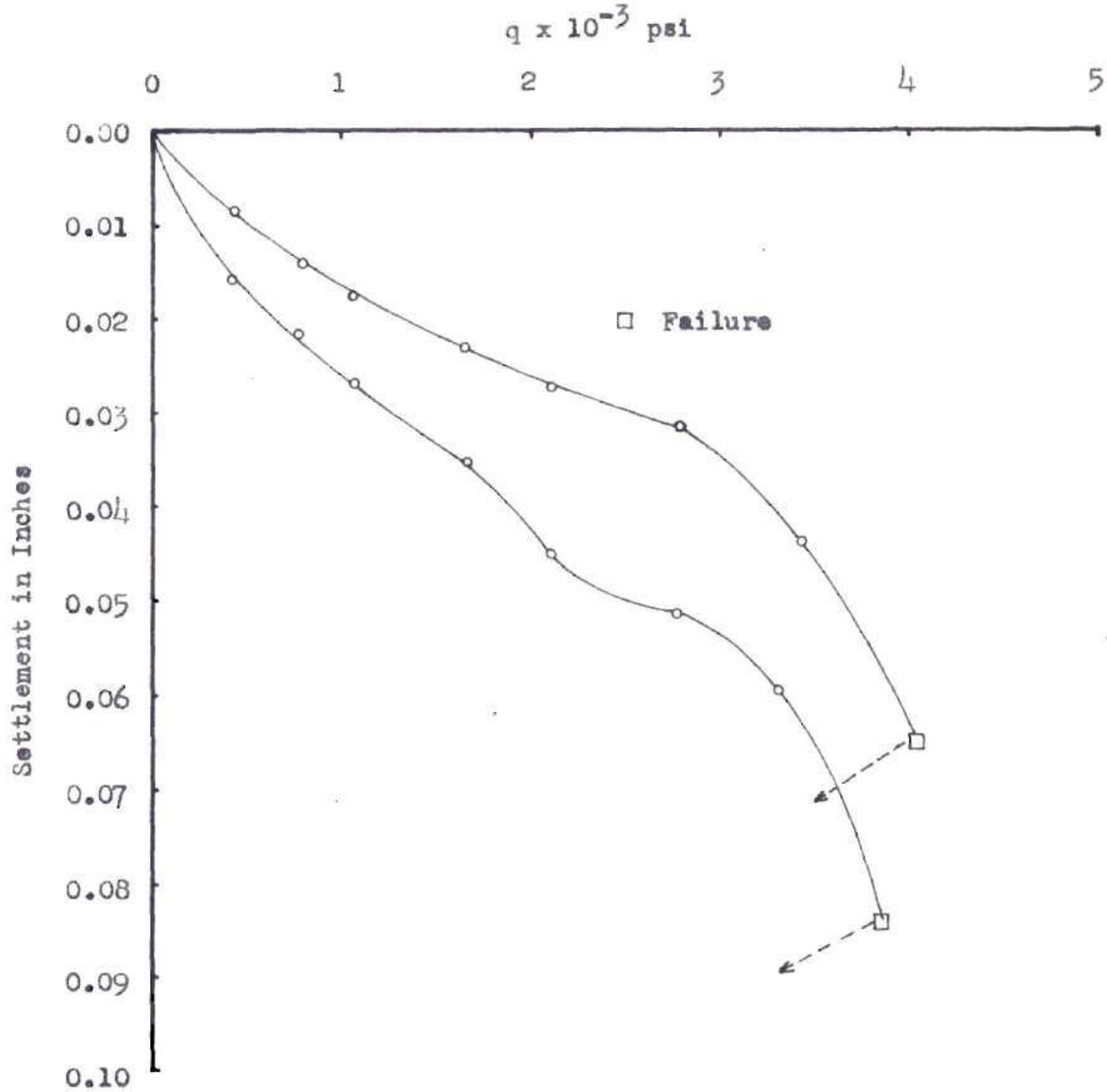

Figure 32. Pressure (q) vs. Settlement, 3.00 Inch Footing at the Edge of a Block

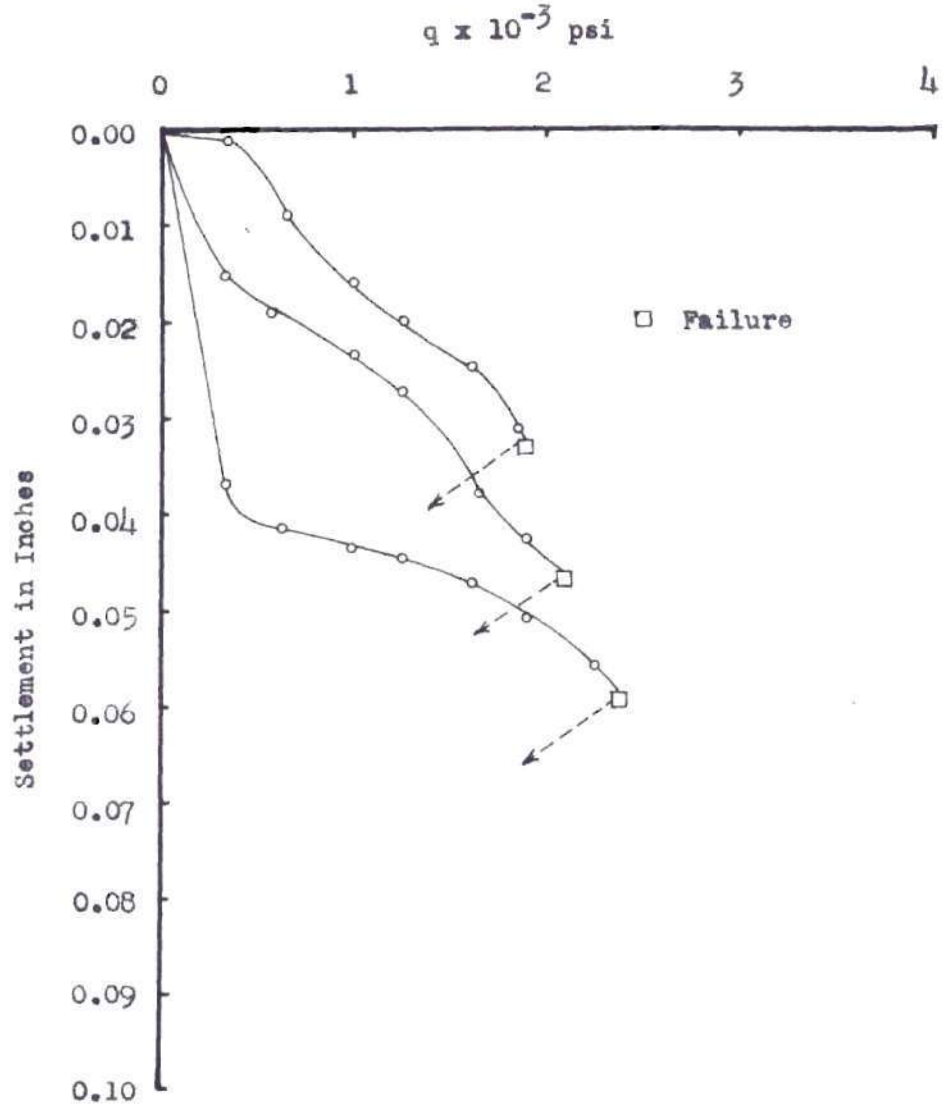

Figure 33. Pressure (q) vs. Settlement, 1.25 Inch Footing at the Corner of a Block

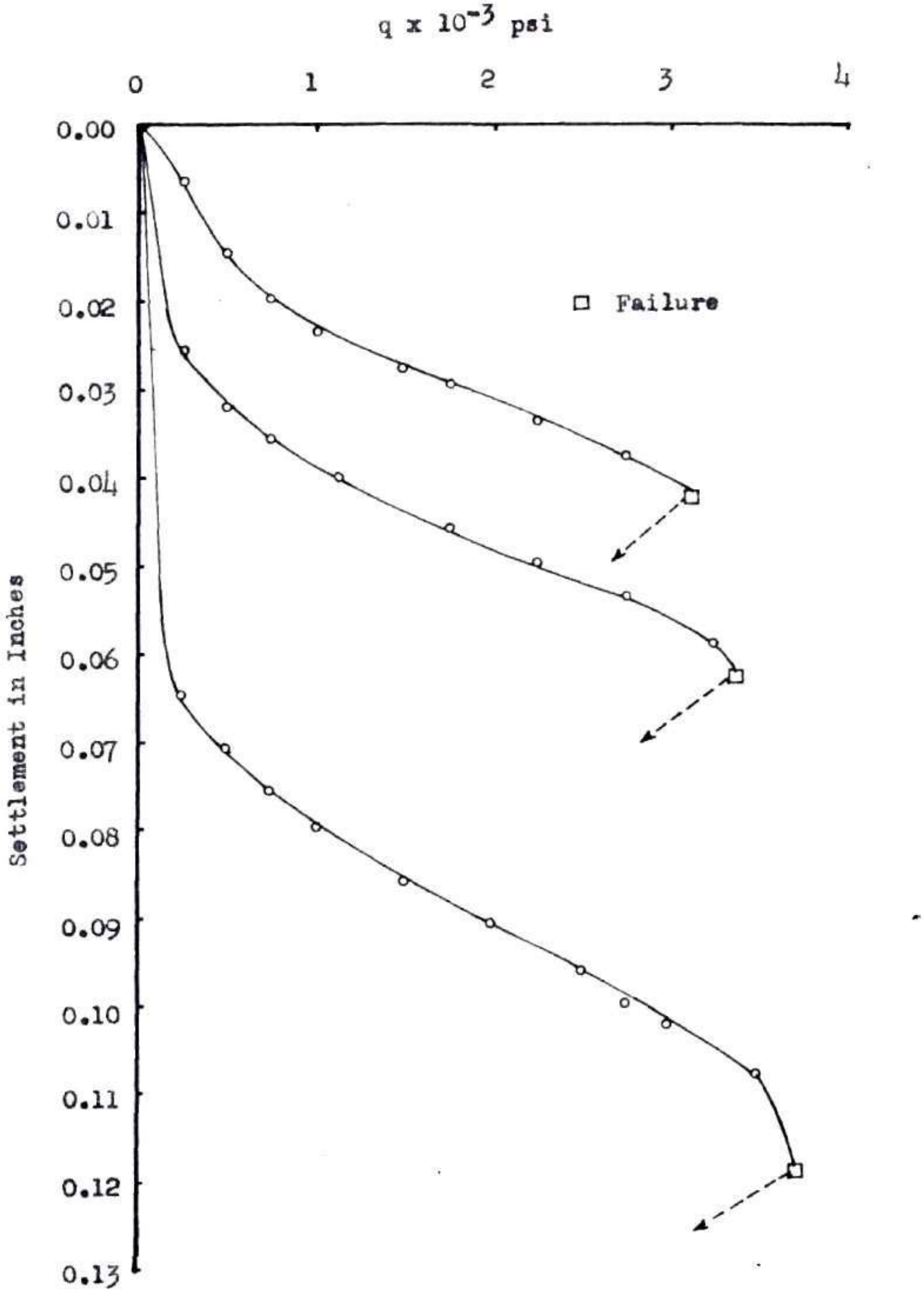

Figure 34. Pressure (q) vs. Settlement, 2.00 Inch Footing at the Corner of a Block

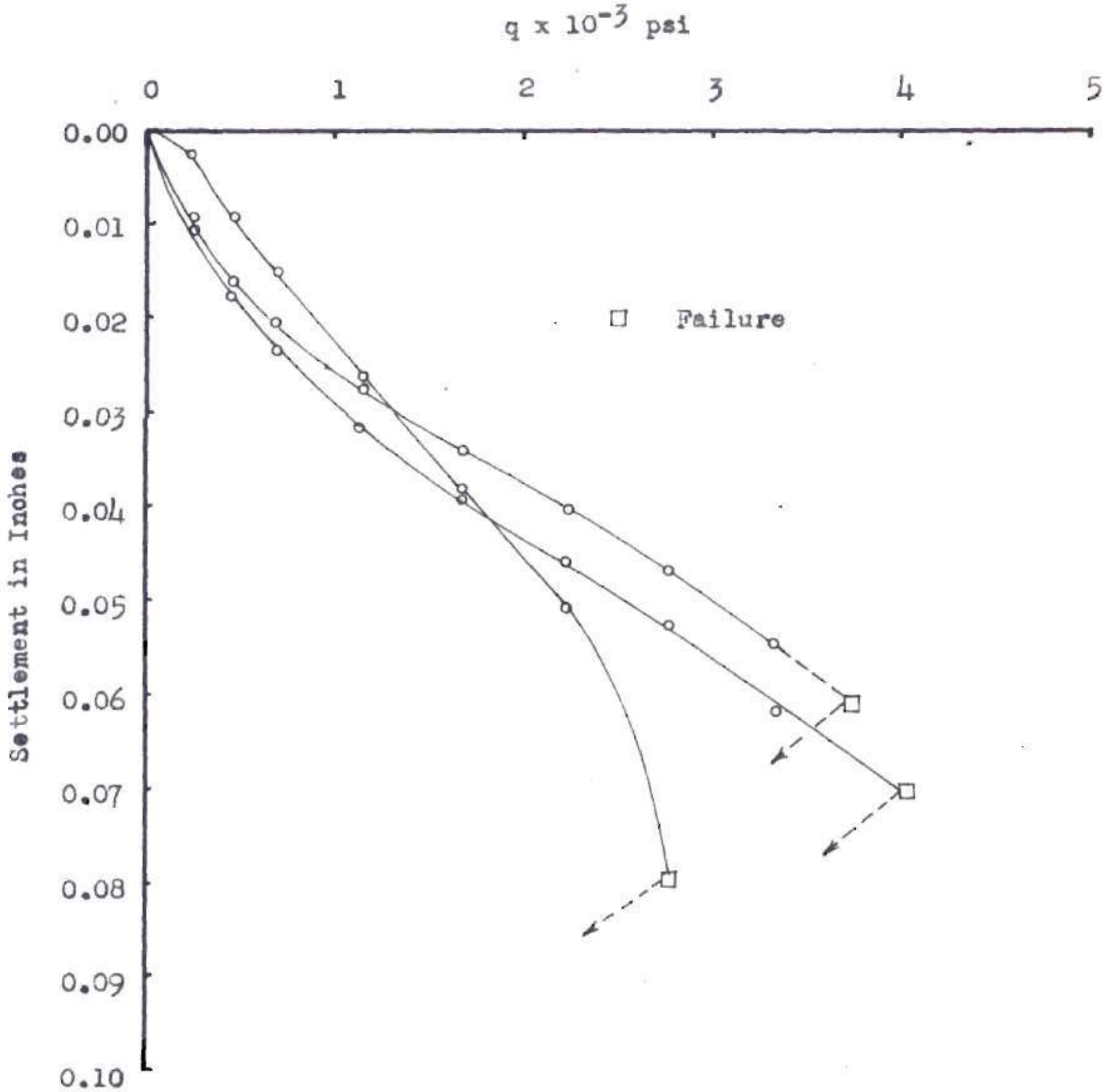

Figure 35 . Pressure (q) vs. Settlement, 3.00 Inch Footing at the Corner of a Block

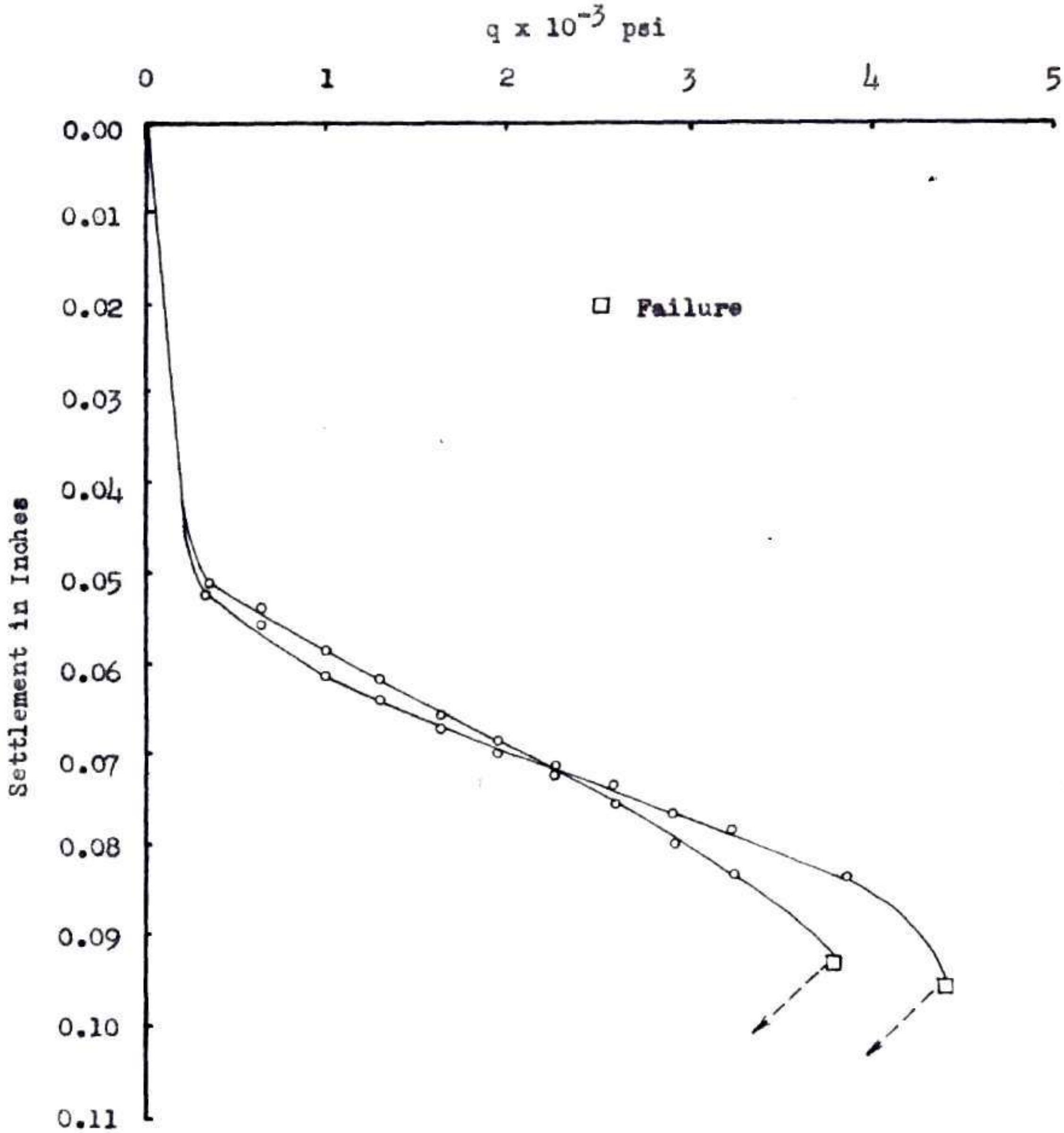

Figure 36. Pressure (q) vs. Settlement, 1.25 Inch Footing Centered over Two Blocks

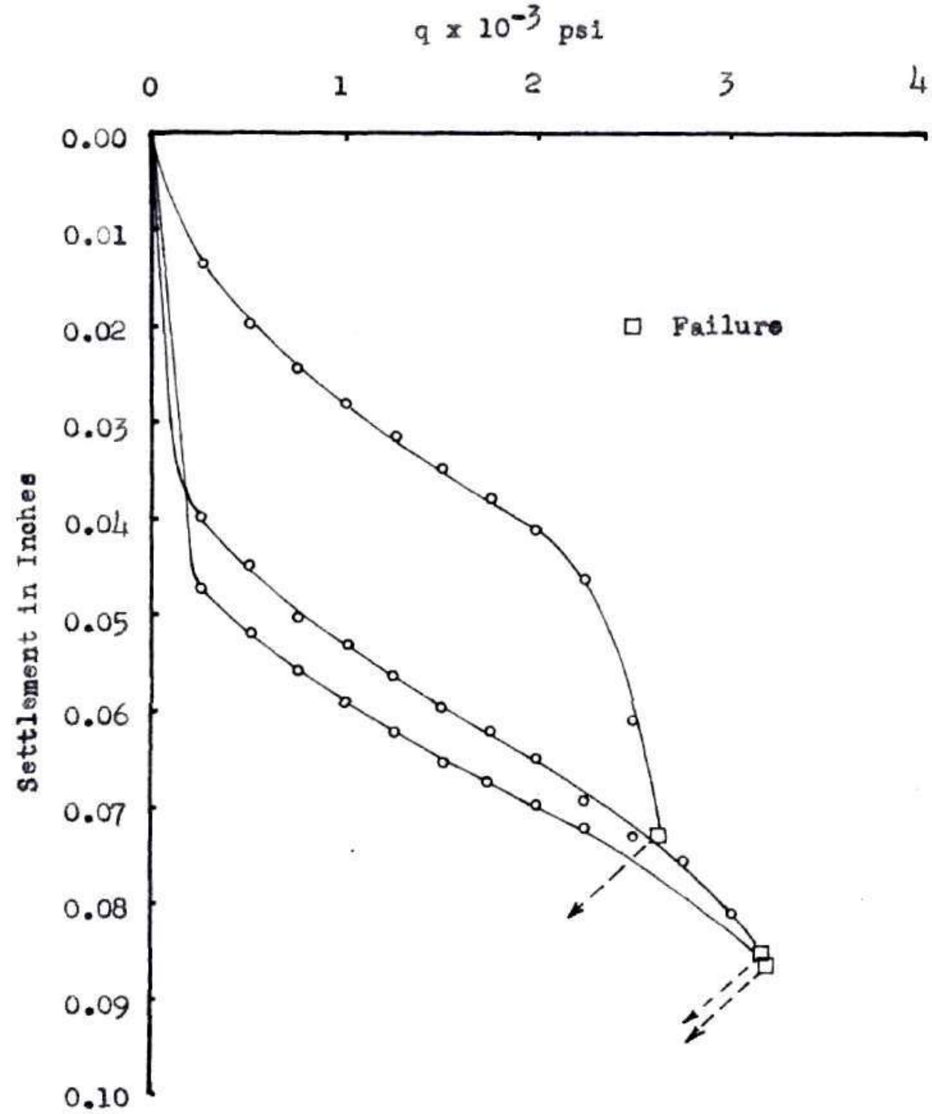

Figure 37. Pressure (q) vs. Settlement, 2.00 Inch Footing Centered over Two Blocks

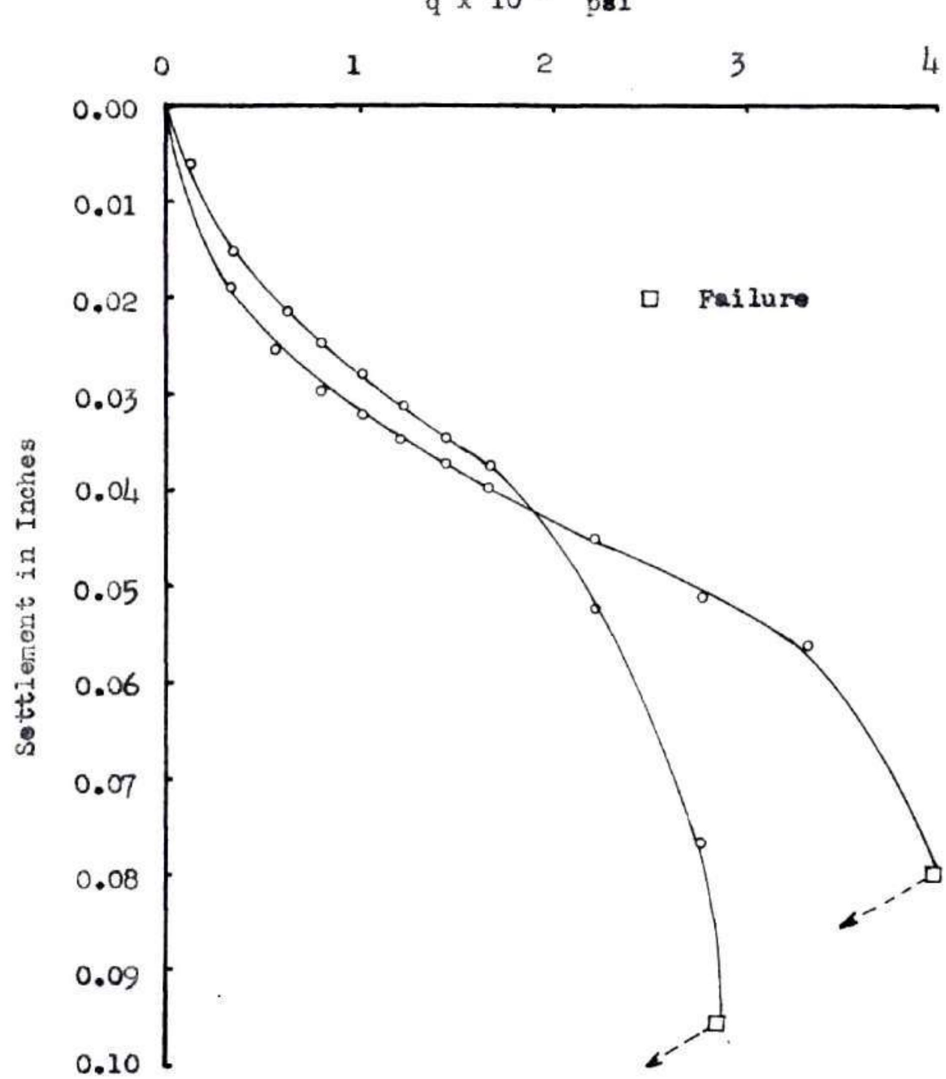

Figure 38. Pressure (q) vs. Settlement, 3.00 Inch Footing Centered over Two Blocks

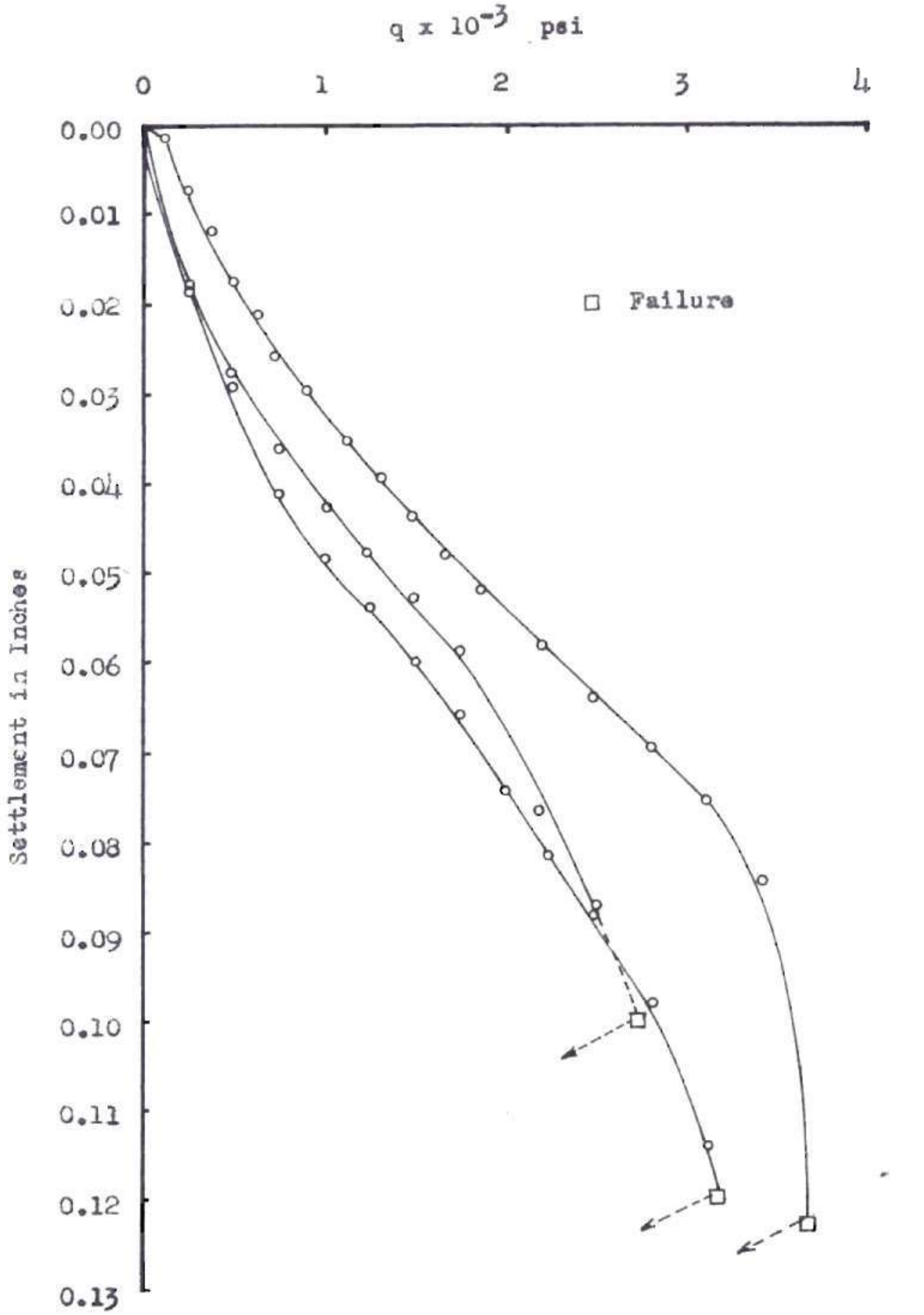

Figure 39. Pressure (q) vs. Settlement, 4.00 Inch Footing Centered over Two Blocks

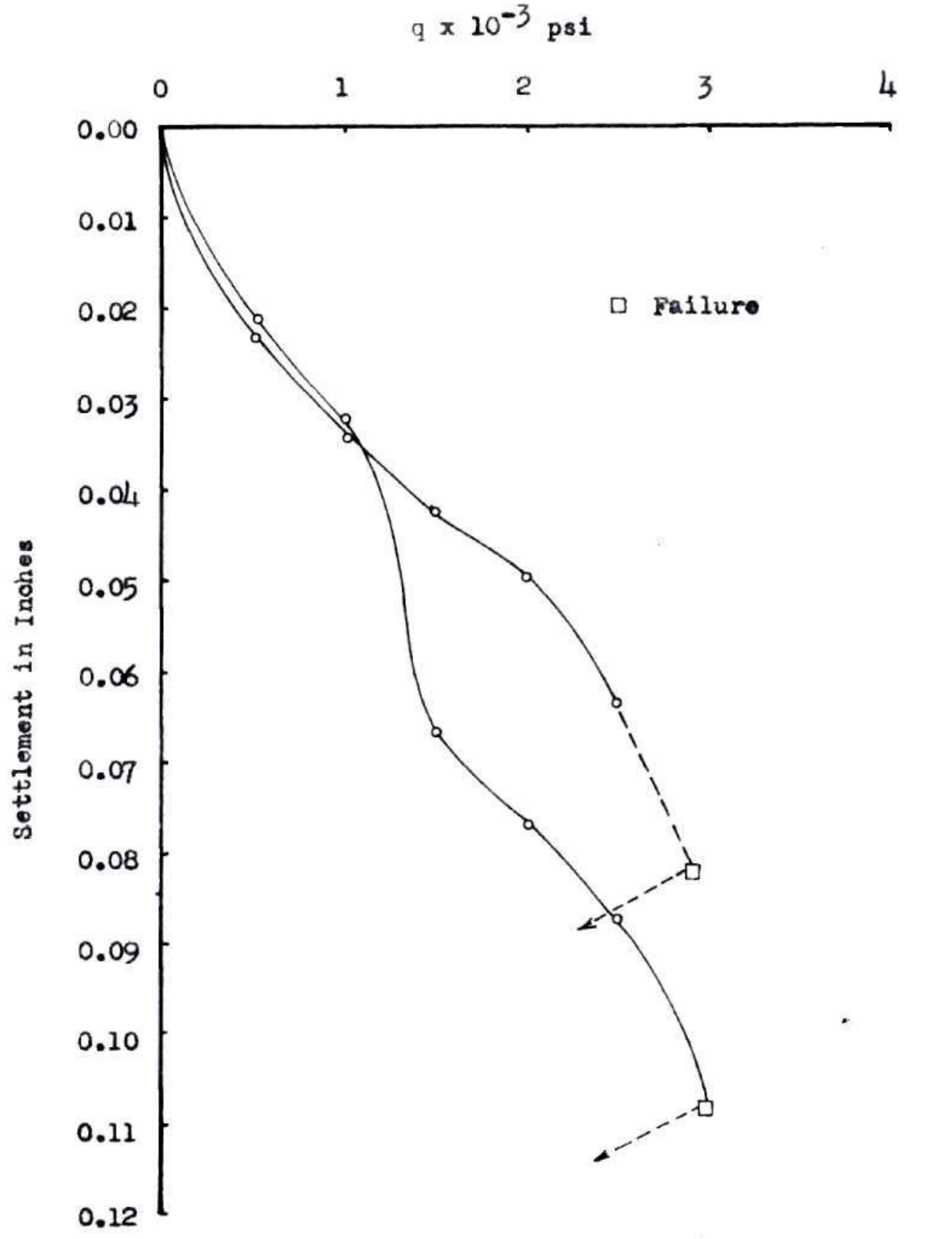

Figure 40. Pressure (q) vs. Settlement, 2.00 Inch Footing Centered over Four Blocks

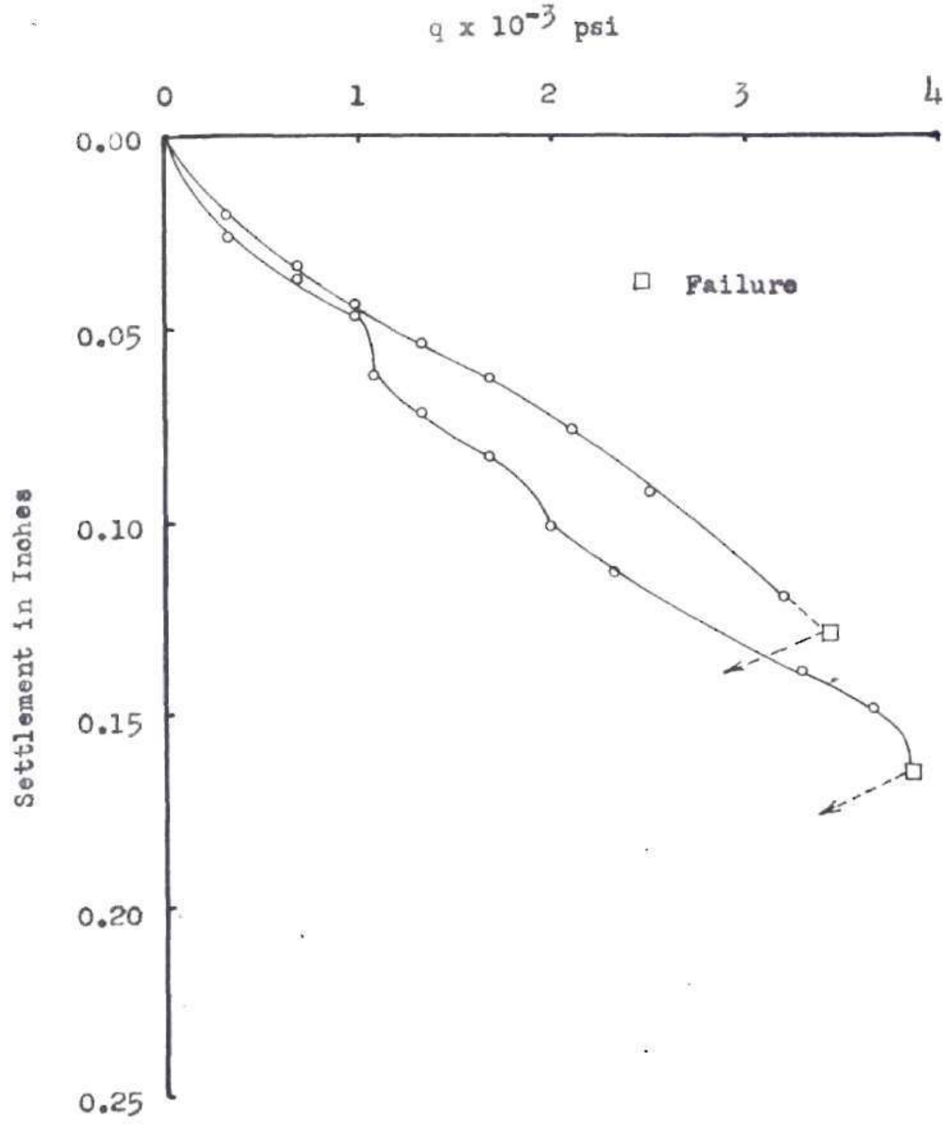

Figure 41 . Pressure (q) vs. Settlement, 3.00 Inch Footing Centered over Four Blocks

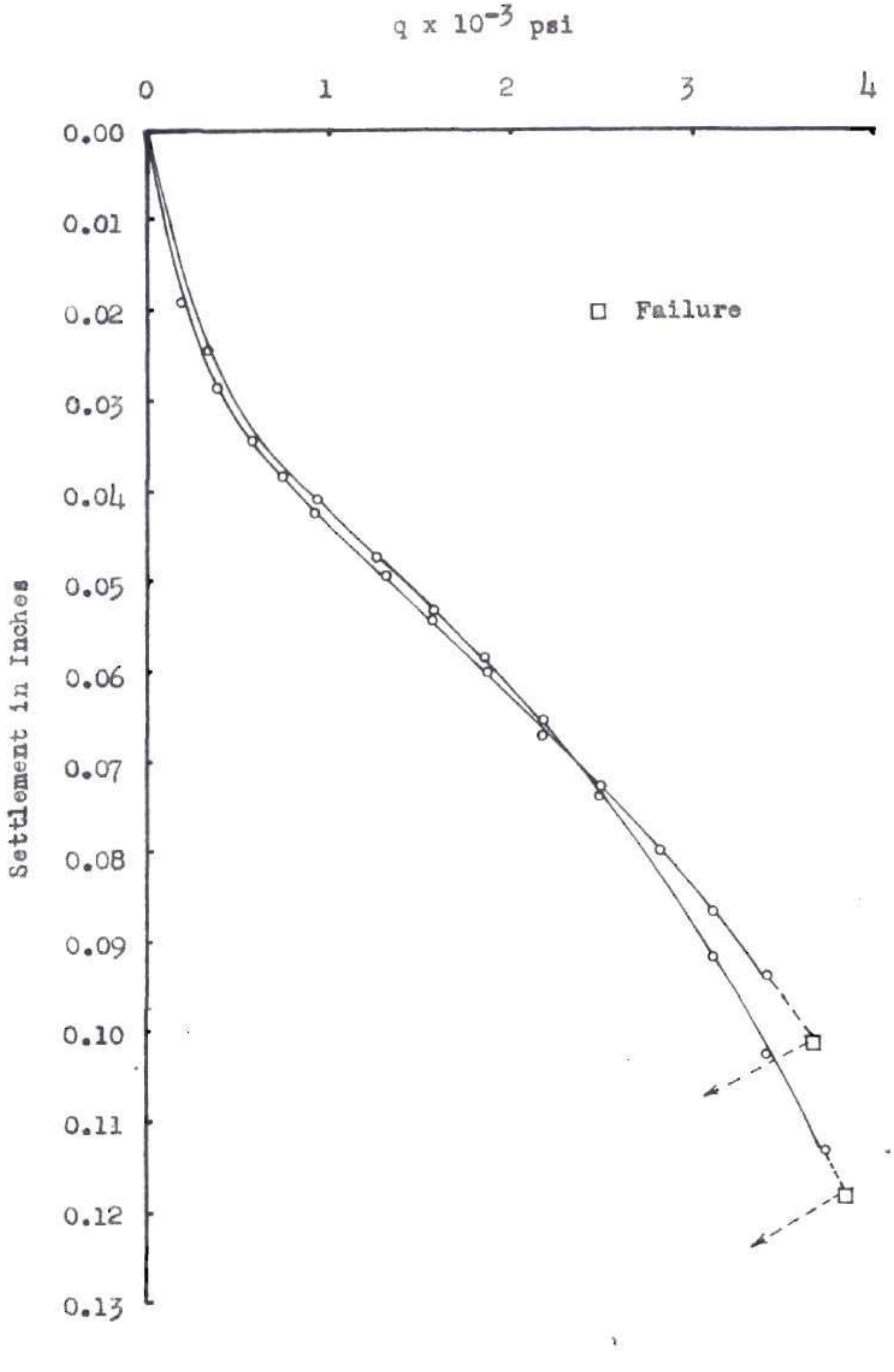

Figure 42. Pressure (q) vs. Settlement, 4.00 Inch Footing Centered over Four Blocks

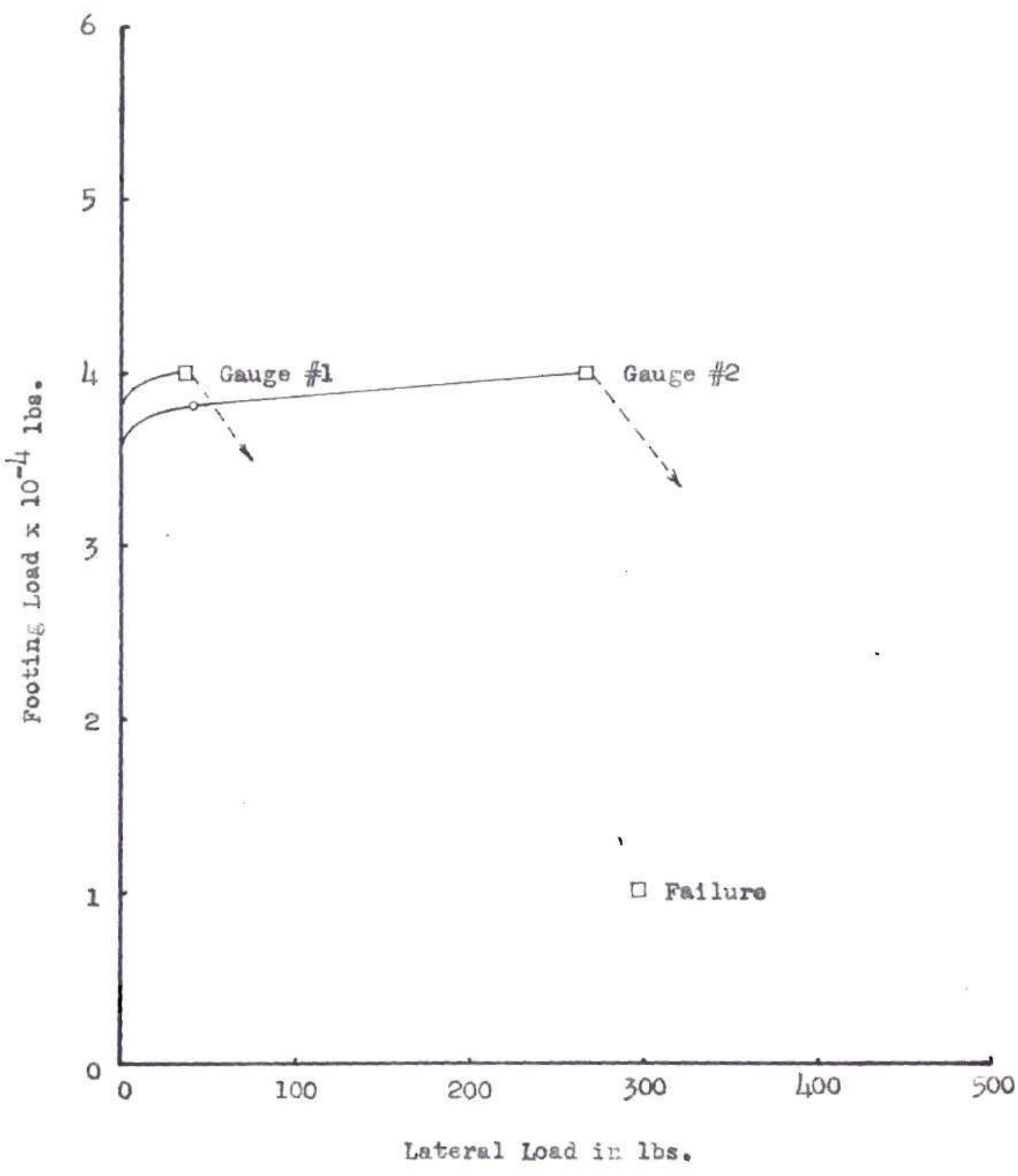

Figure 43. Footing Load vs Lateral Load, 3.00 Inch Footing at the Center of a Block

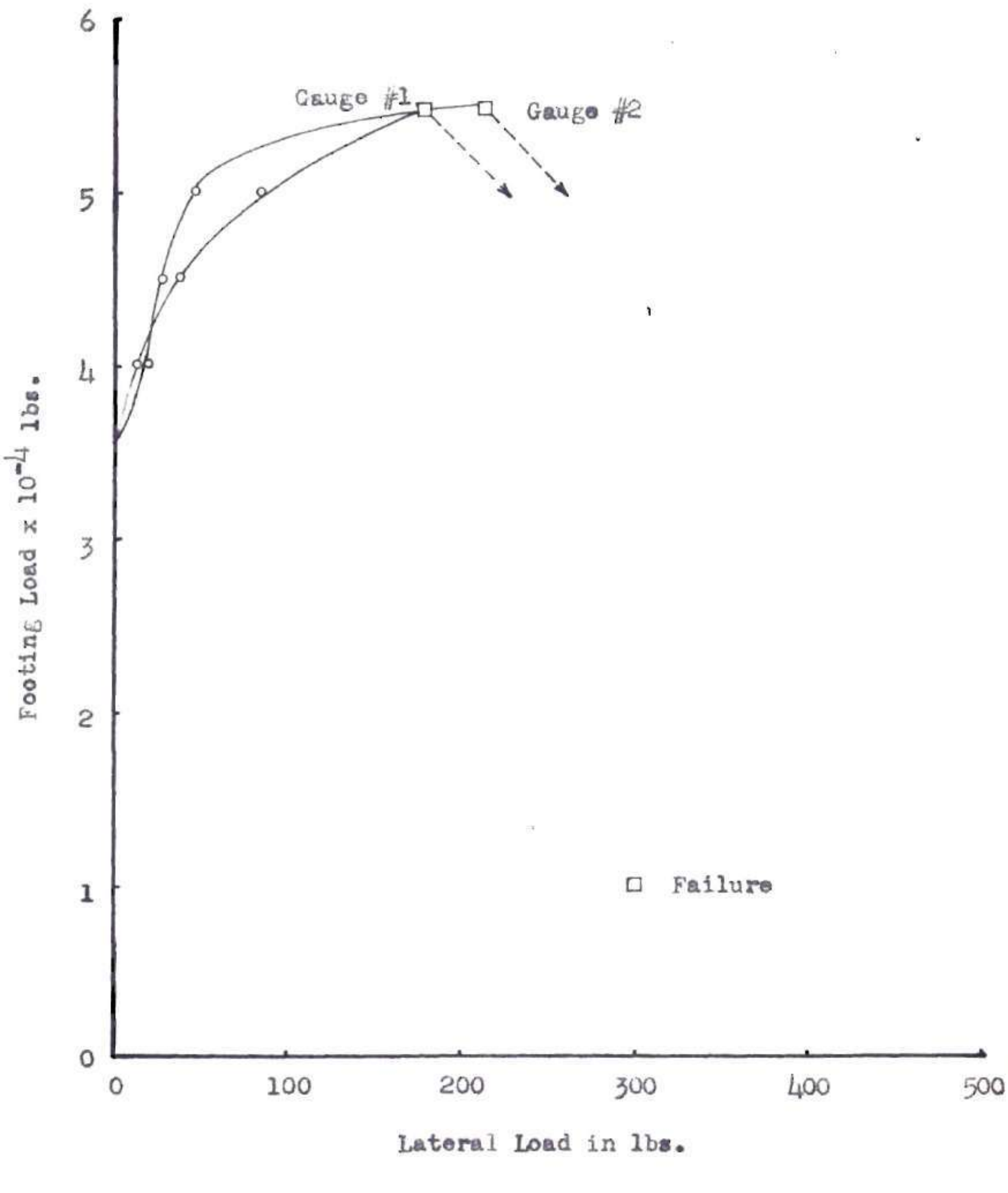

Figure 44 . Footing Load vs. Lateral Load, 4.00 Inch Footing at the Center of a Block

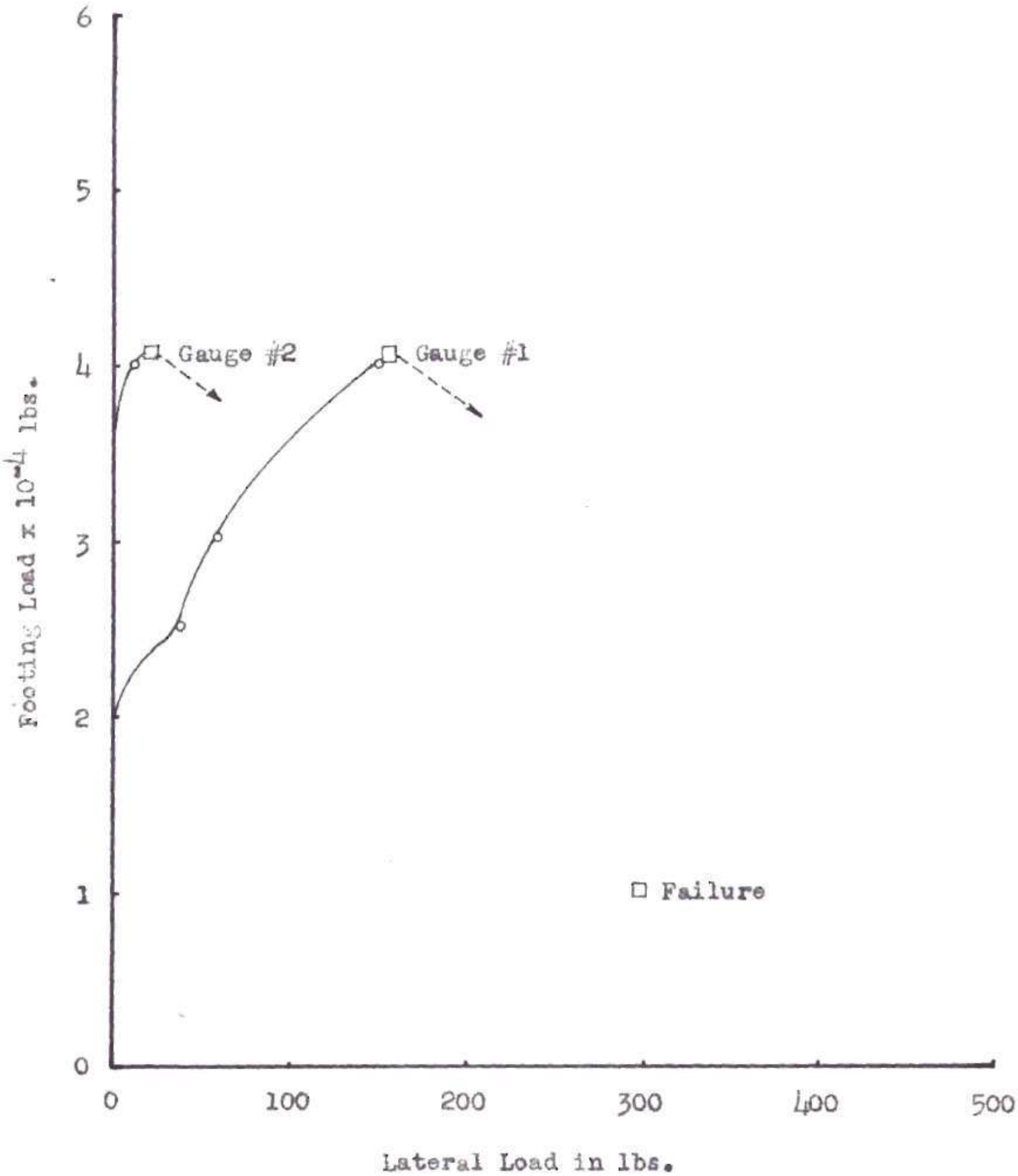

Figure 45 . Footing Load vs. Lateral Load, 3.00 Inch Footing at the Edge of a Block

Page missing from thesis

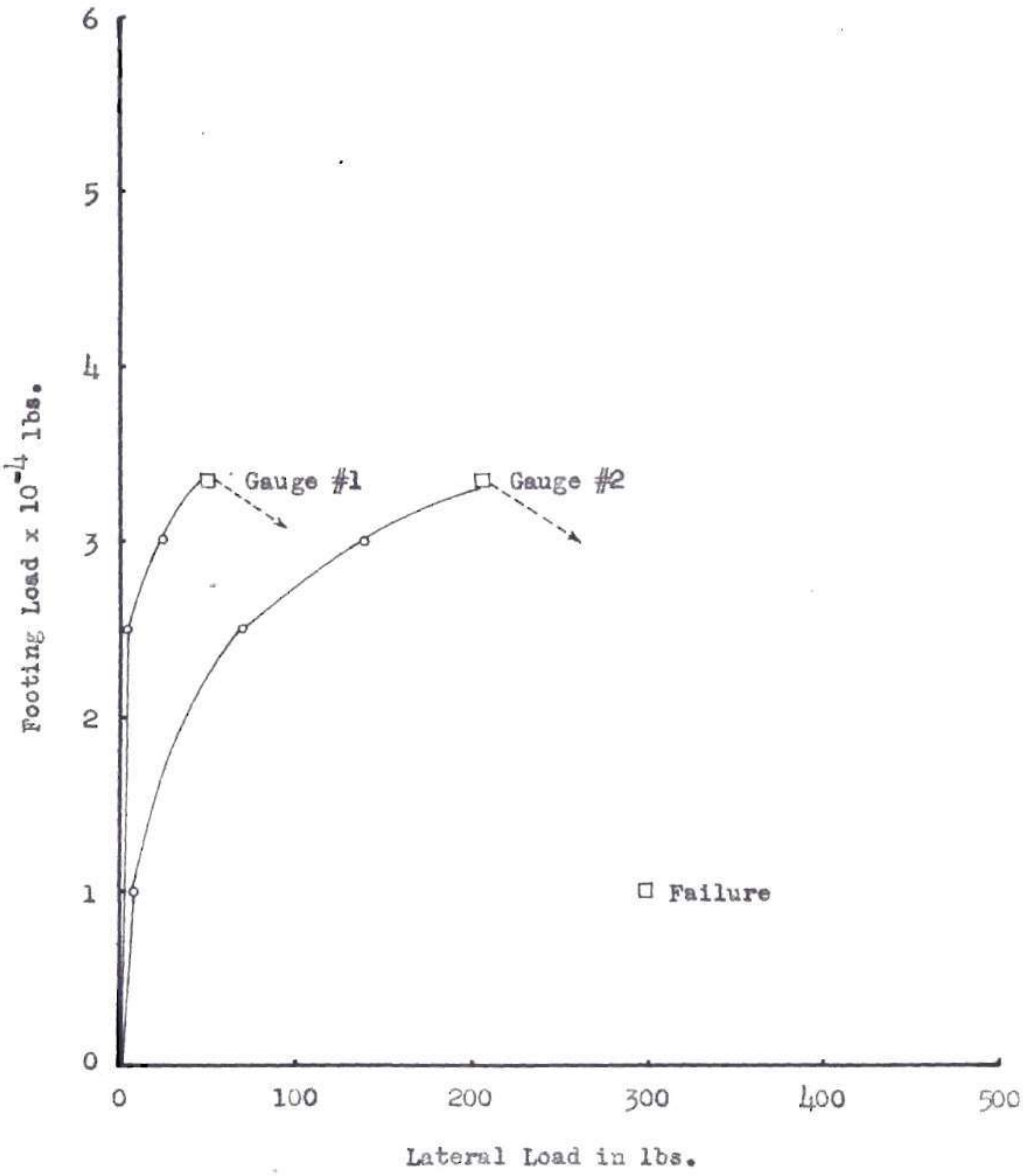

Figure 47. Footing Load vs. Lateral Load, 3.00 Inch Footing at the Corner of a Block

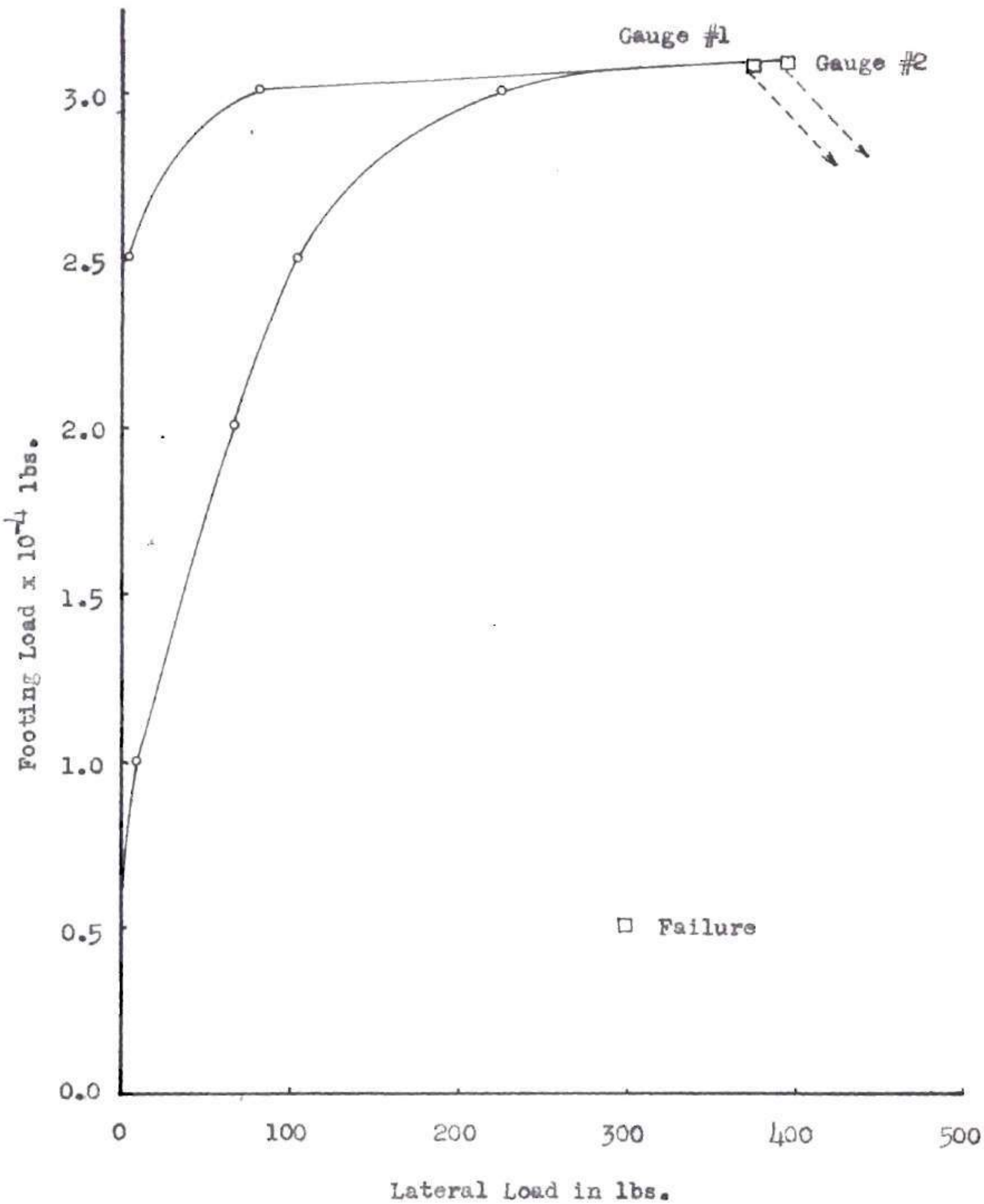

Figure 48. Footing Load vs. Lateral Load, 3.00 Inch Footing Centered over Two Blocks

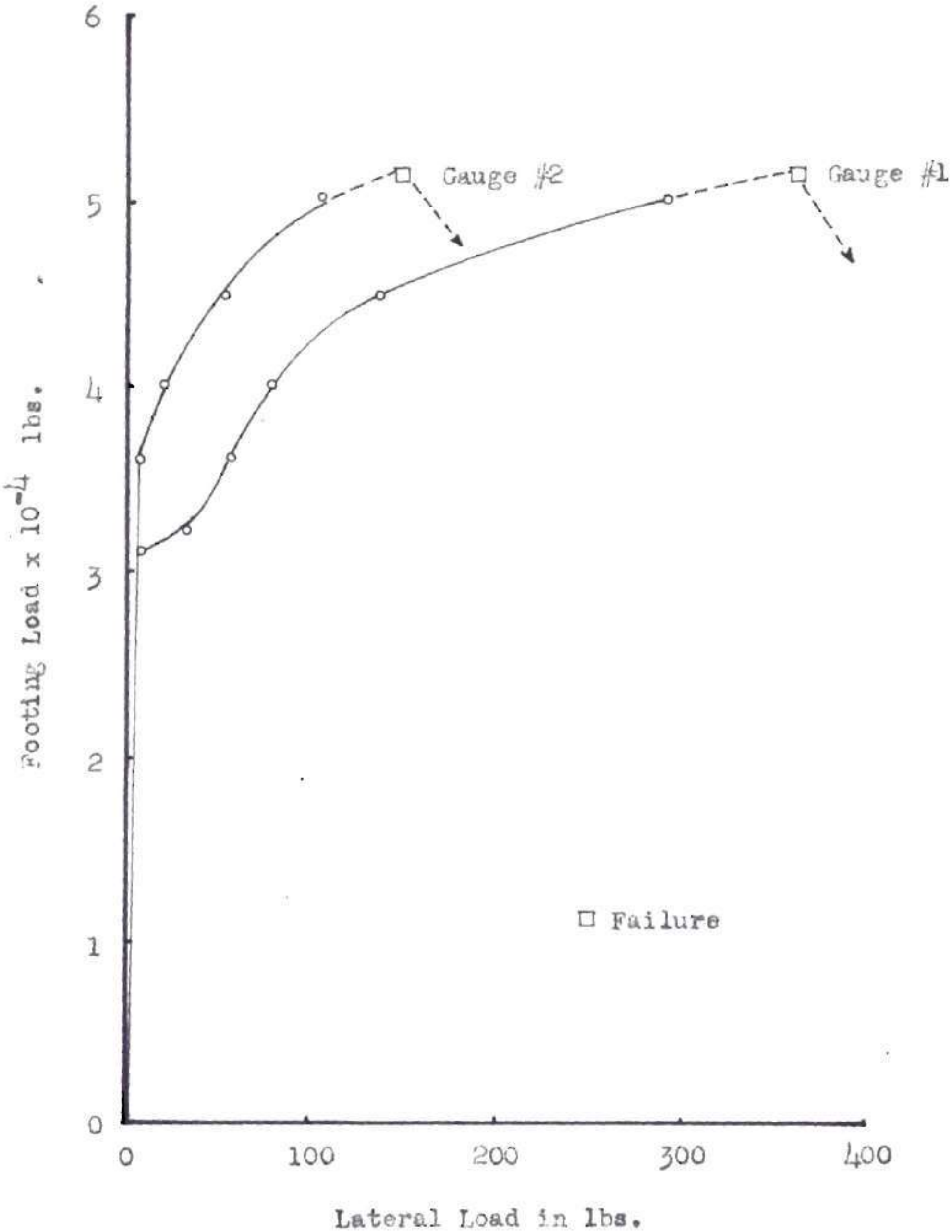

Figure 49. Footing Load vs. Lateral Load, 4.00 Inch Footing Centered over Two Blocks

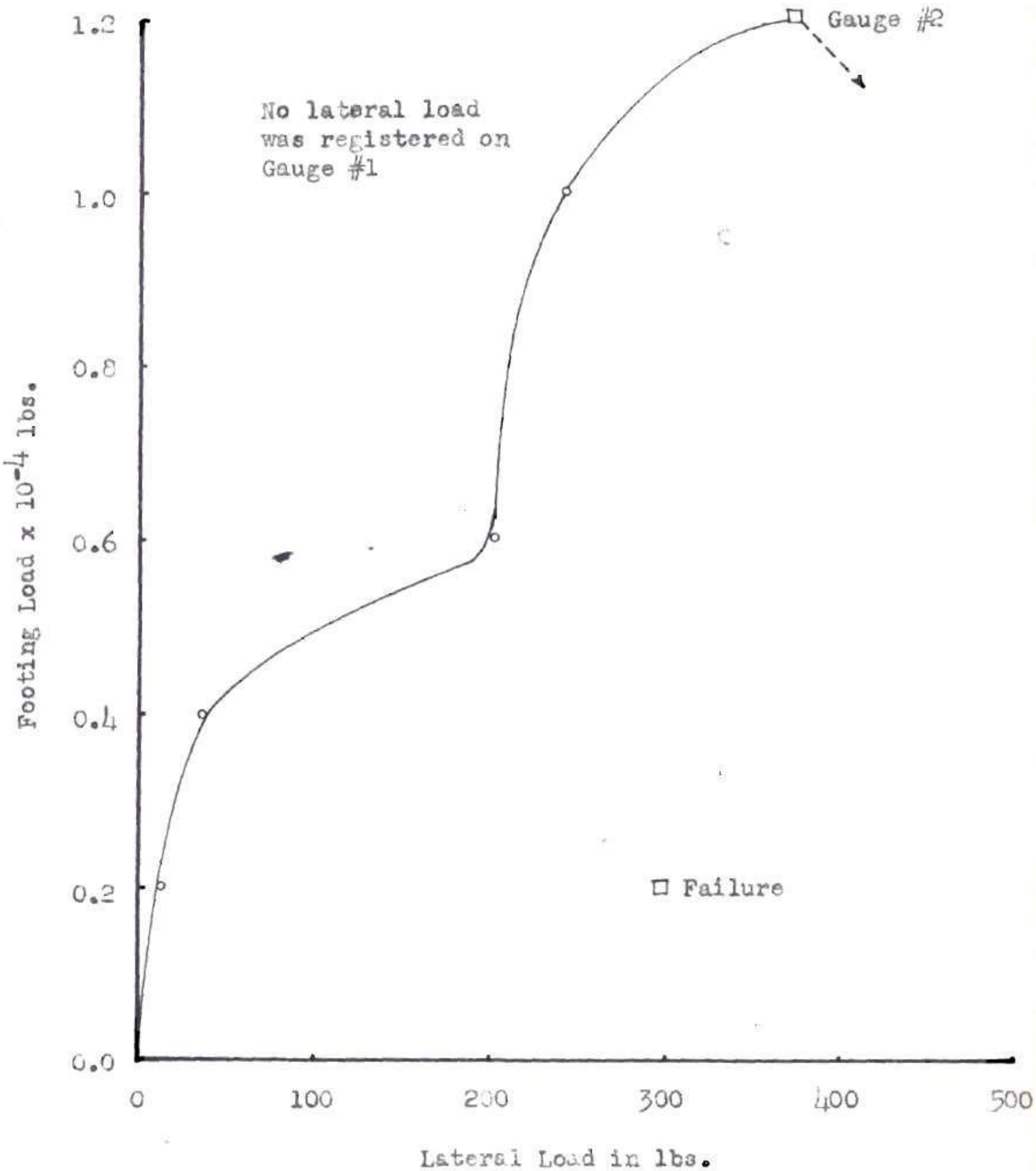

Figure 50 . Footing Load vs. Lateral Load, 2.00 Inch Footing Centered over Four Blocks

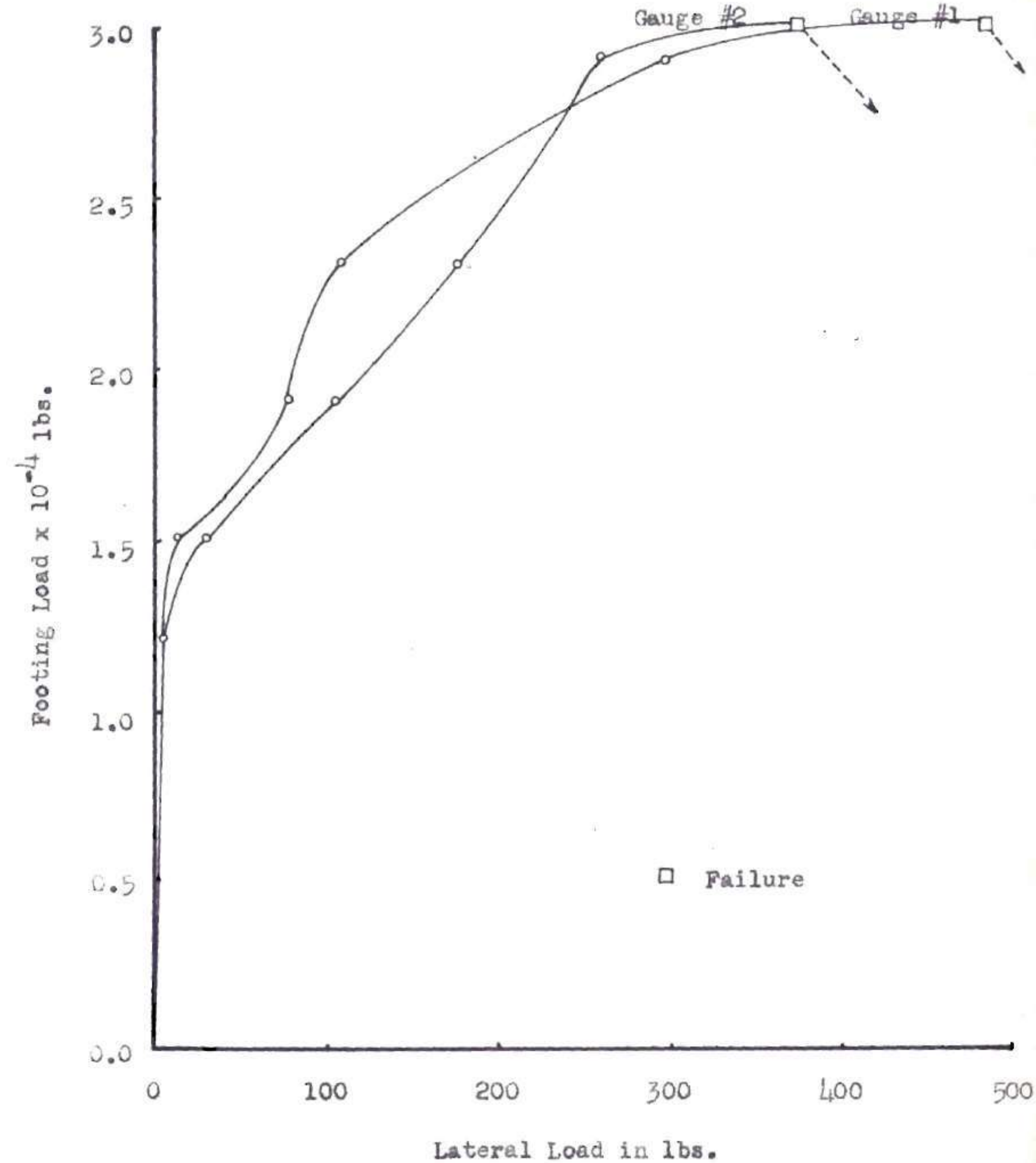

Figure 51 . Footing Load vs. Lateral Load, 3.00 Inch Footing Centered over Four Blocks

BIBLIOGRAPHY

1. Sowers, G. F.: "Shallow Foundations," in Foundation Engineering, ed. by G. A. Leonards, McGraw-Hill Book Company, Inc., New York, 1962, p. 529.

2. John, Klaus W.: "An Approach to Rock Mechanics," Journal of the Soil Mechanics and Foundations Division, Proceedings, A.S.C.E., vol. 88, no. SM-4(7962).

3. Murphy, G.: Similitude in Engineering, The Ronald Press Company, New York, 1950, p. 57.

4. Meyerhof, G. G.: "The Bearing Capacity of Concrete and Rock," Magazine of Concrete Research, vol. 4, no. 12, p. 109 (April, 1953).

5. Bauschinger, J., Versuche mit Quaderne aus Natursteinen. Munich, Mitteilungen aus dem Mechanischtechischen Laboratorium der Kgl. Technischen Hochschule No. 6. 1876, p. 13.

6. Bach, C. and Baumann, R., Elastizität und Festigkeit. Berlin, J. Springer Verlag, 1924, p. 217.

7. Graf, O., Versuch mit Betonquadern zu Brückengelenken und Auflagern. Berlin, Verin Deutscher Ingenieure. Mitteilungen uber Forschung sar beiten, no. 232, 1921, p. 68.

8. Graf, O., Über einige Aufgaben der Eisenbetonforschung aus alterer und neurer Zeit., Beton und Eisen. 1934, Vol. 33, no. 11, June, pp. 165-173.

9. Terzaghi, K.: Theoretical Soil Mechanics, John Wiley and Sons, Inc., New York, 1943, p. 118.

10. Von Kolnitz, G. F.: An Investigation of the Bearing Capacity of a Jointed System, Unpublished Masters Thesis, Georgia Institute of Technology, 1965.

11. ____________: "Specifications and Details," Indiana Limestone Co. Inc., Bedford, Indiana, p. 2.

12. Webster, N.: Webster's New Collegiate Dictionary, G. and C. Merriam Company, Springfield, Mass., © 1953, p. 331.

13. Schwartz, A. E.: An Investigation of the Strength of Rock, Unpublished Ph. D. Thesis, Georgia Institute of Technology, 1963.

14. Robertson, L. H.: "The Mechanics of Rock Failure," Third Symposium on Rock Mechanics, Golden, Colorado, 1959, pp. 177-199.

15. Anderegg, F. D.: "Efflorescence and Staining of Indiana Limestone," Purdue Engineering Experiment Station Report, No. 33, pp. 8-11.